International Journal of Analytical Chemistry

Extraction/Preconcentration Procedures for Determination of Metal and Organometallic Species in Environmental, Biological, and Food Samples

Lead Guest Editor: Marcela Z. Corazza
Guest Editors: Vanessa Egea and Seyyed E. Moradi

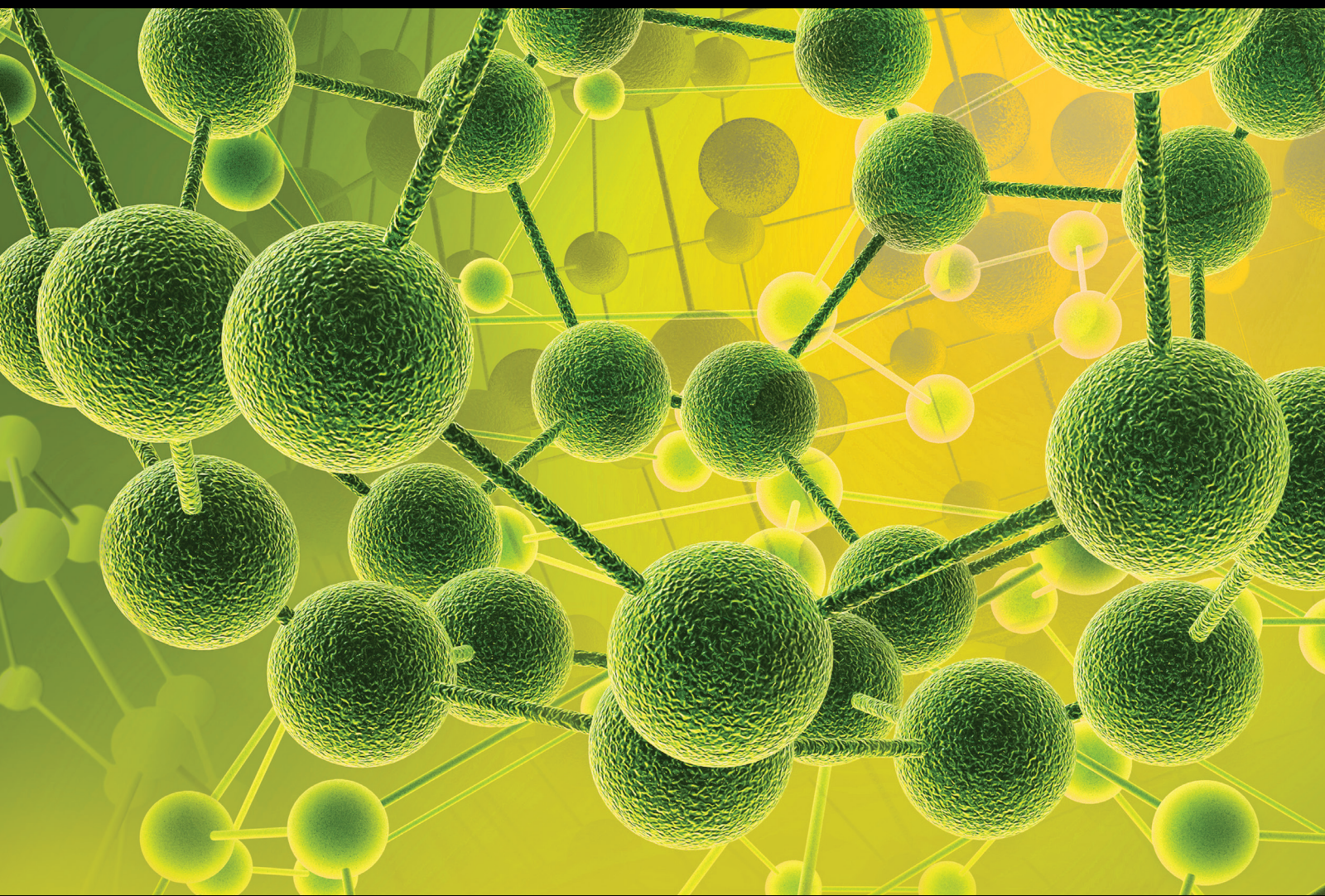

Extraction/Preconcentration Procedures for Determination of Metal and Organometallic Species in Environmental, Biological, and Food Samples

International Journal of Analytical Chemistry

Extraction/Preconcentration Procedures for Determination of Metal and Organometallic Species in Environmental, Biological, and Food Samples

Lead Guest Editor: Marcela Corazza
Guest Editors: Vanessa Egea and Seyyed E. Moradi

Editorial Board

Contents

Hindawi
International Journal of Analytical Chemistry
Volume 2019, Article ID 9465432, 2 pages
https://doi.org/10.1155/2019/9465432

Editorial

Extraction/Preconcentration Procedures for Determination of Metal and Organometallic Species in Environmental, Biological, and Food Samples

Marcela Zanetti Corazza,[1] **Vanessa Egea dos Anjos**,[2] **and Seyyed E. Moradi**[3]

[1]*Faculty of Science and Technology, Federal University of Grande Dourados, Brazil*
[2]*Chemistry Department, State University of Ponta Grossa, Brazil*
[3]*Pharmaceutical Sciences Research Center, Faculty of Pharmacy, Mazandaran University of Medical Sciences, Sari, Iran*

Correspondence should be addressed to Marcela Zanetti Corazza; mazcorazza@yahoo.com.br

Received 2 December 2018; Accepted 2 December 2018; Published 1 January 2019

The development of analytical methods for the determination of trace metals and some organometallic species from complex matrices employing different sample preparation procedures, such as extraction/preconcentration, as well as alternative adsorbent materials, yet is the major challenge for researchers. In addition, the chemical speciation is currently a very important form to enlarge the perspective for environmental, biological, food, and medicinal applications, since toxicity, bioavailability, mobility, and other critical properties of the trace elements depend on this different chemical forms and species in the sample medium. In this special issue on analytical methods of extraction/preconcentration, 6 papers reported different sample preparation for several metals from simple to complex matrix such as geological samples.

One paper published in this special issue reports the application of a novel nanocomposite of nanoporous gold nanoparticles (np-AuNPs) functionalized with 2,2,6,6-tetramethyl-1-piperidinyloxy radical (TEMPO) by the bridge of carboxylate-zirconium-carboxylate chemistry as sensor for the electrochemical detection of H_2O_2 at a trace level. In this work, besides demonstrating a strategy for producing large specific surface area nanoporous gold nanoparticles and TEMPO-functionalized np-AuNPs nanocomposite, the electro-oxidation of H_2O_2 with a high density of radicals on the TEMPO-np-AuNPs surface is also investigated. The new probe constructed by combination of 4-Carboxy-TEMPO and np-AuNPs shows a double effective enhancement in the electrochemical detection of H_2O_2 and wide linear range for H_2O_2 detection due to the enzyme-like activity. The sensor had low detection limit, high sensitivity, low cost, anti-interference, good reproducibility, and stability of this nanocomposite with TEMPO-based ligand, contributing to improve the detection of current signal of H_2O_2.

Another paper published in this special issue reports the development of a simple, effective, environment-friendly and sensitive analytical method for trivalent antimony determination employing single drop microextraction (SDMM) in water samples. In this work [C4mim][PF6] was employed as the extraction solvent and BPHA was used as the complexing agent making it an analytical method of low cost, simple device, easy operation, and high enrichment efficiency and using low amounts of organic solvent. The use of ionic liquid has been explored in SDME since it does not have detectable vapor pressure, can extract metal ions at room temperature, and avoid several safety problems. So, the introduction of BPHA-[C4mim][PF6] system was not only ecofriendly compared with traditional organic solution, but also efficient for extraction.

In addition, exploring the synthesis and application of materials with ability to preconcentrate metals as well as identify and distinguish different molecules, the paper "Host–Guest Extraction of Heavy Metal Ions with p-t-butylcalix[8]arene from Ammonia or Amine Solutions" reports the behavior and ability of calixarenes (macrocyclic

phenolic oligomers) as specific receptor in the extraction of metal ions and/or molecules by modification of the hydroxyl functional group and/or by creating a new cavity size. In calixarenes, the cavity size, position and type of donor groups, and molecular flexibility lead to their high potential for the complexation and extraction of metal ions. It should be noted that the extraction of metal demonstrated to be much higher in some metals when ammonia was used as the aqueous phase.

The fourth paper reported in this special issue "Selective Preconcentration of Gold from Ore Samples" brings the theme of the development of an analytical methodology employing SPE for determination/preconcentration of gold in ores samples. This paper reports the use of an adsorbent Amberlite XAD-16 and N, N-diethyl-N′-benzoylthiourea (DEBT), a selective chelating agent that allowed the selective preconcentration of gold ions from ore samples. It is important to emphasize that low abundance and heterogeneous distribution of gold ions in ore samples require accurate and reliable analytical procedures for its determination. Thus, the accuracy of the proposed method was evaluated by the analyses of two geological samples: Cu-ore and Gold ore (MA-1b) as a certified reference material and the results demonstrated good agreement with the given values. Although there are more sensitive methods applied to similar samples, the proposed method allowed a preconcentration selective of gold ions without any matrix interference using an instrumental technique simple and of low cost (FAAS) when compared to techniques as ICP-MS and GF AAS.

The speciation of Ni in environmental samples has been explored for several years due to carcinogenic potential of water-soluble nickel compounds and nickel tetracarbonyl. However, the analytical techniques for its determination are not always available or easy to use since their limits are threshold values relative to the single species. More specifically, the speciation of Nickel in workplaces airborne particulate is the most important for the assessment of the respiratory health risks. The paper "Development of a New Sequential Extraction Procedure of Nickel Species on Workplace Airborne Particulate Matter: Assessing the Occupational Exposure to Carcinogenic Metal Species" reports a speciation analysis of inorganic Ni compounds such as soluble, sulfidic, metallic, and oxide fractions in airborne particulate matter using a simple selective sequential extraction as sample preparation and analysis by Atomic Absorption Spectroscopy without long evaporation phases. Among the good results obtained by the proposed method stand out the small volumes of solutions and the absence of long evaporation phases. And the last paper published in this special issue, "Simultaneous Determination of Cr, As, Se, and Other Trace Metal Elements in Seawater by ICP-MS with Hybrid Simultaneous Preconcentration Combining Iron Hydroxide Coprecipitation and Solid Phase Extraction Using Chelating Resin", highlights the benefits of the hybrid preconcentration combing iron hydroxide coprecipitation and solid phase extraction using chelating resin for determination of the oxo-anion forming elements such as Cr, As, and Se and other trace metal elements (Ti, V, Co, Ni, Cu, Zn, Zr, Ge, Cd, Sb, Sn, W, Pb, and U) in seawater, whose standard and guideline values were established in environmental quality standards for water pollution in Japan. In addition, the hybrid preconcentration besides demonstrated recoveries of oxo-anion-forming elements higher than single solid phase extraction using chelating resin (InertSep ME2,60-70 μm in diameter, GL Science Inc., Tokyo, Japan) allowed an extraction in a single pH adjustment (pH 6.0) due to groups functional in the resin surface, such as iminodiacetic acid (pKa=2.98) and dimethylamino (pKa=10.77) groups.

Conflicts of Interest

I, Marcela Zanetti Corazza, Lead Guest Editor of Special Issue (Extraction/Preconcentration Procedures for Determination of Metal and Organometallic Species in Environmental, Biological and Food Samples) in the International Journal of Analytical Chemistry, declare there are no conflicts of interest.

Marcela Zanetti Corazza
Vanessa Egéa dos Anjos
Seyyed E. Moradi

Hindawi
International Journal of Analytical Chemistry
Volume 2018, Article ID 3812795, 9 pages
https://doi.org/10.1155/2018/3812795

Research Article

Development of a New Sequential Extraction Procedure of Nickel Species on Workplace Airborne Particulate Matter: Assessing the Occupational Exposure to Carcinogenic Metal Species

Catalani Simona,[1] Fostinelli Jacopo ,[1] Gilberti Maria Enrica,[1] Orlandi Francesca,[1] Magarini Riccardo,[2] Paganelli Matteo,[1] Madeo Egidio,[1] and De Palma Giuseppe[1]

[1] *Unit of Occupational Health and Industrial Hygiene, Department of Medical and Surgical Specialties, Radiological Sciences and Public Health, University of Brescia, Italy*
[2] *PerkinElmer (Italia), Milano, Italy*

Correspondence should be addressed to Fostinelli Jacopo; j.fostinelli@unibs.it

Received 5 July 2018; Revised 10 October 2018; Accepted 30 October 2018; Published 2 December 2018

Guest Editor: Seyyed E. Moradi

Nickel (Ni) compounds and metallic Ni have many industrial and commercial applications, including their use in the manufacturing of stainless steel. Due to the specific toxicological properties of the different Ni species, there is a growing interest about the availability of analytical methods that allow specific risk assessment, particularly related to exposure to the Ni species classified as carcinogenic. In this paper, we described a speciation method of inorganic Ni compounds in airborne particulate matter, based on selective sequential extractions. The analytical method reported in this paper allows the determination of soluble, sulfidic, metallic, and oxide Ni by a simple sequential extraction procedure and analysis by Atomic Absorption Spectroscopy using small volumes of solutions and without long evaporation phases. The method has been initially set up on standard laboratory mixtures of known concentrations of different Ni salts. Then it has then been tested on airborne particulate matter (powder and filters) collected in different workstations of a large stainless steel production facility. The method has occurred effectively in the comparison of the obtained results with occupational exposure limit values set by the main international scientific and regulatory agencies for occupational safety and health, in order to prevent both toxic and carcinogenic effects in humans.

1. Introduction

Nickel (Ni) compounds and metallic Ni have many industrial and commercial applications, including their use in stainless steel production, in a large series of metal alloys, as catalysts, in batteries, pigments, and ceramics [1]. An industrial sector in which Ni exposure can be particularly relevant is the production of special stainless steel in secondary steel foundries: the workers engaged in this industry are potentially exposed to various forms of airborne Ni, in particular during the operations of melting and casting and at all the stages of the process characterized by the need for high temperatures [2, 3]. This kind of production has been widespread for decades in northern Italy, involving thousands of workers and consequently arousing high interest on the related occupational and public health issues. The toxicological properties of Ni compounds yet represent an important challenge in terms of risk assessment and are also of great concern for the necessary enforcement of preventive measures in exposed workers [4, 5].

Exposure to Ni oxides and sulfides, which have low solubility in water, has been recognized as one of the prominent causes for occupational Ni-related lung and nasal cancer [6, 7].

The carcinogenic potential of water-soluble Ni compounds and Ni tetracarbonyl has been continuously discussed for decades [8]. Although there is no evidence that exposure to metallic Ni increases the risk of respiratory

cancer, it is well known as the most important sensitizer among metal elements [9–12].

In 1990, the International Agency for Research on Cancer (IARC) concluded that there were sufficient evidences in humans for the carcinogenicity of Ni sulfate and of combinations of Ni sulfide and oxides in the Ni refining industry [13]. In 2012, with specific referral to the inhalator exposure route, IARC updated the evaluation classifying Ni compounds as "carcinogenic to humans-group 1", whereas metallic Ni and Ni alloys were categorized as "possibly carcinogenic to humans-group 2B", specifically for cancer of the lung and the nasal cavity [14].

The current understanding of the carcinogenic potential of the most prominent Ni species in sulfidic Ni (Ni subsulphide (Ni_3S_2), Ni oxide (NiO), Ni metal (Ni^0), and soluble Ni (primarily Ni sulfate, $NiSO_4$) has been determined through studies based on a combination of animal testing (of pure compounds) and human epidemiological data [15].

Due to the above-mentioned reasons, the speciation of Ni in workplaces' airborne particulate is of the utmost importance for the assessment of the respiratory health risks.

Regarding occupational exposure limits, different threshold levels for Ni and Ni compounds in workplaces and emissions are available (Table 1). In 1998 the American Conference of Governmental Industrial Hygienists (ACGIH) published separated threshold values for the organic and inorganic forms of Ni [16]. In doing so it was recognized that different Ni species had different toxic and carcinogenic properties [17].

In the "Recommendation from the Scientific Committee on Occupational Exposure Limits" for Ni and inorganic Ni compounds", by the European SCOEL, some occupational exposure limits (OELs) aiming to protect both from inflammatory effects in the lung and from cancer were published [18].

The determination of the total concentration of Ni, accordingly, gives no information about environmental risks or knowledge of the various forms, which makes monitoring of specific chemical species of Ni in environmental samples, such as airborne particulates, extremely important [19]. Consequently, the development of analytical techniques for the determination of various compounds of metallic elements in environmental samples, such as ambient aerosols, is presently one of the most challenging tasks for environmental analytical chemistry [20, 21].

Ni determination can be performed with various analytical techniques, including spectrophotometry, atomic absorption spectrometry (FAAS and ETAAS), inductively coupled argon plasma optical emission spectrometry (ICP-OES), inductively coupled plasma mass spectrometry (ICP-MS) and voltammetry. In the past two decades many techniques have been widely developed for the speciation of inorganic contaminants in environmental samples [22, 23]. Several of them make use of sequential extraction schemes to determine the metal distribution over different fractions, usually including species such as soluble, sulfidic, metallic, and oxide fractions. The application of sequential extraction procedures provides relevant environmental information.

Several of the sequential extraction procedures found in the literature are variants of the method proposed by Zatka et al. in the early 1990s [24] in which the solubility of the different fractions was utilized for the sequential determination of Ni ions.

The procedure of Zatka involves a sequential leaching of airborne dust from Ni production sites and Ni-using workplaces by using ammonium citrate, hydrogen peroxide/ammonium citrate, and bromine-methanol. Acceptable recoveries were obtained, for most species better than 95%.

Up to now, the sequential extraction procedure proposed by Zatka has mainly been applied for speciation of Ni in work-room air (for instance, in Ni refinery) present at mg/m^3. These levels however, obtaining correct results for the concentrations of trace elements in out-door air at ng/m^3 levels, are still a great concern, mainly due to the extremely small amounts of sample and analyte.

2. Aims

In consideration of the toxicological properties of Ni compounds, this paper describes a modified method which is mainly based on the fractionation proposed by Zatka et al. [25] but achieving both time optimization and greater sensitivity. The method has been first setup on a mix of different Ni species. Subsequently, the method has been applied on airborne particulate matter sampled in different departments of a steel production facility, in order to assess the airborne levels of different Ni species.

3. Materials and Methods

3.1. Reagents. All chemicals used were of analytical grade. The water used was bidistilled water, for inorganic trace analysis (Merck KgaA, Darmstadt, Germany).

The reagent in the solution for the elution of different Ni species from the filters was as follows:

(A) Ammonium citrate solution: 1.7% ammonium hydrogen citrate and 0.5% citric acid solution, the solution was prepared by dissolving 1.7g of diammonium hydrogen citrate ($(NH_4)2H$-Cit)), CAS No. 3012-65-5, Carlo Erba, Milan, Italy) and 0.5 g of citric acid (99%, $C_6H_80_7$, Sigma Aldrich, Saint Louis, Missouri, USA) in 100ml of bidistilled water.

(B) H_2O_2 citrate: ammonium citrate 0.1M and hydrogen peroxide 30% (w/w) ratio 2:1 (H_2O_2, CAS No. 7722-84-1 Sigma Aldrich, Saint Louis, Missouri, USA).

(C) Methanol-bromine solution: methanol (CH_3OH, Chromasolv ≥99.9%, CAS No. 67-56-1, Honeywell, Thermo Fisher Scientific); Bromine (Br_2, CAS No. 7726-95-6 Sigma Aldrich, Saint Louis, Missouri, USA), 50:1.

(D) Nitric and hydrochloric acid solution: nitric acid (HNO_3 70%, CAS No. 7697-37-2 Sigma Aldrich, Saint Louis, Missouri, USA) and hydrochloric acid (HCl 37%, CAS No. 7647-01-0 Sigma Aldrich, Saint Louis, Missouri, USA) ratio 1:1.

The mixture of Ni compounds was prepared by several salts: Ni(II) sulfate hexahydrate ($NiSO_4$, PM 262.7, reagent plus® 99.99%, CAS No. 7786-81-4 Sigma Aldrich, Saint Louis,

Table 1: Ni species, with chemical formulas, solubility characteristics, 8h-TWA occupational exposure limits proposed by international agencies, and hazard statements assigned by the EU CLP Regulation, ACGIH, SCOEL, and OSHA.

Nickel Species		*Solubility in water (g/100ml) [temperature]*	*CAS Number*	*ACGIH*	*SCOEL*	*OSHA*	*CLP*
Nickel Sulfate	$NiSO_4$	65.5 [0°C]	7786-81-4	A4 0.1 mg/m^3 (Ni Sol)	0.01 mg/m^3 #	-	H351
Nickel subsulphide	Ni_3S_2	poorly soluble	12035-72-2	A1 0.1 mg/m^3	0.005 mg/m^3§ 0.01 mg/m^3 #	0.1 mg/m^3 (Ni insol)	H350i
Nickel monoxide	NiO	poorly soluble	1313-99-1	A1 0.2 mg/m^3 (Ni insol)	0.005 mg/m^3§ 0.01 mg/m^3 #	0.1 mg/m^3 (Ni insol)	H350i
Metallic nickel	Ni	poorly soluble	7440-02-0	A5 1.5 mg/m^3	0.005 mg/m^3§	0.5 mg/m^3	H351

#Inhalable fraction; §respirable fraction.

Table 2: AAS instrumental parameters for determination of Ni

Operating conditions	
Primary source	Nickel Hollow Cathode lamp (Agilent Technologies)
Lamp current	5 mA
Analytical wavelength	232 nm
Background correction system	Zeeman effect based (Transversal)
Slit width	0.2 nm
Mode	Absorbance (peak height)
Graphite furnace operation	
Atomization tube	Partition tubes (coated)-GTA (Agilent Technologies)
Sheath/Purge gas	Argon (Ar) of 99.999% purity
Sample Injection (sample, μL)	30

Missouri, USA), Ni sulfide (Ni_3S_2, 99.7%, PM 240.1 CAS No. 12035-72-2 Sigma Aldrich, Saint Louis, Missouri, USA), Ni powder (PA 58.7, 100mesh, 99.999%, CAS No. 7440-02-0 Sigma Aldrich, Saint Louis, Missouri, USA), and Ni(II)oxide (NiO, PM 74.7, 99.999%, CAS No. 1313-99-1 Sigma Aldrich, Saint Louis, Missouri, USA).

The sequential leaching was carried out in an all hydrophilic Teflon filter holder (DigiFILTER 0.45 micron, SCP Science, Quebec, Canada); the holder was fitted with a 25mm (5μm) PVC filters (SKC Inc. 25mm, 5.0μm) (Figure 1). The filtrates are collected in a test tube (DigiTUBEs 50ml, SCP Science, Quebec, Canada).

A 0.45 micron Teflon membrane inserted in every DigiFILTER guarantees 98% particle retention.

The DigiFILTERs were connected to a vacuum pump; the filtering system is set up so that mild suction can be turned on and off at short intervals if required.

Figure 1: Filter device utilized for sequential extraction of Ni's fractions (DigiFILTER 0.45 micron, SCP Science, Quebec, Canada).

3.2. Determination of Nickel. The determination of different fraction of Ni were performed by atomic absorption spectrometry (AAS Spectra 400 Varian, Medical Systems, Inc. Palo Alto, CA) equipped with a transversal Zeeman-effect background correction system and an auto sampler was used for all measurements. The instrumental operating parameters of the AAS apparatus are reported in Tables 2 and 3.

Table 3: Temperature program of the AAS method for determination of nickel.

Step N°	Temperature °C	Time (sec)	Flow (L/min)	Type of gas
1	40	5.0	3.0	Argon
2∗	150	35.0	3.0	Argon
3∗	150	5.0	3.0	Argon
4^{α}	900	10.0	3.0	Argon
5^{α}	900	15.0	3.0	Argon
6^{α}	900	2.0	0.0	
7^{β}	2400	1.0	0.0	
8^{β}	2400	2.0	0.0	
9	2500	1.0	3.0	Argon
10	2500	2.0	3.0	Argon

∗Drying step, $^{\alpha}$pyrolysis step, and ^{B}atomizing step.

Table 4: Results of dissolution of different nickel fractions (N∘=3).

Nickel Species	Solution	Treatment	Aspect	Ni expected(mg)	Ni determined(mg)	% extracted
$NiSO_4$	ammonium citrate (Sol A)	10mL, 37°C, 60min	clear	1.6	1.70±0.1	102%
	H_2O_2 citrate: ammonium citrate (Sol B)	10mL, ΔT, 60min	clear	2.3	2.1±0.2	91%
	solution methanol:Bromine (solution C)	10mL, ΔT, 2h	clear	1.8	1.6±0.1	89%
	Solution HCl: HNO_3 1:1 (Sol D)	4mL, 70°C, 30min	clear	2.6	2.7±0.3	103%
Ni_3S_2	ammonium citrate (Sol A)	10mL, 37°C, 60min	residue	10.8	0.31±0.1	0.03%
	H_2O_2 citrate: ammonium citrate (Sol B)	10mL, ΔT, 60min	clear	7.6	7.4±1.1	96%
	solution methanol: Bromine (solution C)	10mL, ΔT, 2h	clear	8.0	8.3±0.8	103%
	Solution HCl: HNO_3 1:1 (Sol D)	4mL, 70°C, 30min	clear	7.4	8.8±1.2	118%
Ni (0) metallic	ammonium citrate (Sol A)	10mL, 37°C, 60min	residue	4.6	/	/
	H_2O_2 citrate: ammonium citrate (Sol B)	10mL, ΔT, 60min	residue	12.2	0.5±0.1	4%
	solution methanol: Bromine (solution C)	10mL, ΔT, 2h	clear	8.7	9.2±1.1	105%
	Solution HCl: HNO_3 1:1 (Sol D)	4mL, 70°C, 30min	clear	13.4	15.7±2.3	117%
NiO	ammonium citrate (Sol A)	10mL, 37°C, 60min	residue	7.0	/	/
	H_2O_2 citrate: ammonium citrate (Sol B)	10mL, ΔT, 60min	residue	13.4	0.1±0.1	1%
	solution methanol: Bromine (solution C)	10mL, ΔT, 2h	residue	7.4	/	/
	Solution HCl: HNO_3 1:1 (Sol D)	4mL, 70°C, 30min	clear	10.4	11.8±3.2	114%

Ni stock standard solutions was prepared from 1 mg/mL (1000ppm) of standard solution (Ni(0) in 2% HNO_3, O2Si smart solution, Charleston, USA). Working solutions at 0.05; 0.1; and 0.5 mg/L were prepared by serial dilution in bidistilled water of the standard at 1000 mg/L solution (0.05ppm, 0.1ppm, and 0.5ppm).

The accuracy of the method was evaluated by analyzing certified reference materials (NIST 1643e-1643d trace elements in water for ultrafiltrate).

Instrumental limit of detection (LOD) of the total Ni, calculated as three standard deviations of the background signal obtained on 10 blank samples, was equal to 1 μg/L.

The limit of quantification (LOQ) of the total Ni, calculated as ten standard deviations of the background signal obtained on 5 blank samples, was equal to 3 μg/L.

The relative standard deviation (RSDs) of measurements of Ni solutions was between 5 and 10 %.

3.2.1. Extraction Tests. A little amount of all the Ni salts was treated in falcon with one leaching solution at a time and then the concentration of Ni was then determined.

To facilitate the dissolution the falcons were placed in an ultrasonic bath for 5 minutes.

Several tests have been carried out to evaluate different extraction conditions by using different volumes of solutions, times and temperatures (date not shown). The best conditions are reported in Table 4 which illustrates the composition of the solutions, conditions of the extractions, dissolution of the salts, and the recovery of Ni fraction.

The Ni soluble fraction was effectively extracted by all the solutions. The sulfidic fraction was not solubilized by solution A, while it was dissolved by other solutions. The metallic fraction was well extracted by solution C and D. The Ni oxide is solubilized only by a solution HCl:HNO_3 (1:1); the leaching with the other solutions does not show traces of Ni in solutions.

Table 5: Extraction of specific Ni's compounds in two mixtures of powders. For each Ni species the percentage of recovery with respect to the Ni salt added is reported.

Ni species	Mixture A			Mixture B		
	Ni added (mg)	Ni found (mg)	%	Ni added (mg)	Ni found (mg)	%
$NiSO_4$	0.016	0.013	81	0.054	0.049	91
Ni_3S_2	0.096	0.080	83	0.310	0.290	93
Ni(0)	0.114	0.11	96	0.367	0.371	101
NiO	0.064	0.065	102	0.207	0.220	106

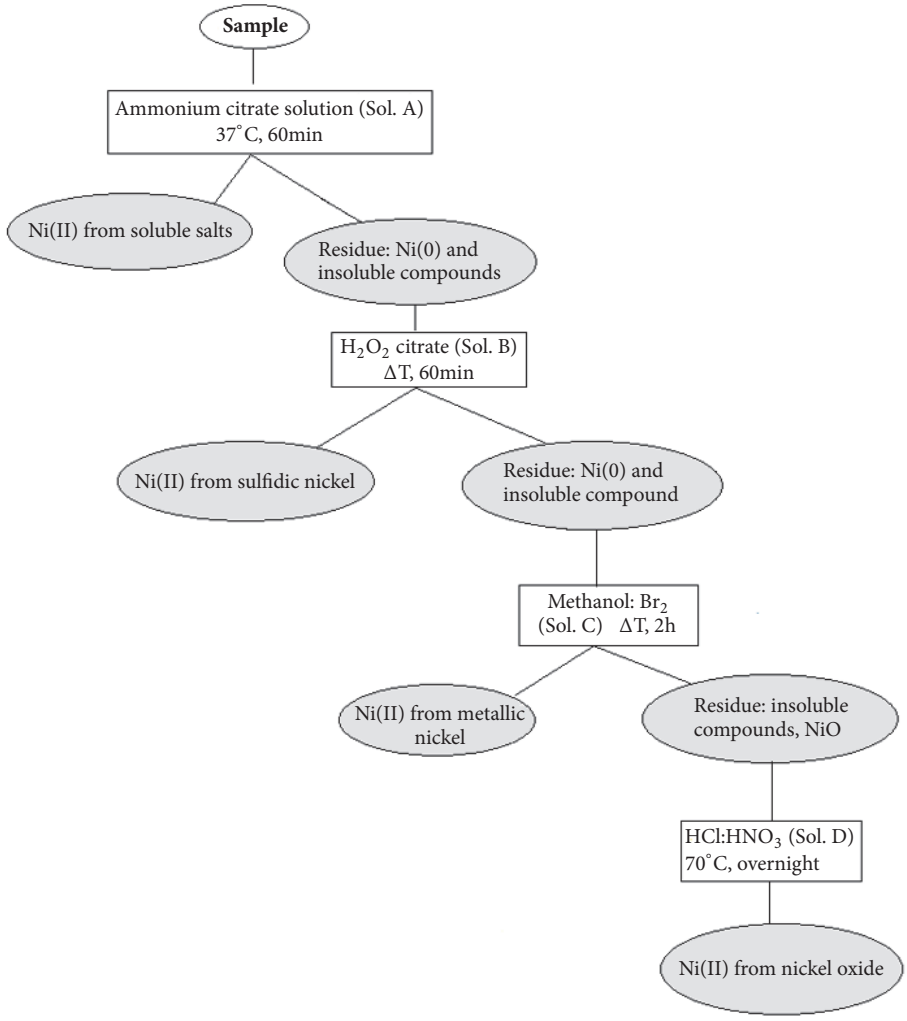

Figure 2: Selective sequential solubilization of inorganic Ni compounds: scheme of the procedure.

The same procedure was carried out on all the solutions (A, B, C, D) without the addition of Ni salts.

3.3. Speciation Procedure. In order to have Ni concentrations nearer to those found in real samples, each Ni compound was homogenously dispersed and grinded in an agate mortar.

The final mixed salts contained 10.4 mg $NiSO_4$ equal to 2.3 mg as Ni, 18.5 mg Ni_3S_2 equal to 113.3 mg as Ni, 15.8 mg Ni(0), and 11.3 mg NiO equal to 8.9 mg as Ni.

Quantities ranging from 1 to 2 mg of the mix weighed to the 5th decimal were deposited in a PVC filter placed on the DigiFILTER (Mix A = 0.4 mg; Mix B = 1.3 mg).

The sequential extraction procedures are illustrated in Figure 2 and the results in Table 5.

3.4. Determination of Soluble Nickel. Add 10mL of ammonium citrate solution (solution A) in DigiFILTER inserted on a falcon; place the DigiFILTER in the oven at 37°C for 60

Table 6: Determination of Ni's fraction in powders (μg/g) and environmental samples (μg/m^3) collected in the departments of the steel production facility.

Powder (μg/g)	**$NiSO_4$**	**Ni_3S_2**	**Ni(0)**	**NiO**	**Σ**	**Ni Tot AAS**
A (1.2 mg)	/	/	145	196	341	423
B (1.1 mg)	2727	395	745	6673	10540	11509
C (0.1mg)	/	/	323	356	679	695
D (1.0 mg)	580	232	2180	4440	7432	7538
Filters (μg/m^3)	**$NiSO_4$**	**Ni_3S_2**	**Ni(0)**	**NiO**	**Σ**	**Ni Tot AAS**
Filter A	0.32	0.07	0.64	1.5	2.53	2.81
Filter B	0.25	0.67	0.94	1.0	2.86	3.12
Filter C	0.76	0.28	1.6	3.5	6.14	6.44
Filter D	0.87	0.73	4.0	5.0	10.6	10.88
Filter E	0.89	0.24	0.55	1.3	2.98	3.50

minutes. With a vacuum pump, draw the solution into the falcon and keep it for the determination of the soluble Ni fraction. Insert a new falcon in the DigiFILTER.

3.5. Determination of Sulfidic Nickel. To the filter from which soluble Ni phases have been leached out add 10mL of the solution H_2O_2 citrate: ammonium citrate (solution B). Keep at room temperature for 60 minutes under a hood.

With a vacuum pump, draw the solution into the falcon and keep it for the determination of the sulfidic Ni fraction. Insert a new falcon in the DigiFILTER.

3.6. Determination of Metallic Nickel. To the filter from which soluble and sulfidic Ni phases have been leached out add 10mL of the solution methanol:bromine (solution C). Keep at room temperature for 2 hours. With a vacuum pump, draw the solution into the falcon and keep it for the determination of the metallic Ni. Insert a new falcon in the DigiFILTER.

3.7. Determination of Oxide Nickel. To the filter from which the first Ni's fraction have been leached, add 5mL of solution HCl:HNO_3 (solution D) and keep at room temperature overnight under the hood. With a vacuum pump, draw the solution in the new falcon. Transfer the filter from the support into the falcon and add another 5 mL of HCl:HNO_3 and heat in a water bath at 70°C for 15 minutes.

4. Application of Sequential Leaching to Real Samples

4.1. Sampling Site and Equipment. The sampling was performed in a steel foundry plant specialized in stainless steels for naval and aerospace industry; the production cycle is based on an electric arc furnace with subsequent casting in a continuous plant. The melting is essentially performed in a three-phase furnace equipped with three graphite electrodes. The different qualities of steel are obtained by mixing recycled scrap with chromium, Ni, and other raw materials. Through the refining in the ladle furnace, specific compositions and quality of the steel are reached (the exact composition of the alloy is proprietary information).

In order to characterize occupational exposure to airborne Ni compounds, we carried out a characterization of Ni species collected on two different types of substrate:

(1) Particulate collected through an IOM (Institute of Occupational Medicine) sampler (SKC Inc.) on PVC membrane filters (diameter: 25 mm; porosity 0.5 μm), according to Italian standards [26]. The sampling time of the inhalable fraction ranged from three to six hours in each location.

(2) Samples of deposition powders generated by industrial processes.

All samples were collected in production areas subjected to possible Ni airborne exposure, i.e., the ladle furnace, the continuous casting area, and the electric arc furnace.

5. Leaching and Results

The speciation procedure described in this paper was applied to real samples of environmental dust and filters.

A small amount of collected powder (in the order of a few mg) was placed on a PVC filter and treated with the sequential leaching described above. The results of speciation are reported in Table 6.

The analysis was also carried out on a PVC filter clean to control any forms of contamination.

In all the samples, the most represented species was NiO (35-63%), followed by metallic Ni (7-48%); the soluble and sulfidic fractions were equally distributed (8-30% and 3-23%, respectively). In two samples of powders (A and C) the soluble and sulfidic fractions were not detectable.

In all remove samples, the sum of the different Ni fractions was comparable with the amount of total Ni. The sum of the fraction was slightly lower than total Ni measured in AAS, and the difference was comprised between 1.4 and 19.4%.

At each analysis set, a sample of weighed salts mix is extracted in parallel to verify the quality and effectiveness of the extraction. The quality of determination of total Ni was checked with certified material (NIST 1640, metallic elements in water).

6. Discussion

The speciation of Ni in environmental air samples has been debated for several years, since there are threshold limits values relative to the single species but the analytical techniques for determining them are not always available or easy to use. The speciation of Ni can be obtained through chemical leaching and subsequent analysis of the solutes with traditional methods of Ni determinations or by X-ray determination [27]. In the literature several authors have tried to standardize the leaching process and the contrasting results demonstrate the high variability of the method.

The first available method was published by Zatka et al. [28], which, through several washings and dry evaporations, determines the soluble Ni fraction, the sulfidic Ni, the metallic Ni, and the oxide in sequence with a relative standard deviation (RSD) ranged from 3.2 to 3.7%.

Over the years, other authors have tried to replace by using different solutions. Bolt et al. [28] have developed an inline system for extracting soluble Ni compounds (with ammonium citrate buffer), Ni sulfide (with ammonium citrate and hydrogen peroxide), and metal Ni (with CuCl2 / KCl). The final digestion of the residues on the membrane with HNO_3/HCl leads to the determination of the Ni oxide fraction. The method is based on the one developed by Zatka but requires much less time in execution. In 2003, Profumo et al. [29] reported a method of speciation based on sequential extraction. The authors succeeded in speciating Ni metal and soluble Ni compounds, such as sulfate and chloride and among from the insoluble Ni oxide and sulfide. The Ni recoveries of the different species were in the range 94/99%.

Also Conard et al. [30] tried to improve the sequence of Zatka especially in the separation step of the Ni sulfide/metal phases with leaching with ammonium citrate and hydrogen peroxide increasing the volume of the solution, time, and percolation methods. Despite the studies and tests to date, there is no standardized extraction method to carry out the chemical speciation of Ni, and the proposed methods are difficult to apply on environmental samples.

Our study allowed us to overcome some of the prominent methodological limits of the previously described speciation techniques: the excessive length of the extraction phase and the powder leak during the leaching process.

This method is based on the different solubility based on the different chemical-physical properties of the inorganic Ni species which allow a sequential extraction of the fraction and a determination of Ni.

The test on all the solutions of each single fraction shows how the solutions selectively dissolve the inorganic Ni species.

$NiSO_4$, more soluble compound, is dissolved by all four solutions with an efficacy ranging from 89 to 103%, while the less soluble Ni dissolves only in a solution of HNO_3 and HCl 1:1.

Compared to the previously published methods we reduced the overall volume of the solvents used to only 10 mL, therefore avoiding the evaporation phase and the issues related to the retaining of the solutes. Previous tests on the same sequence of leaching conducted on a filter placed on a simple vacuum extraction device led to very low retaining rates in the order of 50% (date not shown); the adoption of DigiFILTER devices allowed to improve the retaining rate (reaching 94-99%) probably preventing the loss of small particles independently from the different Ni species.

The determination of species of Ni in real powder or filter allowed identifying the different species associated with the different samples.

In all remove samples, the sum of the different Ni fractions was comparable with the amount of total Ni. The sum of the fraction was slightly lower than total Ni measured in AAS; the difference was comprised between 1.4 and 19.4%.

Moreover, taking into account the great progress that has been made in the identification of new health related particle size exposure assessment, the methods described in this paper could also be applied in analyzes carried out on particulate ultrafine material [31]. The value of inhalable Ni aerosols monitoring by species has been widely demonstrated in a variety of working environments as a fundamental tool in assessing respiratory cancer risk [32, 33]. A species-specific approach to setting occupational exposure limits guarantees that the best available health and exposure data will be used. Future research may lead to consideration of setting species-specific OELs on the basis of certain subfractions of inhalable Ni aerosols.

Better Ni speciation techniques will improve the capability of assessing the occupational exposure to carcinogens together with both the measurement of the inhalable fraction and the particle size distribution, as expected and hoped in previous studies [34].

7. Conclusion

The analytical method described in this paper allows the determination of soluble, sulfidic, metallic, and oxide Ni by a simple sequential extraction procedure and determination by Atomic Absorption Spectroscopy using small volumes of solutions and without long evaporation phases. For the purpose of assessing occupational exposure to carcinogens, the method developed allowed the separation and speciation of the different Ni species on the inhalable fraction of the airborne particulate sampled in different working environments.

The speciation of Ni in real environmental samples allowed us to compare our results with the TLVs proposed by the different agencies and regulations, which is not possible with the sole determination of the total metallic Ni.

Data Availability

All the data from determinations of Ni species in powders and filters, used to support the findings of this study, are included within the article.

Conflicts of Interest

The authors declare no conflicts of interest.

Acknowledgments

The study was supported by University of Brescia.

References

[1] C. Klein and M. Costa, "Nickel," in *Handbook on the Toxicology of Metals*, Academic Press, Waltham, MA, USA, 4th edition, 2014.

[2] M. A. Riaz, A. B. T. Akhtar, A. Riaz, G. Mujtaba, M. Ali, and B. Ijaz, "Heavy metals identification & exposure at workplace environment its extent of accumulation in blood of iron & steel recycling foundry workers of Lahore, Pakistan," *Pakistan Journal of Pharmaceutical Sciences*, vol. 30, no. 4, pp. 1233–1238, 2017.

[3] NiDI (Nickel Development Institute), *Safe Use of Nickel in the Workplace*, Nickel Development Institute, Toronto, Canada, 2nd edition, 1997.

[4] H. Lu, X. Shi, M. Costa, and C. Huang, "Carcinogenic effect of nickel compounds," *Molecular and Cellular Biochemistry*, vol. 279, no. 1-2, pp. 45–67, 2005.

[5] M. Costa, "Molecular mechanisms of nickel carcinogenesis," *Biological Chemistry*, vol. 383, no. 6, pp. 961–967, 2002.

[6] D. Beyersmann and A. Hartwig, "Carcinogenic metal compounds: recent insight into molecular and cellular mechanisms," *Archives of Toxicology*, vol. 82, no. 8, pp. 493–512, 2008.

[7] D. G. Barceloux, "Nickel," *Journal of Toxicology - Clinical Toxicology*, vol. 37, no. 2, pp. 239–258, 1999.

[8] L. T. Haber, L. Erdreicht, G. L. Diamond et al., "Hazard identification and dose response of inhaled nickel-soluble salts," *Regulatory Toxicology and Pharmacology*, vol. 31, no. 2, pp. 210–230, 2000.

[9] M. G. Ahlström, J. P. Thyssen, T. Menné, and J. D. Johansen, "Prevalence of nickel allergy in Europe following the EU Nickel Directive – a review," *Contact Dermatitis*, vol. 77, no. 4, pp. 193–200, 2017.

[10] M. Saito, R. Arakaki, A. Yamada, T. Tsunematsu, Y. Kudo, and N. Ishimaru, "Molecular mechanisms of nickel allergy," *International Journal of Molecular Sciences*, vol. 17, no. 2, article no. 202, 2016.

[11] P. Apostoli and S. Catalani, "Mechanisms of action for metallic elements and their species classified carcinogen R 45 and R 49 by EU," *Giornale Italiano di Medicina del Lavoro ed Ergonomia*, vol. 30, no. 4, pp. 382–391, 2008.

[12] J. Zhao, X. Shi, V. Castranova, and M. Ding, "Occupational toxicology of nickel and nickel compounds," *Journal of Environmental Pathology, Toxicology and Oncology*, vol. 28, no. 3, pp. 177–208, 2009.

[13] IARC, "Chromium, Nickel, and Welding," in *Monographs on the Evaluation of Carcinogenic Risks to Humans*, vol. 49, IARC, Lyon, France, 1990.

[14] IARC, "Arsenic, Metals, Fibers and dust," in *Monographs on the Evaluation of Carcinogenic Risks to Humans*, vol. 100, IARC, Lyon, France, 2009.

[15] G. G. Fletcher, F. E. Rossetto, J. D. Turnbull, and E. Nieboer, "Toxicity, uptake, and mutagenicity of particulate and soluble nickel compounds," *Environmental Health Perspectives*, vol. 102, no. 3, pp. 69–79, 1994.

[16] ACGIH, "Threshold Limit Values and Biological Exposure Indices for Chemical Substances and Physical Agents," in *Proceedings of the American Conference of Governmental Industrial Hygienists*, Cincinnati, OH, USA, 1998.

[17] K. S. Kasprzak, F. W. Sunderman Jr., and K. Salnikow, "Nickel carcinogenesis," *Mutation Research - Fundamental and Molecular Mechanisms of Mutagenesis*, vol. 533, no. 1-2, pp. 67–97, 2003.

[18] SCOEL, "Recommendation from the Scientific Committee on Occupational Exposure Limits for nickel and inorganic nickel compounds," SCOEL/SUM/85, 2011.

[19] P. Apostoli, "The role of element speciation in environmental and occupational medicine," *Fresenius' Journal of Analytical Chemistry*, vol. 363, no. 5-6, pp. 499–504, 1999.

[20] J. Szpunar and R. Łobiński, "Speciation in the environmental field - Trends in analytical chemistry," *Fresenius' Journal of Analytical Chemistry*, vol. 363, no. 5-6, pp. 550–557, 1999.

[21] G. W. Hughson, K. S. Galea, and K. E. Heim, "Characterization and assessment of dermal and inhalable nickel exposures in nickel production and primary user industries," *Annals of Occupational Hygiene*, vol. 54, no. 1, pp. 8–22, 2010.

[22] L. Füchtjohann, N. Jakubowski, D. Gladtke, D. Klockow, and J. A. C. Broekaert, "Speciation of nickel in airborne particulate matter by means of sequential extraction in a micro flow system and determination by graphite furnace atomic absorption spectrometry and inductively coupled plasma mass spectrometry," *Journal of Environmental Monitoring*, vol. 3, no. 6, pp. 681–687, 2001.

[23] D. Schaumlöffel, "Nickel species: analysis and toxic effects," *Journal of Trace Elements in Medicine and Biology*, vol. 26, no. 1, pp. 1–6, 2012.

[24] V. J. Zatka, J. Stuart Warner, and M. David, "Chemical Speciation of Nickel in Airborne Dusts: Analytical Method and Results of An Interlaboratory Test Program," *Environmental Science & Technology*, vol. 26, no. 1, pp. 138–144, 1992.

[25] OSHA—Occupational Health and Safety Administration, "Permissible Exposure Limits – Annotated Tables Z-1," https://www.osha.gov/dsg/annotated-pels/index.html, (accessed on 3rd July 2018).

[26] UNICHIM—Associazione Per l'Unificazione Nel Settore Dell'industria Chimica, "Ambienti di Lavoro—Determinazione Della Frazione Inalabile Delle Particelle Aerodisperse, Metodo Gravimetrico," http://www.uni.com/index.php?option=com_content&view=article&id=454&Itemid=2448&lang=it, (accessed on 26 June 2018).

[27] L. L. Van Loon, C. Throssell, and M. D. Dutton, "Comparison of nickel speciation in workplace aerosol samples using sequential extraction analysis and X-ray absorption near-edge structure spectroscopy," *Environmental Science: Processes & Impacts*, vol. 17, no. 5, pp. 922–931, 2015.

[28] H. M. Bolt, C. Noldes, and M. Blaszkewicz, "Fractionation of nickel species from airborne aerosols: Practical improvements and industrial applications," *International Archives of Occupational and Environmental Health*, vol. 73, no. 3, pp. 156–162, 2000.

[29] A. Profumo, G. Spini, L. Cucca, and M. Pesavento, "Determination of inorganic nickel compounds in the particulate matter of emissions and workplace air by selective sequential dissolutions," *Talanta*, vol. 61, no. 4, pp. 465–472, 2003.

[30] B. R. Conard, N. Zelding, and G. T. Bradley, "Speciation/fractionation of nickel in airborne particulate matter: Improvements in the Zatka sequential leaching procedure," *Journal of Environmental Monitoring*, vol. 10, no. 4, pp. 532–540, 2008.

[31] G. Marcias, J. Fostinelli, S. Catalani et al., "Composition of Metallic Elements and Size Distribution of Fine and Ultrafine

Particles in a Steelmaking Factory," *International Journal of Environmental Research and Public Health*, vol. 15, no. 6, 2018.

[32] D. J. Sivulka, "Assessment of respiratory carcinogenicity associated with exposure to metallic nickel: A review," *Regulatory Toxicology and Pharmacology*, vol. 43, no. 2, pp. 117–133, 2005.

[33] D. J. Sivulka and S. K. Seilkop, "Reconstruction of historical exposures in the US nickel alloy industry and the implications for carcinogenic hazard and risk assessments," *Regulatory Toxicology and Pharmacology*, vol. 53, no. 3, pp. 174–185, 2009.

[34] D. J. Sivulka, B. R. Conard, G. W. Hall, and J. H. Vincent, "Species-specific inhalable exposures in the nickel industry: A new approach for deriving inhalation occupational exposure limits," *Regulatory Toxicology and Pharmacology*, vol. 48, no. 1, pp. 19–34, 2007.

Hindawi
International Journal of Analytical Chemistry
Volume 2018, Article ID 9457095, 8 pages
https://doi.org/10.1155/2018/9457095

Research Article

Simultaneous Determination of Cr, As, Se, and Other Trace Metal Elements in Seawater by ICP-MS with Hybrid Simultaneous Preconcentration Combining Iron Hydroxide Coprecipitation and Solid Phase Extraction Using Chelating Resin

Akihide Itoh,[1] **Masato Ono**,[2] **Kota Suzuki**,[1] **Takumi Yasuda**,[1] **Kazuhiko Nakano**,[1] **Kimika Kaneshima**,[1] **and Kazuho Inaba**[1]

[1]*Department of Environmental Science, School of Life and Environmental Science, Azabu University, 1-17-71, Fuchinobe, Chuo-ku, Sagamihara-shi, Kanagawa 252-5201, Japan*
[2]*GL Science Inc., Shinjuku Square Tower 30F, 6-22-1 Nishi Shinjuku, Shinjuku-ku, Tokyo 163-1130, Japan*

Correspondence should be addressed to Akihide Itoh; a-ito@azabu-u.ac.jp

Received 6 July 2018; Accepted 29 October 2018; Published 13 November 2018

Guest Editor: Marcela Z. Corazza

In the present study, ICP-MS with a new hybrid simultaneous preconcentration combining solid phase extraction using chelating resin and iron hydroxide coprecipitation in one batch at a single pH adjustment (pH 6.0) were developed for multielement determination of trace metal ions in seawater. In multielement determination, the present method makes it possible to determine Cr(III), As(V), Se (IV), and other 14 trace metal elements (Ti, V, Co, Ni, Cu, Zn, Zr, Ge, Cd, Sb, Sn, W, Pb, and U) in seawater. Moreover, for speciation analyses of Cr, As, and Se, the pH dependence on recovery for the different chemical forms of Cr, As, and Se was investigated. In speciation analyses, Cr, As, and Se were determined as the total of Cr (III) and a part of Cr (VI), total of As (III) and As (V), and Se(IV), respectively. Determination of total of Se and Cr(VI) remains as future task to improve. Nevertheless, the present method would have possibility to develop as the analytical method to determine comprehensively most metal elements in all standard and guideline values in quality standard in environmental water in Japan, that is, most toxic metal elements in environmental water.

1. Introduction

ICP-MS has excellent analytical features such as simultaneous multielement capability, extremely high sensitivity, and wide linear dynamic range for most metal elements [1–3]. So, ICP-MS makes it possible to determine comprehensively almost all heavy metals, whose standard values or guideline values were established in water quality standards for human health relating to water pollution in Japan, without any special preconcentration. However, the measurement of trace metals such as heavy metals in seawater is difficult even using ICP-MS, because the salt contents in seawater are approximately 3.5% and they cause not only matrix effect and spectral interference but also the clogging of the torch top and the orifice of cone in ICP-MS [3]. These days, a high matrix introduction (HMI) unit permits the direct introduction of seawater into ICP-MS. In addition, novel ICP-MS with tandem quadrupole mass spectrometer (QMS/QMS) as well as with an octapole reaction cell (ORC) have become commercially available, which provides efficient removal of spectral interferences due to oxide species [4]. However, ICP-MS with preconcentration and desalting remains the most efficient method for the simultaneous and sensitive determination of trace metal elements in seawater without spectral interference and matrix effect.

The chelating resin preconcentration method has excellent analytical features of nonselective multielement

determination for many trace elements in seawater, along with efficient removal of matrix elements such as Na, K, Ca, and Mg [5–10]. However, it is found that the chelating resin provided poor recoveries for some oxoanion-forming elements, such as As, Se, and Cr, which are toxic and important in environmental sciences. Coprecipitation methods [11] such as lanthanum hydroxide [12–14], iron hydroxide [15–17], yttrium hydroxide [18], and magnesium hydroxide [19] are also effective as other preconcentration methods to complement chelating resin technique, because both oxoanion-forming elements and cation-forming trace elements can be concentrated using this method. However, the coprecipitation methods do not allow one to analyze toxic metal elements comprehensively, although they provided good recoveries for some oxoanion-forming elements and/or a part of transition metals. In addition, coprecipitation carrier results in high concentration of matrix components. Accordingly, performing both chelating resin preconcentration and coprecipitation complementally under control of matrix components is effective to determine many trace metal elements including toxic ones simultaneously. Yabutani et al. developed the tandem preconcentration method based on chelating resin adsorption and lanthanum hydroxide coprecipitation method that was continuously used to determine the oxoanion-forming elements and other trace elements [20]. However, this tandem method was time-consuming, because a series of preconcentration procedures including pH adjustment need to be performed for the coprecipitation after the chelating resin preconcentration. In contrast, a proposed new hybrid simultaneous preconcentration method was examined as a batch method that uses a single pH adjustment to achieve solid phase extraction using chelating resin and iron hydroxide coprecipitation. Thus, the potentials of ICP-MS with the present hybrid preconcentration method were investigated for simultaneous preconcentration and determination of the oxoanion-forming elements such as Cr, As, Se, and other trace metal elements, whose standard and guideline values were established in environmental quality standards for water pollution in Japan, even in seawater containing high concentrations of salts.

2. Materials and Methods

2.1. Instruments. An ICP-MS instrument (Agilent 7700x, Agilent Technologies Co., Tokyo, Japan), equipped with a quadrupole mass spectrometer and an octapole reaction cell (ORC), was used for the determination of trace metals in preconcentration solution of seawater. The operating conditions for the ICP-MS instrument were summarized in Table 1. In the ICP-MS measurement, the internal standard correction was performed using Be, In, and Tl as internal standard elements to correct matrix effects due to major elements [21]. The purified water (18.2 MQ cm) used throughout the present experiment was prepared by a Milli Q SP-TOC system (Nihon Millipore Kogyo, Tokyo, Japan).

2.2. Chemicals. The standard solutions for making the calibration curves in the ICP-MS measurements were prepared by diluting commercial multielement standard stock solutions (XSTC-622, 35 elements, 10 mg L^{-1} each), which were purchased from SPEX (Metuchen, NJ, USA). As, Cr, and Se were involved as As(V), Cr(III), and Se(IV) in XSTC-622, respectively. Nitric acid, hydrochloric acid, acetic acid, and aqueous ammonia solution were of electronics industry grade (Kanto Chemical Co., Tokyo, Japan). A single-element standard stock solution of Fe 10000 mg L^{-1} for general tests in the Japanese pharmacopoeia (Wako Pure Chemical Industries Inc., Osaka, Japan) was used as the iron solution for iron hydroxide coprecipitation.

Table 1: Operating conditions for the ICP-MS instrument.

ICP-MS: Agilent 7700x	
Plasma conditions:	
RF power	1.55 kW
Plasma gas flow rate	15.0 L min^{-1} Ar
Auxiliary gas flow rate	0.90 L min^{-1} Ar
Makeup gas flow rate	0 L min^{-1} Ar
Carrier gas flow rate	1.05 L min^{-1} Ar
Sampling depth (mm from load coil)	8.0 mm
Cell gas	He mode:4.3 mL min^{-1}
	H_2 mode:6.0 mL min^{-1}
Nebulizer	Micro Mist
Sample uptake rate	0.45 mL min^{-1}
Data acquisition:	
Accumulation time	0.3-1.0 s / point
Data point	3 points / peak
Repetition	3 times

The added standard solutions to investigate the recovery values were prepared as follows. The standard stock solutions for Cr(III), Cr(VI), and As(V) were prepared by diluting chromium(III) standard for ICP, chromium(VI) standard for ICP, and Arsenic (V) standard solution (1000 mg L^{-1} each, Merck, Darmstadt, Germany), respectively. The standard stock solutions for As(III) and Se(IV) were prepared by diluting standard solution of arsenic (III) and selenium (IV) for chemical analysis (1000 mg L^{-1} each, Kanto Chemical Co.), respectively. The standard solution for Se(VI) was prepared by extra grade of dissolving sodium selenite (Wako Pure Chemical Industries Inc.) in ultrapure water.

The chelating resin particles (InertSep ME2, 60-70 μm in diameter, GL Science Inc., Tokyo, Japan) have iminodiacetic acid (pK_a = 2.98) and dimethylamino (pK_a =10.77) groups on methacrylate resin. This resin was beforehand conditioned with ethanol, 2 M HNO_3, purified water, and 0.1 M ammonium acetate solution, which was used for chelating resin preconcentration of seawater samples. The ammonium acetate solution (pH 6) used for the pH adjustment was prepared by mixing equivalent molar amounts of acetic acid and ammonia solution.

The artificial seawater was prepared as follows using some reagents of extra grade purchased from Wako Pure

Chemical Industries Inc.: 28.5 g of sodium chloride, 6.82 g of magnesium sulfate heptahydrate, 5.16 g of magnesium chloride hexahydrate, 1.47 g of calcium chloride dehydrate, 0.725g of potassium chloride, 0.084 g of sodium bromide, and 0.0273 g of boric acid were dissolved in ultrapure water. Then, the volume of the solution was adjusted to be 1 L with ultrapure water.

2.3. Procedure of the Hybrid Preconcentration Combing Iron Hydroxide Coprecipitation and Solid Phase Extraction Using Chelating Resin. In the preconcentration procedure, 50 mL of a sample solution was initially taken in a 50 mL plastic bottle (DigeTUBEs, SCP SCIENCE, Canada, Montreal) and then 250 mg of the chelating resin particles, 50 μL of 10000 mg L^{-1} iron standard solution, 1 mL of 1.0 M ammonium acetate (buffer solution), and 100 μL of 400 μg L^{-1} methyl red solution (pH indicator) were added into the sample solution. The pH of the sample solution was adjusted to 6.0±0.1 using 6 M ammonia solution. As described in Results and Discussion, the optimal pH value for seawater samples in the iron hydroxide precipitation was pH 6.0, which was also appropriate for solid phase extraction using chelating resin. In the process of hybrid preconcentration procedure, it is considered that some cation-forming trace metals were complexed on the surface of the chelating resin particles and some oxoanion-forming elements such as Cr, As, and Se were adsorbed on and/or occluded in iron hydroxides coprecipitation. Changes in color were monitored during the pH adjustment for a preliminary estimation, but the final pH of the sample solution was confirmed using with a compact pH meter (Twin pH meter, Horiba Ltd., Kyoto, Japan). Next, the iron hydroxide coprecipitations formed were ripened for 2 h at 70°C in a water bath. Then, all the solutions were filtered using ϕ25 mm the glass fiber filter (Digi Filter, SCP SCIENCE, Canada, Montreal) with pore size of 1 μm, and the chelating resin particles and iron hydroxide coprecipitates were collected on the filter simultaneously. They were then washed with 50 mL purified water several times. Trace metals from the chelating resin particles and iron hydroxide coprecipitates were eluded with an acid solution. In the elution process, 5 mL of 2.6 M nitric acid solutions was added divisionally twice (2 and 3 mL) into chelating resin particles and iron hydroxide coprecipitates on the filter. When the first 2 mL of 2.6 M nitric acid solution was added, the solution was maintained for 10 min before removing to dissolve adequately the iron hydroxide coprecipitates. Subsequently, 5 mL of ultrapure water and 3 mL of the 2.6 M nitric acid solution were added as elutants and aspirated by vacuum pump (MDA-05, ULVAC, Chigasaki, Japan). Totally, 10 mL of elutant was obtained per each sample. Hence, ca. 5-fold preconcentration was achieved for the analysis solution in the present procedure, which was subjected to the simultaneous multielement determination of Cr, As, and Se and other trace metals using ICP-MS.

In the recovery test for investigation for the added amount of Fe^{3+} and analysis of coastal seawater, 50 μL of a mixed standard solution (XSTC-622, SPEX) containing 35 trace metals (1.0 mg L^{-1} each), in which Cr, As, and Se were contained as As(V), Cr(III), and Se(IV), was added into 50 mL of an artificial seawater. Then, the preconcentration procedure described above was carried out for the spiked and the unspiked artificial seawaters to estimate the recovery values. The recovery values for analyte elements were obtained as the percentages of the differences between the amounts of analyte elements in the spiked and unspiked artificial seawater samples, which was measured by ICP-MS after the present hybrid simultaneous preconcentration procedure, to the amounts added to the artificial seawater (50 ng each). In recovery test for speciation analysis of Cr, As, and Se, two kinds of recovery tests were separately performed using the stock solution for lower oxidation state of Cr(III), As(III), and Se(IV) and that for higher oxidation state of Cr(VI), As(V), and Se(VI) to avoid the oxidation-reduction reaction among these elements. 50 μL of the mixed standard stock solution of Cr(III), As(III), and Se(IV) (1.0 mg L^{-1} each) was added to the artificial seawater sample to prepare 50 mL of the spiked test solution for the lower oxidation state, and those of Cr(VI), As(V), and Se(VI) (1.0 ngL^{-1} each) were added to another sample of the artificial seawater to prepare 50 mL of the spiked test solution for the higher oxidation state. These two kinds of the spiked test solutions and unspiked artificial seawater without addition of any standard solution were analyzed by ICP-MS with the present hybrid simultaneous preconcentration to investigate the pH dependence on recovery of each oxidation state of Cr, As, and Se. The recovery for each chemical form of Cr, As, and Se was calculated in a similar manner to the recovery test for investigation for the added amount of Fe^{3+} and analysis of coastal seawater described above.

2.4. Seawater Samples. Seawater samples were collected at the Senzu coast in Izu-Oshima Island, Tokyo, Japan. Collected samples were filtered through the membrane filters of ϕ47 mm with a pore size 0.45 μm (Omnipore filter, Millipore, Bedford, MA, USA) immediately after sampling. The dissolved samples filtered with the membrane filters were acidified to pH 1 by adding concentrated HNO_3 (EL grade, Kanto Chemical Co.) and then subjected to hybrid preconcentration.

3. Results and Discussion

3.1. Investigation for Added Amounts of Fe^{3+}. In the present study, iron hydroxide coprecipitation was employed along with solid phase extraction using chelating resin to develop a hybrid simultaneous preconcentration method, because $Fe(OH)_3$ precipitates have a positive charge at pH 4-8 [22]. Moreover, $Fe(OH)_3$ precipitates can form at pH 5-6 [16]: this acidic condition is also optimal for solid phase extraction using chelating resin. In iron hydroxide coprecipitation, the added amounts of Fe^{3+} are generally 1.5-50 mg for 50 mL of each seawater sample [15, 16]. In the present study, however, it was set as 0.5 mg for 50 mL samples, because the added

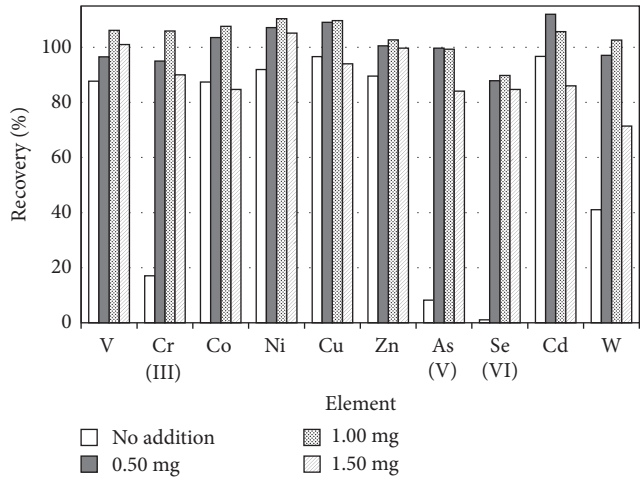

Figure 1: Comparison of recoveries of V, Cr(III), Co, Ni, Cu, Zn, As(V), Se(IV), Cd, and W in changing the added amount of Fe^{3+} in the hybrid preconcentration.

amount of Fe^{3+} as coprecipitation carrier should be kept minimal to decrease total matrix concentration and not to block the performance of chelating resin particles. Thus, the optimal added amount of Fe^{3+} was investigated in the present hybrid simultaneous preconcentration. When 0 mg, 0.50 mg, 1.0 mg, and 1.5 mg of Fe^{3+} were added to 50 mL of seawater sample with 250 mg of powdered chelating resin particles, respectively, and adjusted to pH 6.0, the recoveries of V, Cr(III), Co, Ni, Cu, Zn, As(V), Se(IV), Cd, and W are shown in Figure 1. As can be seen in Figure 1, the recoveries of most analyte elements were found to be higher at 0.50 mg and 1.0 mg. From this result, it was determined that the optimal amount of added Fe^{3+} was 0.50 mg, which resulted in the smaller total matrix and provided the smaller blank values. Then, Fe concentration was maintained below 50 mg L^{-1} in the 5-fold concentrated solutions and total residual concentrations of major ions such as Mg^{2+}, Ca^{2+}, Na^{+}, and K^{+} were below 20 mg L^{-1}. Thus, the matrix effect caused by the added Fe and the residual concentration of major ions was so small to be corrected using the internal standard method [21].

3.2. Comparison of Recoveries in the Hybrid Preconcentration with Those in Solid Phase Extraction Using Chelating Resin. The recovery of each element in the developed hybrid preconcentration was investigated. The results are shown in Figure 2 with those in a single solid phase extraction using chelating resin. As seen in Figure 2, for single solid phase extraction using chelating resin, the recoveries of Cr(III), Ge, As(V), Se(IV), Zr, and Sb were very low below 10%, and those of Sn and W were below 60%, whereas those of V, Co, Ni, Cu, Zn, Cd, Pb, and U were over 80% and high enough for determination of trace metals in seawater. As reported in previous studies [14], it is considered that oxoanion-forming elements such as Cr, Ge, As, Se, Sb, and W provided poor recoveries in single chelating resin preconcentration, which may be ascribed to their low adsorption on the chelating resin with cation-exchange functional groups.

However, in the present hybrid preconcentration, the recoveries of oxoanion-forming elements such as As(V), Cr(III), Se(IV), Ge, Sb, and W were remarkably higher than those in single solid phase extraction using chelating resin, as seen in Figure 2. Particularly, the recoveries of As(III), Cr(III), Se(IV), and W were over 80%. Moreover, those of Ti, Cd, Zr, and Sn were 70-95% and become remarkably higher than those in single chelating resin preconcentration. The precisions of the recoveries were almost below 5% for the present hybrid method. Recovery values and precisions obtained were high enough to determine simultaneously the oxoanion-forming elements and other trace metals.

3.3. pH Dependence on the Recovery of Different Chemical Forms of Cr, As, and Se for Speciation Analysis. Cr, As, and Se are present as two different oxidation states in seawater and environmental water. Cr exists as either Cr^{3+} or CrO_4^{2-} (VI) in seawater, As as either AsO_3^{3-} (III) or AsO_4^{3-} (V), and Se as either SeO_3^{2-} (IV) or SeO_4^{2-} (VI) [23]. Because the toxicity and bioavailability of these elements to aquatic animals and plants depend on the oxidation state, speciation analysis for these elements was very important to evaluate the effects on the aquatic ecosystem. Thus, the pH dependence on recovery of each oxidation state of Cr, As, and Se in seawater samples was investigated for speciation analysis. The results are shown in Figure 3. It can be seen from Figure 3 that the optimal pH to recover Se (IV), As (III), As(V), and Cr(III) simultaneously was pH 6.0. At this pH, the recovery of As was over 80%, regardless of the oxidation state. On the other hand, the recoveries of Cr(VI) and Se(VI) were ca.30% and 2%, respectively, whereas those of Cr(III) and Se (IV) were 100% and 80%, respectively. Moreover, even in different pH value, the recovery of each chemical form was not enough for its determination. Therefore, the optimal pH is also 6.0 for the speciation analyses that allows determining separately each chemical form of Cr, As, and Se. Under these conditions, the total concentrations of As, the sum of As(III) and As (V), and the concentration of Se(IV) were determined.

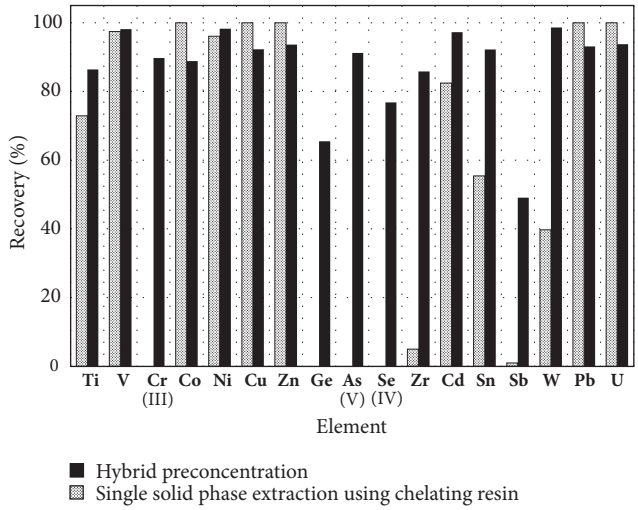

Figure 2: Comparison of the recoveries of Cr, As, Se, and other trace metal elements by the hybrid preconcentration with those by single preconcentration using chelating resin.

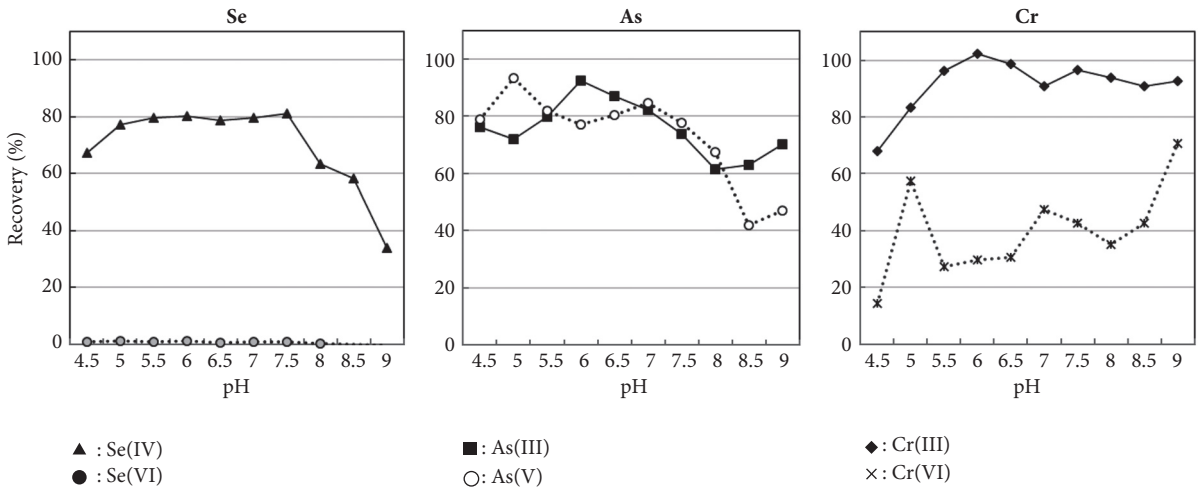

Figure 3: pH dependence on recovery of different chemical forms of Cr, As, and Se.

However, it was difficult to determine separately Cr(III) and Cr(IV).

3.4. Simultaneous Determination of Cr, As, and Se and Other Trace Metals in Coastal Seawater. Analytical results for the oxoanion-forming elements and other trace metals dissolved in coastal seawater collected at Izu-Oshima Island are shown in Table 2 with the recovery values, blank values, instrumental detection limits (DL_{instru}), and analytical detection limits (DL_{anal}). The recovery values were calculated as the percentages of analyte element amounts recovered after preconcentration to those added before preconcentration (50 ng each), as described in "Experimental" section. The recovery of As in Table 2 was obtained for As (V). However, as the recovery of As(III) was as high as that of As(V) at pH 6.0 in Figure 3, the analytical result of As in coastal seawater is shown as As (III+V) in Table 2. The DL_{instru} of the analyte elements was obtained at the concentrations corresponding to 3-fold the standard deviation (3σ) of the background signal intensities for the blank solution (2 M HNO_3), where the standard deviation (σ) was calculated from 10-times repeated measurement at each mass number. As it is confirmed that the linearities of the calibration curves for all analyte elements ranged from DL_{inst} to over 100 ng L^{-1}, all analyte elements in the concentrated sample solutions were measured within the liner range of the calibration curves. The DL_{anal} was estimated from the instrumental detection limits, taking into consideration the concentration factors and recovery values. The concentrations for 17 trace metals, which were corrected by the recovery values, concentration factors, and blank values, are shown in Table 2. The observed values and relative standard deviations (RSDs) were estimated from mean values and standard deviation (σ) of the independent 3-times analyses. As can be seen in Table 2, the concentrations of Cr (III), As (III+V), Se (IV), and other trace metals (Ti, V, Co, Ni, Cu, Zn, Ge, Zr, Cd, Sb, Sn, W, Pb, and U) were in the

Table 2: Analytical results for Cr, As, Se and other trace metals in coastal seawater (Izu Oshima, the senzu coast) determined by ICP-MS with hybrid preconcentration combining iron hydroxide coprecipitation and solid phase extraction using chelating resin.

Element	Cell gas mode	m/z	Concentration		Recovery		Blank value/ μgL^{-1}	DL_{instru} [(b)]/ μgL^{-1}	DL_{anal} [(c)]/ μgL^{-1}
			Observed [(a)] / μgL^{-1}	RSD/%	Mean [(a)] / %	RSD/%			
Ti	He	47	0.027 ± 0.009	32.7	96.9 ± 0.85	0.88	n.d. [(d)]	0.072	0.0074
V	He	51	1.87 ± 0.08	4.0	100.5 ± 0.99	0.99	0.001	0.0024	0.00024
Cr (III)	He	52	0.24 ± 0.02	7.4	96.3 ± 0.5	0.56	0.018	0.013	0.0013
Co	He	59	0.012*± 0.001	7.1	88.6 ± 0.57	0.64	0.006	0.0012	0.00014
Ni	He	60	0.22 ± 0.01	5.8	105.0 ± 3.2	3.3	0.012	0.0031	0.0031
Cu	He	63	0.17 ± 0.02	10.3	104.7 ± 1.9	2.0	0.034	0.021	0.0021
Zn	He	66	1.85 ± 0.03	1.8	86.8 ± 1.9	2.2	0.077	0.058	0.0067
Ge	He	72	0.72*± 0.04	5.2	65.5 ± 1.9	2.8	0.31	0.0018	0.00027
As (III + V)	He	75	1.34 ± 0.05	4.0	90.8 ± 0.84	0.92	0.0012	0.0024	0.00026
Se (IV)	H_2	78	0.0324 ± 0.0002	0.8	71.1 ± 0.17	0.24	n.d. [(d)]	0.0021	0.00029
Zr	He	90	0.055 ± 0.004	6.9	85.8 ± 2.3	2.6	n.d. [(d)]	0.0072	0.00084
Cd	He	111	0.013 ± 0.002	11.7	91.5 ± 0.53	0.58	n.d. [(d)]	0.0006	0.00007
Sn	He	118	0.065 ± 0.008	12.7	99.1 ± 0.57	0.57	0.0061	0.011	0.0011
Sb	He	121	0.23 ± 0.03	11.5	49.1 ± 0.39	0.80	0.0008	0.0003	0.00006
W	He	182	0.020 ± 0.001	5.1	98.6 ± 0.16	0.17	0.002	0.0029	0.00029
Pb	He	208	0.087 ± 0.01	10.4	98.9 ± 3.8	3.9	0.0023	0.0055	0.00056
U	He	238	3.0 ± 0.2	5.2	103.0 ± 0.010	0.010	n.d. [(d)]	0.0011	0.00011

(a) Mean $\pm\sigma$(standard deviation),n=3, The observed values with asterisk were corrected by the blank values over 10% of the observed values.
(b) DL_{instru}: instrumental detection limit. (c) DL_{anal}: analytical detection limit. (d) Not detected.

range of 3.0 μg L^{-1} for U to 0.012 μg L^{-1} for Co, which were determined with low RSDs below ca. 10% except for Ti. The recovery values for most elements in Table 1 were large (more than 85%) enough to obtain reliable analytical data, whereas those for Ge, Se(IV), and Sb were below 70%. However, they were employed for correction of the determined values, because the RSDs for these recoveries were below 3% and the precisions were very high. The blank values for most elements were below sub μg L^{-1} and low enough to correct the determined values. However, those for Co and Ge were over 10% of the observed values and relatively high. Therefore, these determined values were showed with asterisk in Table 2, as they may be less reliable than those for other elements.

4. Conclusion

In the present study, ICP-MS with a new hybrid simultaneous preconcentration combining the solid phase extraction using chelating resin and iron hydroxide coprecipitation in one batch at a single pH adjustment (pH 6.0) were developed for multielement determination of trace metal ions in seawater. In multielement determination, the present method made it possible to determine Cr(III), As(V), Se(IV), and 14 other trace metal elements (Ti, V, Co, Ni, Cu, Zn, Ge, Zr, Cd, Sb, Sn, W, Pb, and U). However, in speciation analyses, Cr, As, and Se were determined as the total of Cr (III) and a part of Cr (VI), total of As (III) and As (V), and Se(IV), respectively. Determination of total of Se and Cr (VI) remains as future task to improve. Nevertheless, the present method would have possibility to develop as the analytical method to determine comprehensively most metal elements in all standard and guideline values in quality standard in environmental water in Japan, that is, most toxic metal elements in environmental water.

Data Availability

The output data obtained to support the findings of this study are available from the corresponding author upon request.

Conflicts of Interest

The authors declare that they have no conflicts of interest.

Acknowledgments

We would like to thank Mr. Kunihisa Yamaguchi and his colleagues in Metropolitan Islands Area Research and Development Center of Agriculture, Forestry and Fisheries for sampling of coastal seawater in Izu-Oshima Island, Japan.

References

[1] M. Dziewatkoski, *Inductively Coupled Plasma Mass Spectrometry*, A. Montaser, Ed., Wiley-VCH, New York, NY, USA, 1998.

[2] H. E. Taylor, *Inductively Coupled Plasma-Mass Spectrometry*, Academic Press, San Diego, Calif, USA, 2001.

[3] H. Haraguchi, "Multielement Profiling Analyses of Biological, Geochemical, and Environmental Samples as Studied by Analytical Atomic Spectrometry," *Bulletin of the Chemical Society of Japan*, vol. 72, pp. 1163–1186, 1999.

[4] Y. Zhu and A. Itoh, "Direct Determination of Cadmium in Seawater by Standard Addition ICP-QMS/QMS with an ORC," *Analytical Sciences*, vol. 32, pp. 1301–1305, 2016.

[5] T. Yabutani, S. Ji, F. Mouri et al., "Multielement Determination of Trace Elements in Coastal Seawater by Inductively Coupled Plasma Mass Spectrometry with Aid of Chelating Resin Preconcentration," *Bulletin of the Chemical Society of Japan*, vol. 72, p. 2253, 1999.

[6] H. Sawatari, T. Toda, T. Saizuka, C. Kimata, A. Itoh, and H. Haraguchi, "Multielement Determination of Rare Earth Elements in Coastal Seawater by Inductively Coupled Plasma Mass Spectrometry after Preconcentration Using Chelating Resin," *Bulletin of the Chemical Society of Japan*, vol. 68, pp. 3065–3070, 1995.

[7] Y. Zhu, A. Itoh, and H. Haraguchi, "Multielement Determination of Trace Metals in Seawater by ICP-MS Using a Chelating Resin-Packed Minicolumn for Preconcentration," *Bulletin of the Chemical Society of Japan*, vol. 78, pp. 107–115, 2005.

[8] Y. Zhu, A. Itoh, E. Fujimori, T. Umemura, and H. Haraguchi, "Multielement Determination of Trace Metals in Seawater by Inductively Coupled Plasma Mass Spectrometry after Tandem Preconcentration Using a Chelating Resin," *Bulletin of the Chemical Society of Japan*, vol. 78, no. 4, pp. 659–667, 2005.

[9] A. Itoh, T. Ishigaki, T. Arakaki, A. Yamada, M. Yamaguchi, and N. Kabe, "Determination of trace metals in coastal seawater around Okinawa and its multielement profiling analysis," *Bunseki Kagaku*, vol. 58, no. 4, pp. 257–263, 2009.

[10] A. Itoh, T. Kodani, M. Ono et al., "Potential anthropogenic pollution by Eu as well as Gd observed in river water around urban area," *Chemistry Letters*, vol. 46, no. 9, pp. 1327–1329, 2017.

[11] S. Kagaya, "Rapid coprecipitation technique for the separation and preconcentration of trace elements," *Bunseki Kagaku*, vol. 65, no. 1, pp. 13–23, 2016.

[12] T. Yabutani, S. Ji, F. Mouri, A. Itoh, and H. Haraguchi, "Simultaneous multielement determination of hydride- and oxoanion-forming elements in seawater by inductively coupled plasma mass spectrometry after lanthanum coprecipitation," *Bulletin of the Chemical Society of Japan*, vol. 73, p. 895, 2000.

[13] D. Rahmi, Y. Zhu, E. Fujimori et al., "An in-syringe Lacoprecipitation Method for the Preconcentration of Oxo-anion Forming Elements in Seawater Prior to an ICP-MS Measurement," *Analytical Sciences*, vol. 24, pp. 1189–1192, 2008.

[14] T. Arakaki, T. Ishigaki, M. Yamaguchi, and A. Itoh, "Characteristics of concentrations and chemical forms of trace elements in deep seawater near kume island in Okinawa prefecture as studied by multielement profiling analysis," *Bunseki Kagaki*, vol. 58, p. 707, 2009.

[15] H. Daidoji, S. Tamura, and M. Natsubara, "Determination of rare earth elements and thorium in sea water by inductively coupled plasma atomic emission spectrometry," *Bunseki Kagaku*, vol. 34, p. 340, 1985.

[16] T. Fujinaga, M. Koyama, M. Kawashima, K. Izutsu, and S. Himeno, "Coprecipitation of Arsenic (V), (III) and Antimony (III) on Iron (III) and Aluminium Hydroxides," *Nippon Kagaku Kaishi*, vol. 1974, no. 8, pp. 1489–1493, 1974.

[17] M. Raso, P. Censi, and F. Saiano, "Simultaneous determinations of zirconium, hafnium, yttrium and lanthanides in seawater

according to a co-precipitation technique onto iron-hydroxide," *Talanta*, vol. 116, pp. 1085–1090, 2013.

[18] S. Kagaya, S. Miwa, T. Mizuno, and K. Tohda, "Rapid Coprecipitation Technique Using Yttrium Hydroxide for the Preconcentration and Separation of Trace Elements in Saline Water Prior to Their ICP-AES Determination," *Analytical Sciences*, vol. 23, pp. 1021–1024, 2007.

[19] Z. Arslan, T. Oymak, and J. White, "Triethylamine-assisted Mg(OH) 2 coprecipitation/preconcentration for determination of trace metals and rare earth elements in seawater by inductively coupled plasma mass spectrometry (ICP-MS)," *Analytica Chimica Acta*, vol. 1008, pp. 18–28, 2018.

[20] T. Yabutani, K. Chiba, and H. Haraguchi, "Multielement Determination of Trace Elements in Seawater by Inductively Coupled Plasma Mass Spectrometry after Tandem Preconcentration with Cooperation of Chelating Resin Adsorption and Lanthanum Coprecipitation," *Bulletin of the Chemical Society of Japan*, vol. 74, pp. 31–38, 2001.

[21] H. Sawatari, E. Fujimori, and H. Haraguchi, "Multi-Element Determination of Trace Elements in Seawater by Gallium Coprecipitation and Inductively Coupled Plasma Mass Spectrometry," *Analytical Sciences*, vol. 11, pp. 369–374, 1995.

[22] M. Sugiyama, "Ocaeanochemistry, 1998".

[23] Y. Nozaki, "EOS Trans. AGU, 1997".

Hindawi
International Journal of Analytical Chemistry
Volume 2018, Article ID 7503202, 8 pages
https://doi.org/10.1155/2018/7503202

Research Article

Selective Preconcentration of Gold from Ore Samples

Hurmus Refiker,[1,2] **Melek Merdivan**,[3] **and Ruveyde Sezer Aygun**[1]

[1]*Department of Chemistry, Middle East Technical University, Ankara, Turkey*
[2]*Institute of Applied Sciences, University of Kyrenia, Sehit Bakir Yahya Street, Kyrenia, North Cyprus, Mersin 10, Turkey*
[3]*Department of Chemistry, Dokuz Eylul University, Izmir, Turkey*

Correspondence should be addressed to Hurmus Refiker; hurmus.refiker@kyrenia.edu.tr

Received 24 May 2018; Revised 2 August 2018; Accepted 27 August 2018; Published 12 September 2018

Academic Editor: Seyyed E. Moradi

A simple and selective method has been developed for preconcentration of gold in ore samples. The method is based on use of N, N-diethyl-N'-benzoylthiourea (DEBT) as selective chelating agent and Amberlite XAD-16 as solid sorbent. Sorption behavior of gold with DEBT impregnated resin under optimized conditions has been studied in batch process. The gold ion capacity of the impregnated resin is calculated as 33.48 mg g^{-1} resin (0.17 mmol g^{-1} resin). The selective preconcentration of metal was examined using gold chelates prepared in column process under optimized conditions: pH, flow rate, volume of sample solution, nature of eluent, flow rate, and volume of eluent. Under optimum conditions, gold ions at the concentration of 0.015 μg mL^{-1} with a preconcentration factor of 6.7 have been determined by flame atomic absorption spectrometry (FAAS). The accuracy of the proposed method was validated by the analysis of a Cu-ore (semi-certified) supplied by CMC (Cyprus Mining Company, North Cyprus) and a certified reference material, Gold Ore (MA-1b Canmet-MMSL). Satisfactory results were obtained with a RSD of 7.6%. The highly selective proposed method does not require any interference elimination process.

1. Introduction

Gold is one of the precious metals which occurs in very low natural contents such as 4 ng g^{-1} in basic rocks, 1 ng g^{-1} in soils, 0.05 μg L^{-1} in sea water, and 0.2 μg/L in river water. Due to its specific physical and chemical properties, gold is widely used in industry, agriculture, and medicine [1]. Low abundance and heterogeneous distribution of gold in geological samples and various interfering matrices requires the development of accurate and reliable analytical procedures for determination of gold in environmental samples. Therefore, a selective separation and preconcentration method is a critical need for sensitive, accurate, and interference free determination of gold [2].

In literature, various techniques have been recorded for separation and preconcentration of gold, such as liquid-liquid extraction [3], coprecipitation [4], solid-phase extraction [5], cloud point extraction [6], and electrodeposition [7]. Solid-phase extraction (SPE) is preferable over all these techniques due to its advantages like high enrichment factor, high recovery, rapid phase separation, low cost, minimum solvent waste generation, and sorption of the target species on the solid surface in a more stable chemical form [8, 9].

The use of solid sorbents for preconcentration and separation has received great attention from analytical chemists [10]. Among wide range of solid phases such as multi-walled carbon nanotubes [11], surfactant coated alumina [12], styrene-divinylbenzene matrix [5, 13, 14], and silica gel [10, 15] have gained much importance for the metal ion enrichment. Amberlite XAD series have been more preferably used as solid support due to their good physical properties such as high porosity, uniform pore size distribution, high surface area as chemical homogenous non-ionic structure, and good adsorbent properties for great amounts of uncharged compounds [5, 16, 17]. Compared to Amberlite XAD-2 and XAD-4 resins, Amberlite XAD-16 has larger surface area [9], which makes possible to increase the number chelating sites hence increasing the selectivity towards target metal ions. This can be achieved by selecting suitable chelating agents. The chelating groups that are widely used for preconcentration of precious metals are imidazole, thioguanidine, dithizone, mercapto groups, amino groups, and thioureas [18]. In several

studies, N, N-diethyl-N'-benzoylthiourea (DEBT) has been recorded as a selective complexing agent for precious metals [19, 20]. Its selectivity is mainly controlled by pH. It has very high resistance to hydrolysis and oxidation. In addition to high pKs values, with resonance effects, DEBT can increase the electron density at sulfur donor atom when suitable acceptors are available. DEBT forms stable complexes only with Class b and border line acceptors. Noble metal ions, due to their specific Class b properties, form chelates with DEBT in low oxidation states in strongly acidic solutions [19, 20].

In the present study, DEBT as a chelating ligand and Amberlite XAD-16 as solid support have been used for selective separation and preconcentration of gold which is determined by flame atomic absorption spectrometry (FAAS). Optimum conditions for batch and column processes have been studied in detail. Then the proposed method has been applied to two real samples: Cu-ore supplied from CMC, North Cyprus, and a certified reference material Gold Ore (MA-1b) supplied by Canmet-MMSL, Ontario.

2. Experimental

2.1. Apparatus and Instrumentation. In order to prevent sorption of gold on silica surfaces, equipment made of polytetrafluoroethylene (PTFE) was used. 100 mL DuPont polyethylene containers for the storage and 5-50 and 100-1000 μL adjustable micropipettes (Transferpette, Treff Lab) with disposable polyethylene tips for preparation of solutions were used. In batch process, optimum conditions such as pH, stirring time, metal ion capacity, and agents suitable for desorption were studied by using 50-mL of Falcon tubes. NÜVE SL 350 horizontal shaker was used during sorption optimizations in batch process.

Columns were prepared from 12-mL syringe barrels (1.5 cm i.d., 7.8 cm height, PTFE, Supelco) where disposable porous frits were placed at the bottom of the barrels. 1.0 g resin (unless otherwise stated) slurred in 50 mL water was uniformly placed in column and was covered with cotton wool to prevent dispersion by the addition of sample solution. Tygon® tubing was used to connect the outlet tip of the syringe barrel to a Gilson Miniplus peristaltic pump. A calibration, flow rate mL min^{-1} versus rpm was carried out. This calibration was repeated for each column before the application. Each time, 15 mL blank solutions at a flow rate of 1 mL min^{-1} were passed before sorption and desorption studies.

Philips PU 9200 Atomic Absorption Spectrometer with Epson FX-850 printer was used for determination of gold ions.

2.2. Chemicals. All the reagents were of analytical reagent grade. Deionized water from a Milli-Q system was used throughout the study unless otherwise stated. Amberlite XAD-16 resin was supplied by Sigma. Gold standard solutions were prepared by diluting of 1000 μg mL^{-1} stock solution (Spectrosol) with 1 mol L^{-1} HCl (J.T. Baker, 36-38% w/w). During batch process, pH-adjustments were done using NaOH (Acros, 50% w/w). For desorption studies, $Na_2S_2O_3$ (extra pure, Bilesik Kimya Mekanik) was used.

2.3. Synthesis of DEBT and Impregnation Process. DEBT was synthesized according to the procedure modified in our laboratory [20] where potassium thiocyanate (Fischer, 0.1mol) was dissolved in anhydrous acetone (Riedel-deHaen, 100 mL) by stirring and heating in a reflux condenser. After cooling to room temperature, benzoyl chloride (Merck, 0.1 mol) was added dropwise and stirred for 30 minutes. Then potassium salt was filtered off. The filtrate in orange was reacted with 0.1 mol of diethylamine (Merck) dropwise. The reaction mixture was crystallized in 250 mL of 1 mol L^{-1} HCl solution. After filtering the mixture, the residue was recrystallized with ethanol.

Since the impregnation process deals with physical interactions between the chelating agent and solid support by either inclusion in the pores of the support material or adhesion process or electrostatic interaction, some parameters controlling the impregnation such as stirring time and chelating agent capacity have been optimized as mentioned elsewhere [21].

2.4. Batch Method. With batch studies, sorption behavior of high concentrations of gold on DEBT impregnated Amberlite XAD-16 was investigated. Some critical parameters such as pH, stirring time, and metal ion capacity of resin capacity have been studied to find out the optimum conditions for recovery of gold.

2.4.1. pH Effect. In order to investigate the pH effect on sorption of gold onto impregnated resin, different sets of 10 mL of 10 mg L^{-1} of Au^{3+} solution in the pH range of 1-5 were stirred with samples of 0.1 g impregnated resin for 50 minutes. After filtration under vacuum, metal ions in the filtrate were determined by FAAS.

2.4.2. Stirring Time. Three different sets of 2 mg L^{-1}, 10 mg L^{-1}, and 100 $mg^{-1}L$ of 10 mL of Au^{3+} solutions in 1 mol L^{-1} HCl were stirred with samples of 0.1 g impregnated resin from the periods of 5 minutes to 1 hour. Then solutions were filtered and filtrates were aspirated into FAAS for metal ion determination.

2.4.3. Gold Ion Capacity of Resin. In order to determine the resin capacity, samples of 0.1 g of impregnated resin (1 mmol DEBT g^{-1} resin) were stirred with 10 mL of gold ions solutions in the concentration range of 2 mg L^{-1} to 600 mg L^{-1} in 1 mol $/L^{-1}$ HCl for 15 minutes. Then the solutions were filtered and metal ion concentrations were determined by FAAS.

2.5. Column Method. Since the kinetic and equilibrium aspects of column process are different than batch process, optimization of column conditions is needed. Effect of flow rate and volume of ligand solution on impregnation and effect of ligand concentration on amount of metal chelate adsorption have been studied in column process.

2.6. Proposed Method for Preconcentration of Gold. 100 mL of gold chelate solutions (0.15 μg mL^{-1} Au^{3+} and 3 mL of $2x10^{-3}$ mol L^{-1} DEBT) was percolated through the column (1.0 g pure resin) at a flow rate of 0.5 mL min^{-1}. Then metal ions

could be eluted with 15 mL of 0.2 mol L^{-1} $Na_2S_2O_3$ in water with a recovery of 97.6 ± 2.3% (N=2).

2.7. Preparation of Ore Samples. An acid digestion procedure was applied to Cu-ore and Gold Ore (MA-1b) samples as suggested elsewhere [22]. Accordingly, two parallel 10.0 g of Cu-ore sample and 1.0 g of Gold Ore (MA-1b) were transferred into Teflon beakers. 20 mL of HCl was added to each where the beakers were covered and placed on a warm hot plate. After 15 minutes of digestion, 15 mL of concentrated nitric acid was added and the contents were digested for 20 minutes. Then 25 mL of concentrated HCl and 25 mL of deionized water were added. The contents were boiled to expel nitric acid digestion gases and to dissolve all soluble salts. After cooling they were filtered through Whatman white band filter paper into 100 ml PTFE flask. Once 3 mL of 2 X 10^{-3} mol L^{-1} DEBT solution was added, final volume was completed to 100 mL with deionized water. Later, the proposed procedure for preconcentration of gold was applied.

3. Results and Discussion

3.1. Characterization Studies. The structure of DEBT was characterized by FTIR and UV-VIS spectrophotometer. The synthesized DEBT exhibited 2 strong broad UV-absorption peaks at 237 and 278 nm which were consistent with those given in literature [20]. The characteristic absorption bands for N-H, C–H, and amide I (C=O), amide II, and amide III at 3276, 3066-2936, 1656, 1537, and 1306 cm^{-1}, respectively, appeared in both of the spectra. FTIR studies for pure resin, DEBT, DEBT impregnated resin, and DEBT-metal chelates have been carried out [20]. The characteristic absorption bands for C-H and amide I (C=O), amide II, and amide III at 3276, 3066-2936, 1656, 1537, and 1306 cm^{-1}, respectively, appeared only in the spectra of DEBT and impregnated resin. While the characteristic IR band of $-N(CH_2CH_3)_2$ group in the ligand at 2875 cm^{-1} remained almost unchanged in the spectrum of the complex showing that this group is not involved in coordination, C-H vibration in the aromatic ring is blue shifted upon metal-ligand bond formation. The position of amide I, amide II, and III bands at 1656, 1537, and 1306 cm^{-1}, respectively, arising from the carbonyl of the benzamide moiety and secondary amide of DEBT at 3276 cm^{-1} disappeared in the complex.

3.2. Parameters Optimized in Batch Method

3.2.1. pH Effect. In literature, it is noted that DEBT forms stable and selective complexes with noble metals only in acidic or strongly acidic media [19]. Moreover, Shuster and coworker reported optimum pH range as 0-5 for liquid-liquid extraction of gold with DEBT was previously reported as 0-5 by Schuster and coworkers [31]. Therefore, the pH effect on chelation of gold ions with DEBT impregnated resin is investigated within the pH range from 1 to 5.

It was shown that the maximum percent sorption is obtained at pH ~ 1 (see Figure 1). Therefore, standard solutions were prepared by diluting AAS standard stock solutions with 1 mol L^{-1} HCl.

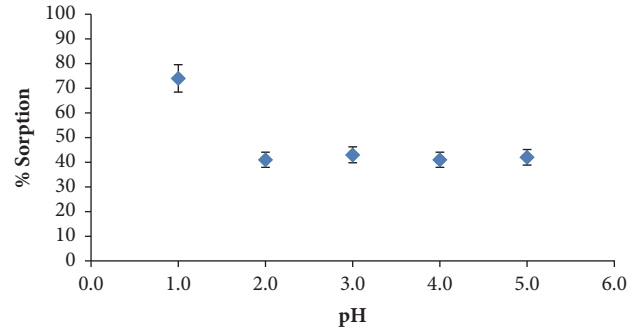

Figure 1: Effect of pH on sorption. Amount of resin: 0.1 g resin, amount of DEBT: 1mmol g^{-1} resin, and stirring time: 50 minutes.

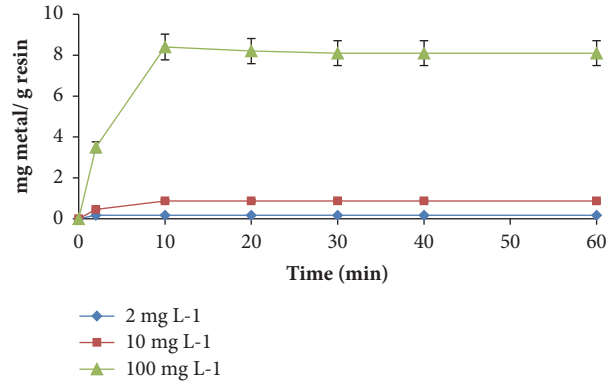

Figure 2: Stirring time of gold. Amount of resin: 0.1 g and amount of DEBT: 1 mmol g^{-1} resin.

3.2.2. Effect of Stirring Time. Referring to Figure 2, it can be concluded that 15 minutes of stirring is sufficiently good enough to achieve sorption equilibrium for three different concentrations of gold ion. Higher gold ion concentrations have no effect on the optimum time of sorption. Actually, fast kinetics can be expected in applications of macroporous resins. In addition, high ligand concentration, 1 mmol g^{-1} resin, used in impregnation may increase selectivity of the resin which can also be a reason for fast sorption rate.

As a result, 15 minutes of stirring can be accepted as a suitable stirring time during loading of resin with possible higher concentrations of gold ions to determine gold ion capacity of the resin.

3.2.3. Gold Ion Capacity of Impregnated Resin. Referring to Figure 3, after 500 mg L^{-1} of gold ions solutions, the impregnated resin reaches to saturation. The metal ion capacity of the resin is calculated as 33.48 mg Au^{3+} g^{-1} resin (0.17 mmol Au^{3+} g^{-1} resin) applying the following formula [32].

$$Q = \frac{(C_o - C_A) \times V}{W} \quad (1)$$

where Q is the metal ion capacity (mg/g),

C_o is the initial concentration of metal ion (mg/L),

C_A is the equilibrium concentration of metal ion (mg/L),

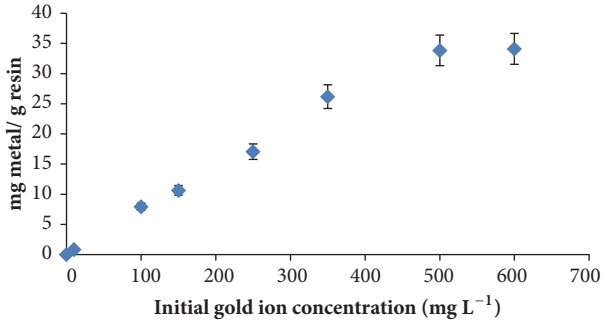

Figure 3: Gold ion capacity of resin. Amount of resin: 0.1 g, amount of DEBT: 1 mmol g^{-1} resin, and stirring time: 15 minutes.

V is the volume of the solution (L),

W is the weight of the resin (g).

3.3. Optimized Parameters in Column Method. During the application of the proposed method in column process, it was noticed that excess volume of sample solutions during sorption leached the impregnated DEBT that lead to loss of selectivity and analyte. Moreover, the partial exhaustion of available chelating sites due to leaching of impregnated ligand caused irreproducible results of sorption percentages of metal ion [5]. Therefore, research was continued with preparation of metal chelates before transferring to column and certain limited volume of chelate solution would be percolated through the column containing pure resin under the optimized conditions.

3.3.1. Sample Flow Rate of Gold Chelates. During batch studies, it was recognized that DEBT showed similar kinetics during chelation with gold as that of silver which was reported in the previous study [5], as long as DEBT concentration is kept the same or close optimum pH for sorption is maintained [21]. In the previous study, considering application of larger volume of sample solutions for preconcentration, to be on safe 0.5 mL min^{-1} had been accepted as optimum sample flow rate [5]. The same was also found to be optimum sample flow rate for gold studies.

3.3.2. Effect of Ligand Volume on Impregnation of Gold Chelates onto Resin. Maximum applicable ligand volume and concentration on analyte sorption are important. Therefore, maximum applicable ligand volume on retention is studied before further application of metal chelates for solid-phase extraction. For this reason, 3 mL of 3.75x10^{-4} mol L^{-1} DEBT solution was percolated through column for 4 times and DEBT concentration in the effluent determined by UV spectrometry. In Figure 4, it can be seen that maximum amount of DEBT retained on Amberlite XAD-16 was achieved with the first 3 mL of DEBT solution. Following additions of 3 mL of 3.75x10^{-4} mol L^{-1} DEBT solution showed a decrease in amount of DEBT retained on resin. This may be because of the leaching effect of ethanol on DEBT.

3.3.3. Effect of Optimized Ligand Concentration on Amount of Gold Chelates. Ligand concentration is also important

Table 1: Effect of ligand concentration of retention of metal chelates.

Amount of DEBT	Amount of Au^{3+} in sample solution (μg)	% Sorption of gold chelates on resin
3mL of 2x10^{-3} mol L^{-1}	15	100 ± 2
3mL of 2x10^{-3} mol L^{-1}	100	100 ± 2
3mL of 2x10^{-3} mol L^{-1}	500	94 ± 3

Amount of resin: 1.0 g, sample volume: 10 mL, and sample flow rate: 0.5 mL min^{-1}.

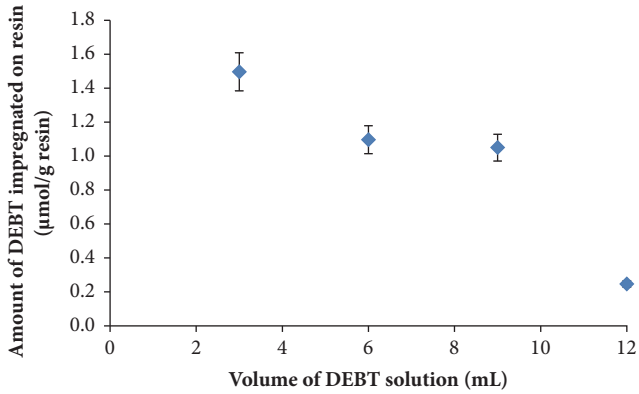

Figure 4: Effect of ligand volume on impregnation. Initial DEBT-ethanol concentration: 3.75 x 10^{-4} mol L^{-1} and flow rate: 0.5 mL min^{-1}.

because if it is not excessively present, the chelate formation may not be complete so metal ions may not be selectively retained on resin. However, excess DEBT (in case of inadequate amount of resin) may prevent retention of metal chelates because of the competition for sorption on resin between excess DEBT and metal chelates.

Considering the further applications of the proposed method to a real sample and limitations related to ligand mentioned above, it was decided to use 1.0 g of resin and amount of DEBT as 3 mL of 2x10^{-3} mol L^{-1}. This amount of DEBT is always in excess considering the amounts of analyte metal that is our concern (15 μg gold ions).

As indicated in Table 1, up to 100 μg gold ions in 10 mL sample solution can be safely retained on 1.0 g of resin as metal chelates. When 10 mL of 50 μg mL^{-1} metal chelate solution was passed through the column, a decrease in percent retention was observed.

During this study, we dealt with quite low amounts of metal ions and carried out the optimizations accordingly. Referring to results in Table 1, any researchers interested in higher amounts of gold up to 100 μg can study safely with the proposed method under the same conditions (such as amount of resin, sample flow rate, pH of sorption media, and ligand volume) as long as only the concentration of eluent and its volume are reoptimized according to the interested amount of metal ions.

3.3.4. Choice of Eluent: Its Nature, Concentration, Volume, and Flow Rate. In the previous study, we used sodium thiosulfate

Table 2: Analytical figures of merit.

Initial concentration of solution[a]	Regression equation[b]	R^2	LOD[c] (μg mL^{-1})	LOQ[d] (μg mL^{-1})	%RSD[e]	PF[f]
0.15 μg mL^{-1}	A = 0.0125C + 0.0003	0.9998	0.025	0.085	7.56	6.7

[a]sample volume = 100 mL, [b]A(absorbance) = slope x C(concentration μg mL^{-1}) + intercept, [c]limit of detection (2.5 μg g^{-1} ore), [d]limit of quantitation (8.5 μg g^{-1} ore), [e]percentage relative standard deviation, and [f]preconcentration factor.

Table 3: Determination of Au in CMC ore sample and Gold Ore (MA-1b) CRM.

Samples	Au concentration (mgkg^{-1})	Corrected values according to 97% desorption
CMC sample		
Au (found) ∗	< LOD	< LOD
Au (claimed)	1.34	1.34
Au (spiked found) ∗	13.6 ± 0.6	14.1 ± 0.6
Au (spiked)	15	15
Gold Ore (MA-1b)		
Au (found) ∗	15.0 ± 1.0	15.5 ± 1.0
Au (certified value)	17.0 ± 0.3	17.0 ± 0.3

∗ Values are given as mean ± SD, N = 3 (number of replicates).

which was found as the most suitable eluent for desorbing silver ions from Amberlite XAD-16 [5]. The sorption of silver ions was governed by the chelation mechanism in that silver ions (belong to class of soft acids) have affinity for (S-O) chelating group of DEBT. During desorption, (S-S) chelating groups of $Na_2S_2O_3$ provide a stronger complex formation as silver has a higher affinity for (S-S) than (S-O) chelating group [21]. Since gold metal also belongs to class of soft acid and same discussion could be valid as well, as a result, $Na_2S_2O_3$ was selected as suitable eluent for desorbing gold ions.

Series of experiments were conducted to optimize the concentration and the volume of eluent [21]. When 0.1 mol L^{-1} $Na_2S_2O_3$ in water was used as an eluent, at a flow rate of 0.3 mL min^{-1}, only 65% desorption was obtained. Later, it was found that the highest recovery with 97.6 ± 2.3% desorption was achieved when 15 mL of 0.2 mol L^{-1} $Na_2S_2O_3$ in water was percolated through the column at a flow rate of 0.3 mL min^{-1}.

3.4. Effect of Electrolytes and Competing Ions. In geological samples like ores, some metals in higher concentrations such as Na^+, K^+, Cu^{2+}, Ni^{2+}, Pb^{2+}, Mn^{2+}, Fe^{3+}, Zn^{2+}, Al^{3+}, and Cr^{3+} can coexist with gold. The anions Cl^-, NO_3^-, SO_4^{2-}, PO_4^{3-}, and ClO_4^- are the anions that are capable of forming complexes with several metal ions.

Considering the real sample amount weighed according to gold digestion procedure (at least 10.0 g), 50 mL of 300 μg mL^{-1} of copper standard solution was prepared in 1 mol L^{-1} HCl. Initial metal ion concentration was determined by FAAS. Then the proposed method was applied. The metal ion concentration in the effluent was determined by FAAS. Initial metal ion concentration was found to be 292 μg mL^{-1} and the metal ion concentration in the effluent was found as 288 μg mL^{-1}. As a result, only 1.37% of copper ions was adsorbed on resin. Although it is known that copper ion forms complex with DEBT in pH range of 0-7 [20], this result showed that the formation of Cu-DEBT complex in 1 mol L^{-1} HCl is quite lower to compete with gold ions. N-benzoylthioureas are bidentate chelating ligands with S and O as donor atoms. The possibility of increasing the electron density at the sulfur atom by means of resonance effect leads to selective complex behavior of DEBT which can be influenced by the adjustment of pH, where competing metal ions could be eliminated.

The effect of various electrolytes like $NaNO_3$, Na_2SO_4, Na_3PO_4, and Na_2CO_3 on the sorption of gold (1 mg L^{-1}) as Au-DEBT chelate on Amberlite XAD-16 resin was studied as well. Na_2SO_4 was tolerable up to 0.04 mol L^{-1}, Na_3PO_4 up to 0.1 mol L^{-1}, and $NaNO_3$ and Na_2CO_3 up to 0.15 mol L^{-1}.

3.5. Analytical Figures of Merit. The calibration graph for the determination of gold was plotted according to the proposed procedure under the optimum conditions. The equation of the line was derived as A = 0.0125C + 0.0003 with the regression coefficient 0.9998 where A is the absorbance and C is concentration of the metal ion (μg mL^{-1}).

The limit of detection (LOD) and limit of quantitation (LOQ) for gold ions were determined employing the standard solutions giving absorbance signal slightly recognizable than blank. The LOD and LOQ were calculated based on 3s/slope and 10s/slope of 10 measurements of the blank, respectively, where s is the standard deviation of the sample solution. The results of the LOD, LOQ, and precision (RSD %) for gold and its concentration are shown in Table 2.

3.6. Analysis of Real Samples. In order to demonstrate the accuracy of the proposed method, analyses of two real samples, one of which is the Cu-ore supplied by Cyprus Mining Company (CMC), North Cyprus, and the other one certified Gold Ore (MA-1b) by Canmet, Ontario, were carried out and the results were compared with the values reported. The results of spiked CMC samples and the results that were corrected for 97% desorption recovery value which was found for 100 mL sample solution were also tabulated in Table 3. Student's t-test was performed to statistically evaluate

Table 4: Comparison of the proposed method with some studies based on SPE and determination of gold reported in literature.

Adsorbent	Medium	Eluent	D. M.	LOD	Matrix	Ref.
Octadecyl silica membrane discs modified with pentathia-15-crown-5	pH 4.5-7.00	0.5 mol L^{-1} Sodium thiosulphate	FAAS	1.0 μg L^{-1}	Pharmaceutical and water samples	[23]
Diethyldithiocarbamate complex on Amberlite XAD-2000	0.5-2.5 mol L^{-1} HNO_3	1 mol L^{-1} HNO_3 in acetone	FAAS	16.6 μg	Environmental samples	[14]
1-phenyl-1,2-propanedione-2-complex on oximethiosemicarbazone SP Sephadex C25	pH 3	—	ICP-MS	$1.6X10^{-8}$-$141X10^{-8}$ mol L^{-1}	Minerals and natural water samples	[24]
Poly(N-(hydroxymethyl)methacylamide 0-1-allyl-thiourea) hydrogels	pH 0.5	0.8 mol L^{-1} thioura in 3 mol L^{-1} HCl	GFAAF	3 ng L^{-1}	Anode slime and geological samples∗	[25]
Dowex M 4195 chelating resin	pH 4	2 mol L^{-1} H_2SO_4 + 2 mol L^{-1} NH_3	FAAS	1.61 μg L^{-1}	Water, soil and sediment samples	[26]
Multi-walled carbon nanotubes	pH 1-6	3% thiourea in 1 mol L^{-1} HCl	FAAS	0.15 μg L^{-1}	Geological and water samples	[11]
2-pyridine-5-(4-tolyl)-1,3,4-oxadiazole complex on Amberlite XAD-4	0.5 mol/L HNO_3	1 mol/L HCl in acetone	FAAS	1.03 μg L^{-1}	Environmental Samples	[27]
Polyethylenimine coated on Al_2O_3	pH 5.7	0.5 mol L^{-1} thiourea then 1.0 mol/L HCl	FAAS	26.2 ng L^{-1}	Water Samples	[28]
Rubeanic acid complex on silica gel	pH 3.5	0.5 mol L^{-1} thiourea then 1.0 mol L^{-1} HCl	FAAS	0.80 ng mL^{-1}	Water Samples	[29]
Silica gel (SG-CIPrNTf_2)	pH 2	—	ICP-OES	—	Water Samples	[30]
DEBT complex on Amberlite XAD-16	pH~1	0.2 mol L^{-1} sodium thiosulphate	FAAS	0.025 μg mL^{-1}	Cu and Au Ores	This study

D.M.: detection method, Ref.: references. ∗Matrix elimination method is used.

the found and certified values. The found values were in good agreement with the certified ones and the difference was found to be statistically insignificant (at 95% confidence interval level).

4. Conclusions

Highly selective, reliable, and low cost method has been proposed for preconcentration of gold ions from highly interfering matrices, namely ores. The validity of the proposed method was demonstrated by the analyses of two geological samples: Cu-ore (supplied by CMC) and Gold Ore (MA-1b) as a certified reference material. The results are in good agreement with the given values. Comparison of the proposed method with some similar studies in literature is summarized in Table 4. Although there are more sensitive methods applied to similar samples, such as ICP-MS and GFAAS, these are much more expensive and sophisticated. The gold ion at such a low concentration of 0.15 μg mL^{-1} could be preconcentrated selectively and determined by the proposed method without any matrix elimination processes.

Data Availability

No data were used to support this study.

Disclosure

Present address for Hurmus Refiker is Institute of Applied Sciences, University of Kyrenia, Sehit Bakir Yahya Street, Kyrenia, North Cyprus, Mersin 10, Turkey.

Conflicts of Interest

Hereby I declare that there are no conflicts of interest for the publication of this manuscript.

Acknowledgments

This study is the unpublished part of Hurmus Refiker's thesis [21] and the authors thank Middle East Technical University-Scientific Research Fund, Project No.: 2002-07-02-00-39 for financial assistance.

References

[1] H. Fazelirad and M. A. Taher, "Ligandless, ion pair-based and ultrasound assisted emulsification solidified floating organic drop microextraction for simultaneous preconcentration of ultra-trace amounts of gold and thallium and determination by GFAAS," *Talanta*, vol. 103, pp. 375–383, 2013.

[2] R. Dobrowolski, M. Kuryło, M. Otto, and A. Mróz, "Determination of gold in geological materials by carbon slurry sampling graphite furnace atomic absorption spectrometry," *Talanta*, vol. 99, pp. 750–757, 2012.

[3] S. Rastegarzadeh, N. Pourreza, and A. Larki, "Determination of trace silver in water, wastewater and ore samples using dispersive liquid-liquid microextraction coupled with flame atomic absorption spectrometry," *Journal of Industrial and Engineering Chemistry*, vol. 24, pp. 297–301, 2015.

[4] A. Iraji, D. Afzali, and A. Mostafavi, "Separation for trace amounts of gold (III) ion using ion-pair dispersive liquid-liquid microextraction prior to flame atomic absorption spectrometry determination," *International Journal of Environmental Analytical Chemistry*, vol. 93, no. 3, pp. 315–324, 2013.

[5] H. Refiker, M. Merdivan, and R. S. Aygün, "Solid-phase extraction of silver in geological samples and its determination by FAAS," *Separation Science and Technology*, vol. 43, no. 1, pp. 179–191, 2008.

[6] G. Hartmann and M. Schuster, "Species selective preconcentration and quantification of gold nanoparticles using cloud point extraction and electrothermal atomic absorption spectrometry," *Analytica Chimica Acta*, vol. 761, pp. 27–33, 2013.

[7] E. A. Moawed and M. F. El-Shahat, "Synthesis, characterization of low density polyhydroxy polyurethane foam and its application for separation and determination of gold in water and ores samples," *Analytica Chimica Acta*, vol. 788, pp. 200–207, 2013.

[8] J. S. Fritz, *Analytical Solid-Phase Extraction*, Wiley-VCH, New York, NY, USA, 1999.

[9] R. K. Sharma and P. Pant, "Preconcentration and determination of trace metal ions from aqueous samples by newly developed gallic acid modified Amberlite XAD-16 chelating resin," *Journal of Hazardous Materials*, vol. 163, no. 1, pp. 295–301, 2009.

[10] M. Ghaedi, M. Rezakhani, S. Khodadoust, K. Niknam, and M. Soylak, "The solid phase extraction of some metal ions using palladium nanoparticles attached to silica gel chemically bonded by silica-bonded N-propylmorpholine as new sorbent prior to their determination by flame atomic absorption spectroscopy," *The Scientific World Journal*, vol. 2012, Article ID 764195, 9 pages, 2012.

[11] P. Liang, E. Zhao, Q. Ding, and D. Du, "Multiwalled carbon nanotubes microcolumn preconcentration and determination of gold in geological and water samples by flame atomic absorption spectrometry," *Spectrochimica Acta Part B: Atomic Spectroscopy*, vol. 63, no. 6, pp. 714–717, 2008.

[12] Ş. Tokalıoğlu, A. Papak, and Ş. Kartal, "Separation/preconcentration of trace Pb(II) and Cd(II) with 2-mercaptobenzothiazole impregnated Amberlite XAD-1180 resin and their determination by flame atomic absorption spectrometry," *Arabian Journal of Chemistry*, vol. 10, no. 1, pp. 19–23, 2017.

[13] S. Sivrikaya, B. Karslı, and M. Imamoglu, "On-line Preconcentration of Pd(II) Using Polyamine Silica Gel Filled Mini Column for Flame Atomic Absorption Spectrometric Determination," *International Journal of Environmental Research*, vol. 11, no. 5-6, pp. 579–590, 2017.

[14] H. B. Senturk, A. Gundogdu, V. N. Bulut et al., "Separation and enrichment of gold(III) from environmental samples prior to its flame atomic absorption spectrometric determination," *Journal of Hazardous Materials*, vol. 149, no. 2, pp. 317–323, 2007.

[15] R. Liu and P. Liang, "Determination of gold by nanometer titanium dioxide immobilized on silica gel packed microcolumn and flame atomic absorption spectrometry in geological and water samples," *Analytica Chimica Acta*, vol. 604, no. 2, pp. 114–118, 2007.

[16] A. Ahmad, J. A. Siddique, M. A. Laskar et al., "New generation Amberlite XAD resin for the removal of metal ions: A review," *Journal of Environmental Sciences*, vol. 31, pp. 104–123, 2015.

[17] D. A. Chowdhury, M. I. Hoque, and Z. Fardous, "Solid Phase Extraction of Copper, Cadmium and Lead Using Amberlite XAD-4 Resin Functionalized with 2-Hydroxybenzaldehyde Thiosemicarbazone and its Application on Green Tea Leaves," *Jordan Journal of Chemistry*, vol. 8, no. 2, pp. 90–102, 2013.

[18] V. Losev, E. Elsufiev, O. Buyko, A. Trofimchuk, R. Horda, and O. Legenchuk, "Extraction of precious metals from industrial solutions by the pine (Pinus sylvestris) sawdust-based biosorbent modified with thiourea groups," *Hydrometallurgy*, vol. 176, pp. 118–128, 2018.

[19] M. Schuster and M. Schwarzer, "Selective determination of palladium by on-line column preconcentration and graphite furnace atomic absorption spectrometry," *Analytica Chimica Acta*, vol. 328, no. 1, pp. 1–11, 1996.

[20] M. Merdivan, "The Analysis of Platinum Metals in Platinum Catalysts by Thin Layer Chromatography," *PhD Thesis*, Middel East Technical University, Ankara, Turkey, 1997.

[21] H. Refiker, "Preconcentration of Some Precious Metals Using Debt Impregnated Resin," MSc Thesis, Middle East Technical University, Ankara, Turkey, 2005.

[22] Perkin Elmer, "Analytical methods for Absorption spectrometry, manual, United States of America," 1996.

[23] M. Bagheri, M. H. Mashhadizadeh, and S. Razee, "Solid phase extraction of gold by sorption on octadecyl silica membrane disks modified with pentathia-15-crown-5 and determination by AAS," *Talanta*, vol. 60, no. 4, pp. 839–844, 2003.

[24] L. Morales and M. I. Toral, "Simultaneous determination of Au(III) and Cu(II) with 1-phenyl-1,2-propanedione-2-oximethiosemicarbazone (PPDOT) on solid phase," *Minerals Engineering*, vol. 20, no. 8, pp. 802–806, 2007.

[25] B. Salih, Ö. Çelikbıçak, S. Döker, and M. Doğan, "Matrix elimination method for the determination of precious metals in ores using electrothermal atomic absorption spectrometry," *Analytica Chimica Acta*, vol. 587, no. 2, pp. 272–280, 2007.

[26] M. Tuzen, K. O. Saygi, and M. Soylak, "Novel solid phase extraction procedure for gold(III) on Dowex M 4195 prior to its flame atomic absorption spectrometric determination," *Journal of Hazardous Materials*, vol. 156, no. 1-3, pp. 591–595, 2008.

[27] H. Elvan, D. Ozdes, C. Duran, V. N. Bulut, N. Gümrükçüoglu, and M. Soylak, "Development of a new solid phase extraction procedure for selective separation and enrichment of Au(III) ions in environmental samples," *Journal of the Brazilian Chemical Society*, vol. 24, no. 10, pp. 1701–1706, 2013.

[28] D. Afzali, Z. Daliri, and M. A. Taher, "Flame atomic absorption spectrometry determination of trace amount of gold after separation and preconcentration onto ion-exchange polyethylenimine coated on Al2O3," *Arabian Journal of Chemistry*, vol. 7, no. 5, pp. 770–774, 2014.

[29] F. Sabermahani, M. A. Taher, and H. Bahrami, "Separation and preconcentration of trace amounts of gold from water samples prior to determination by flame atomic absorption spectrometry," *Arabian Journal of Chemistry*, vol. 9, pp. S1700–S1705, 2016.

[30] H. M. Marwani, A. E. Alsafrani, H. A. Al-Turaif, A. M. Asiri, and S. B. Khan, "Selective extraction and detection of noble metal

Based on ionic liquid immobilized silica gel surface using ICP-OES," *Bulletin of Materials Science*, vol. 39, no. 4, pp. 1011–1019, 2016.

[31] M. Schuster, B. Kugler, and K. König, "The chromatography of metal chelates Fresen," *Journal of Analytical Chemistry*, vol. 338, no. 6, pp. 717–720, 1990.

[32] E. A. Moawed, I. Ishaq, A. Abdul-Rahman, and M. F. El-Shahat, "Synthesis, characterization of carbon polyurethane powder and its application for separation and spectrophotometric determination of platinum in pharmaceutical and ore samples," *Talanta*, vol. 121, pp. 113–121, 2014.

Hindawi
International Journal of Analytical Chemistry
Volume 2018, Article ID 8045324, 8 pages
https://doi.org/10.1155/2018/8045324

Research Article

Determination of Trace Antimony (III) in Water Samples with Single Drop Microextraction Using BPHA-[C_4mim][PF_6] System Followed by Graphite Furnace Atomic Absorption Spectrometry

Xiaoshan Huang, Mingxin Guan, Zhuliangzi Lu, and Yiping Hang

School of Chemistry and Chemical Engineering, South China University of Technology, Guangzhou 510640, China

Correspondence should be addressed to Yiping Hang; yphang@scut.edu.cn

Received 21 March 2018; Accepted 28 June 2018; Published 1 August 2018

Academic Editor: Marcela Z. Corazza

A new sensitive method for antimony (III) determination by graphite furnace atomic absorption spectrometry (GFAAS) has been developed by using N-benzoyl-N-phenylhydroxylamine (BPHA) and 1-butyl-3-methylimidazolium hexafluorophosphate ([C_4mim][PF_6]) single drop microextraction. The single drop microextraction (SDMM) system is more competitive compared with other traditional extraction methods. Under the optimized conditions, the limit of detection (signal-to-noise ratio is 3) and the enrichment factor of antimony (III) are 0.01 $\mu g \cdot L^{-1}$ and 112, respectively. The relative standard deviation of the 0.5 $\mu g \cdot L^{-1}$ antimony (III) is 4.2% (n=6). The proposed method is rather sensitive to determinate trace antimony (III) in water.

1. Introduction

Antimony (Sb) compounds have been extensively applied for various industrial materials such as glass, semiconductors, and pharmaceutical products [1–3]. As Sb can be easily exposed to the surface water, it has been considered as a priority pollutant in drinking water in the United States, Canada, Europe, and Japan while their action levels are ranged from 2 to 6 $\mu g \cdot L^{-1}$ [4]. Sb has two kinds of valence states including Sb (III) and Sb (V), and different chemical forms of them have different levers of toxicity. In inorganic chemistry, the compounds of Sb (III) are almost ten times more poisonous than the compounds of Sb (V) [5–7]. Many diseases including respiratory tract irritation, dermatitis, conjunctivitis, suppuration of the nasal septum, gastritis, or cellular damage in the lungs, heart, and kidneys will be triggered by excessive exposure to Sb (III) [8, 9]. Thus, a reliable and accurate method for the determination of Sb (III) is very necessary.

Several techniques including UV-visible spectrophotometry [10, 11], inductively coupled plasma mass spectrometry [12, 13], hydride generation atomic fluorescence spectrometry [14, 15], flame atomic absorption spectrometry [16–18], and electrothermal atomic absorption spectrometry [19–21] have been used for the determination of antimony species in various samples. Considering the poor sensitivities of flame atomic absorption spectrometry and UV-visible spectrophotometry, the more limited condition of hydride generation atomic fluorescence spectrometry, and the expensive price and analysis cost of inductively coupled plasma mass spectrometry, graphite furnace atomic absorption spectrometry (GFAAS) is an efficient alternative to determinate trace and ultratrace amounts of antimony. Besides the requirement of a relatively small injection volume, a partially eliminated matrix during the pyrolysis is another advantage of GFAAS. Despite the high sensitivity of GFAAS, it is still necessary to use separation techniques that allow preconcentration of antimony species, due to the complex matrix interferences and the low concentration of antimony species in water sample.

Many miniaturized techniques such as homogenous liquid-liquid microextraction [22, 23], solid phase extraction technology [24–26], cloud point extraction [2, 27], single drop microextraction [28–30], hollow-fiber liquid phase microextraction [17, 31], and dispersive liquid phase microextraction [32, 33] have been used as the processing methods of preconcentration. Also, these methods have been applied to preconcentration of antimony species. Compared with

Table 1: Graphite furnace atomizer temperature-rising program.

Steps	Temperature (°C)	Ramp time (s)	Hold time (s)	Argon flow rate ($mL \cdot min^{-1}$)
Drying	120	10	15	250
Pyrolysis	600	5	20	250
Atomization	2000	0	5	0
Cleaning	2400	1	3	250

other methods, SDMM is a new and environmentally friendly sample pretreatment technology. It has the advantages of low cost, simple device, easy operation, very low amounts of organic solvent, and high enrichment efficiency. For its striking advantages, SDMM was selected as the preconcentration methods in our study. Moreover, considering the toxicity and flammability of organic solvents, the ionic liquid of 1-butyl-3-methylimidazolium hexafluorophosphate ($[C_4mim][PF_6]$) has been employed in SDME because of its environmental friendliness. As reported, ionic liquids have been used as novel solvents for the extraction of metal ions at room temperature [34–37]. Ionic liquid does not have detectable vapor pressure and it can avoid environmental and safety problems. Up till now, few analytical applications of SDME method based on $[C_4mim][PF_6]$ for extraction and preconcentration of Sb (III) have been reported. Thus, further studies into the use of $[C_4mim][PF_6]$ in SDME are important in order to improve existing methods.

In this study, a method for Sb (III) determination in water samples by SDME combined with GFAAS was proposed. BPHA and $[C_4mim][PF_6]$ were employed as complexing agent and extraction solvent, respectively. The SDME system was fully characterized through optimizations of the relevant variables influencing the extraction of Sb (III).

2. Materials and Methods

2.1. Reagents. All the reagents were of analytical grade. The experiment water was double distilled deionized water purified by Millipore (Millipore, Bedford, MA, USA). Potassium antimony tartrate was from Tianjin Kemiou Chemical Reagent Co. Ltd., Tianjin, China. N-Benzoyl-N-phenylhydroxylamine (BPHA), sodium thiosulphate, hydrochloric acid, ammonia solutions oxine, dpy, dichloromethane (CH_2Cl_2), and trichloromethane ($CHCl_3$) were bought from Aladdin (Aladdin Industrial Co., Shanghai, China). 1-Butyl-3-methylimidazolium hexafluorophosphate ($[C_4mim][PF_6]$) was bought from J&K (J&K Scientific Ltd., Beijing, China). The 1000 $mg \cdot L^{-1}$ Sb (III) stock solution was prepared by amounts of potassium antimony tartrate dissolved in double distilled deionized water. The pH of the Sb (III) stock solution was adjusted to 2.0 with 0.1 M hydrochloric acid and 0.1 M ammonia solution. 1×10^{-3} M BPHA was dissolved in methanol.

2.2. Instruments. Atomic absorption spectra were performed by a Perkin-Elmer 900T atomic absorption spectrometer (Perkin-Elmer, USA) equipped with transverse heated graphite atomizer, pyrolytic graphite coated tubes (Beijing, China), and an antimony hollow cathode lamp (Perkin-Elmer, USA) recommended by the manufacturer. In the whole operation, except for atomization mode, argon 99.99% was used as protective and purge gas, and the flow rate was 250 $mL \cdot min^{-1}$. The pH of all solutions was performed by pHB-3C (Shanghai Weiye Instrument Factory). And all the stir in this study was performed by 85-2A magnetic stirrer (Changzhou Aohua Instrument Co. Ltd.). Some instrumental parameters of GFAAS were as follows: the lamp current was 10 mA, the wavelength was 217.6 nm, the spectral bandpass was 0.7 nm, and the background correction was Zeeman. Table 1 showed graphite furnace atomizer temperature-rising program.

2.3. Preparation of Samples. All the water samples were filtered through a 0.45 μm pore size membrane filter to remove the suspended particulate matters and the pH of all the water samples was adjusted to 2.0 by using 0.1 M hydrochloric acid and 0.1 M ammonia solution. Water samples including bottled mineral water, river water (pH=6.2, Beijiang River, Shaoguan, China), and tap water were collected locally. Each of the treated water samples was preserved at 1.9 mL for the later determination.

2.4. Process of Single Drop Microextraction. The apparatus of SDME was the same as what we studied before [39]. 1.9 mL treated water sample or 1 $\mu g \cdot L^{-1}$ Sb (III) standard solution and 100 μL 1×10^{-4} M BPHA solution were added to a 5 mL vial. Microsyringe with 5 μL of $[C_4mim][PF_6]$ was positioned above the vial, and the needle was inserted through the septum. The tip of syringe needle was attached to a flared polytetrafluoroethylene tube. Then, the needle tip was immersed into the sample solution, and the microsyringe was pushed slowly in order to make the microdrop hang under the needle tip steadily. The time of the extraction was 6 min under the stirring rate of 600 rpm. After extraction, microdrop was inhaled into the microsyringe and injected into the graphite furnace atomic absorption spectrometer for analysis manually.

3. Results and Discussion

3.1. Chelating Agent and Extraction Solvent. A chelating agent has a great influence on the extraction efficiency of Sb (III). Thus, a suitable chelating agent is very important. Figure 1(a) showed the pattern of the atomic absorbance of Sb (III) with different chelating agents (BPHA, Oxine, and Dpy) and their

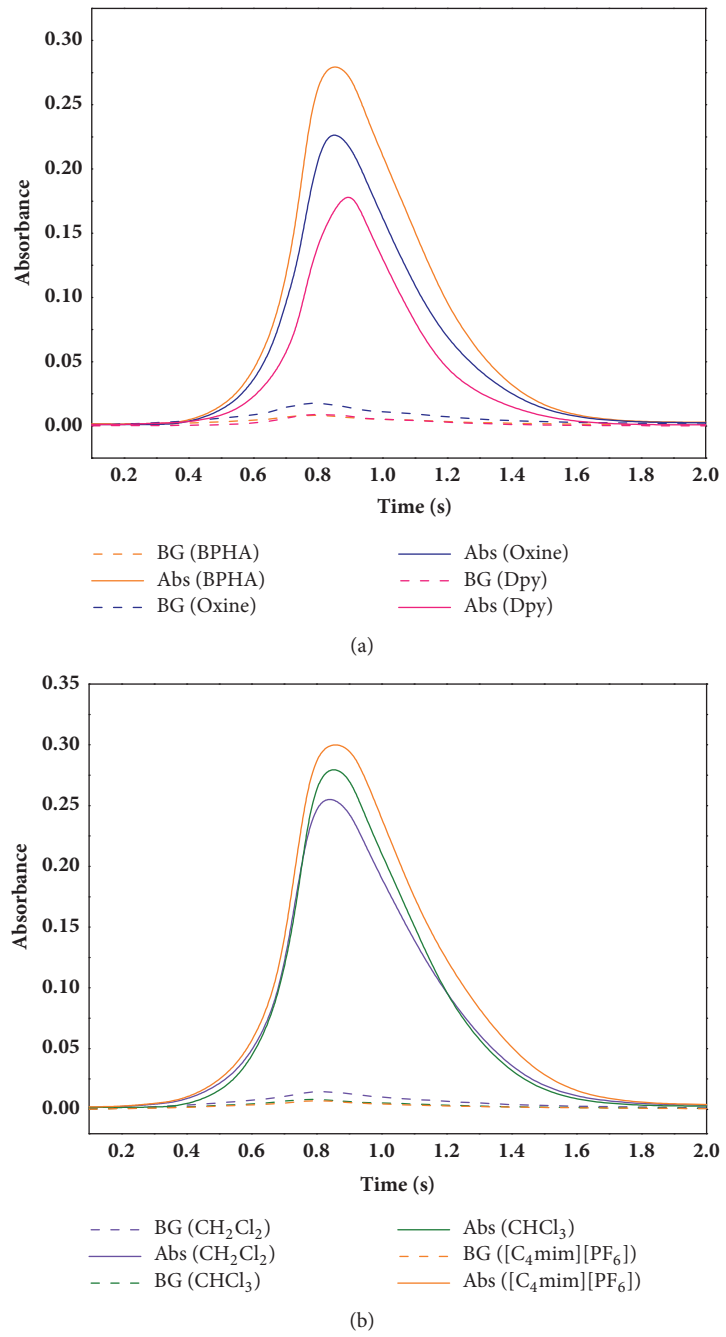

FIGURE 1: (a) The atomic absorbance of Sb (III) with different chelating agents such as BPHA, Oxine, and Dpy and their background absorbance. (b) The atomic absorbance of Sb (III) in different extraction solvents such as CH_2Cl_2, $CHCl_3$, and [C_4mim][PF_6] and their background absorbance; BG: background absorbance without Sb (III); Abs: absorbance.

background absorbance. It was found that the absorbance signal of Sb (III) with the chelating agent of BPHA was stronger than others. Although the absorbance signal of Sb (III) with Oxine was good, it had the stronger background interference. The absorbance signal of Sb (III) with Dpy had weaker signal compared with BPHA and Oxine. As a result, BPHA was selected as the chelating agent for SDME.

A suitable extraction solvent is also important for SDME. The density of the extraction solvent can be supposed to be higher than water so that it could keep the drop stable. CH_2Cl_2, $CHCl_3$, and [C_4mim][PF_6] that were used in liquid-liquid extraction were evaluated as the extraction solvents. Each extraction solvent was dealt with via three different chelating agents, and then the method of SDME-GFAAS was applied to determine the amounts of Sb (III), and the results were shown in Table 2. Whatever the chelating agent was, [C_4mim][PF_6] always had the strongest signal. Figure 1(b) described the atomic absorbance of Sb (III) in different extraction agents (CH_2Cl_2, $CHCl_3$, and [C_4mim][PF_6]) with BPHA as the chelating agent and their background

Table 2: The atomic absorbance of three chelating agents in three different extraction solvents.

Chelating agent	Extraction solvent		
	CH_2Cl_2	$CHCl_3$	$[C_4mim][PF_6]$
Oxine	0.287	0.274	0.294
Dpy	0.158	0.143	0.176
BPHA	0.322	0.355	0.364

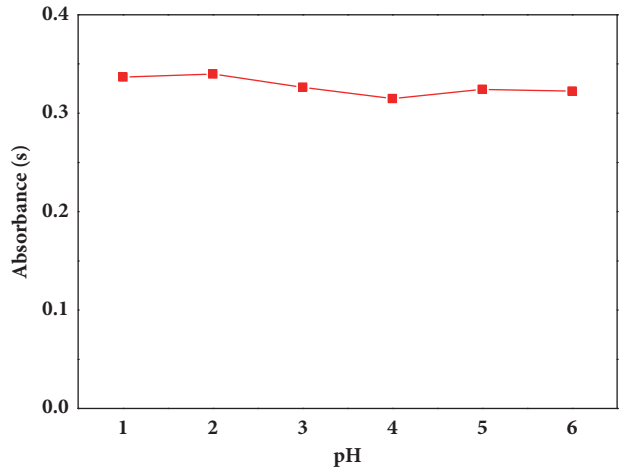

Figure 2: The atomic absorbance of Sb (III) in solutions with the pH value from 2.0 to 6.0.

absorbance. Therefore, $[C_4mim][PF_6]$ was selected as the extraction solvent for SDME.

3.2. Optimization of Single Drop Microextraction Conditions

3.2.1. pH. The pH of the solution played an important role in the formation of metal chelate and the influence of the stability of chemicals. Also, it could affect the extraction of Sb (III) in the BPHA-$[C_4mim][PF_6]$ system. The study of the pH was ranged from 1.0 to 6.0 and the results were shown in Figure 2. The absorbance signals of Sb (III) were high and less volatile in the range of 1.0-6.0. Considering that there may be interferences due to the competitive complexation reaction of other metal ions when the pH value was at a high level, pH=2.0 was chosen for the further study.

3.3. BPHA Concentration. It was also necessary to find the minimal concentration of BPHA. The effect of BPHA concentration on the extraction efficiency of Sb (III) was investigated. The results were illustrated in Figure 3(a) and, as can be seen from it, the absorbance signal of Sb (III) increased with the BPHA concentration from 6×10^{-5} to 8×10^{-5} M and remained constant when the concentration of BPHA was above 8×10^{-5} M. To make the treatment easier, the value of 1×10^{-4} M was chosen for the further study.

3.4. Solvent Drop Size. The effect of drop size was shown in Figure 3(b), and it was found that the absorbance of Sb (III) increased with the increase of the drop size from 2.0 to 6.0 μL. However, the drop size increasing usually resulted in the fall of the microdrop. In general, the stability of the microdrop depends on upward floating force, downward gravity, and adhesion forces [18]. In order to enhance the adhesion force of the microdrop, a flared polytetrafluoroethylene tube was attached to the tip of syringe needle. All these things were taken into account, and then 5.0 μL was chosen as the drop size for extraction.

3.5. Stirring Rate. It was well known that the stirring rate could affect the extracting speed by changing the mass transfer in the sample solution. The effect of stirring rates on extraction efficiency was studied in the range of 200 to 800 rpm. The results in Figure 3(c) showed that the increasing stirring rate of the sample greatly improved the absorbance of Sb (III). However, the microdrop easily fell off the needle of the microsyringe when the stirring rate was above 600 rpm. Increasing stirring rate could also cause a reduction of $[C_4min][PF_6]$ microdrop volume, because the dissolution of ionic liquid was enhancing. Thus, 600 rpm was selected as the best stirring rate in this study.

3.6. Extraction Time. The extraction efficiency depended on the length of the extraction time until the equilibrium was reached. Although the maximum sensitivity was achieved in equilibrium, complete equivalent was not necessary to obtain accurate analysis. Thus, the effect of extraction time on extraction efficiency had been studied from 2 to 10 min. The results were illustrated in Figure 3(d). There were a sharp increase from 2 to 6 min and a slow increase from 6 to 10 min. As the time went on, microdrop would fall into solutions. In order to avoid it, 6 min was selected as the extraction time which was enough for extracting Sb (III) for determination.

3.7. Optimization of Graphite Furnace Atomic Absorption Spectrometry. In order to reduce the chemical interference and the background signal, the work investigated the influence of pyrolysis temperature from 400°C to 800°C and atomization temperature from 1800°C to 2200°C. The 0.5 $\mu g\cdot L^{-1}$ Sb (III) standard solutions were dealt with via the pretreatment of SDME and determined by GFAAS. As shown in Figure 4(b), background signals were stronger when the pyrolysis temperature was lower because of the excessive vaporization of BPHA and ionic liquid at atomization stage, and the strongest signal appeared at 2000°C. It was found in Figure 4(a) that the matrix was sufficiently eliminated and maximum absorbance was achieved at the pyrolysis

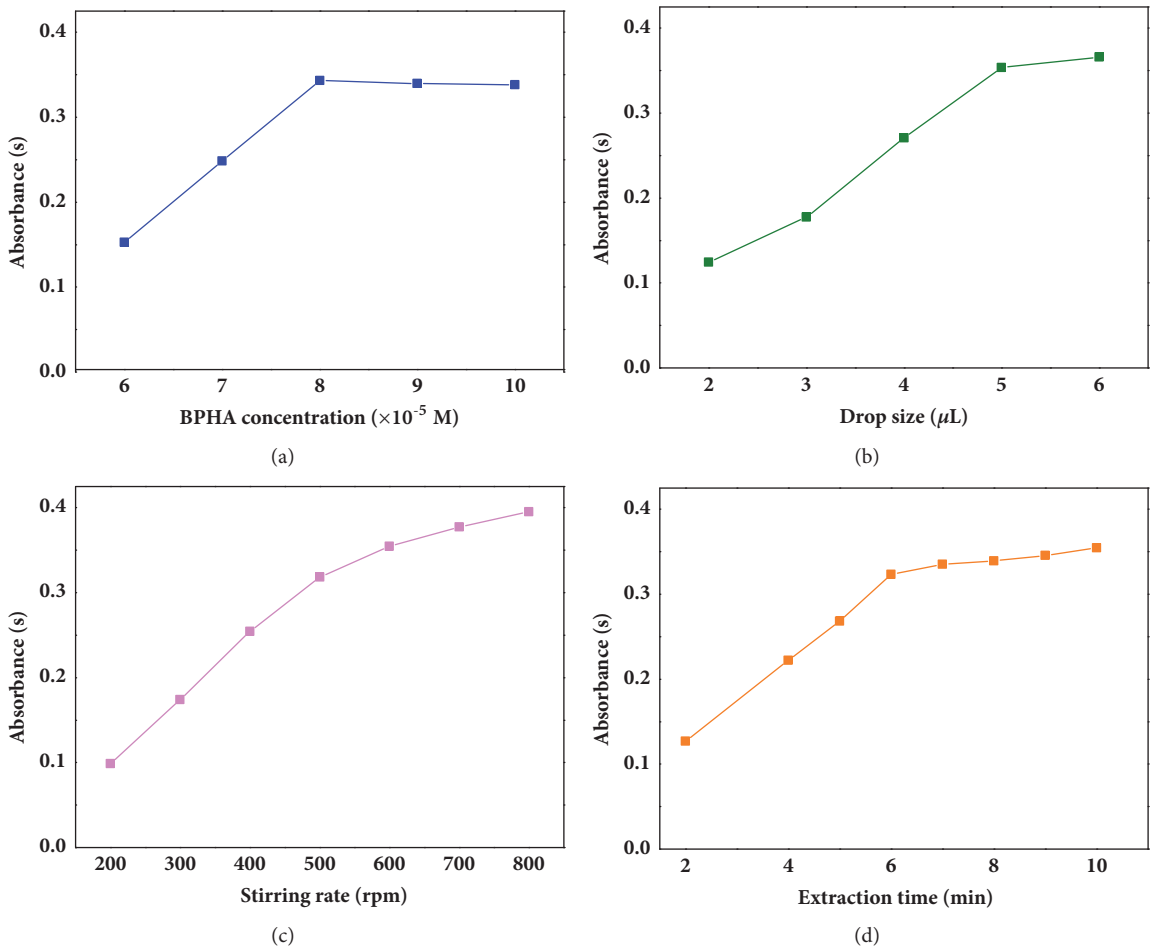

Figure 3: (a) The atomic absorbance of Sb (III) in solutions with the concentration of BPHA from 6×10^{-5} M to 10×10^{-5} M. (b) The atomic absorbance of Sb (III) in solutions with the drop size from 2.0 to 6.0 μL. (c) The atomic absorbance of Sb (III) in solutions with the stirring rate from 200 to 800 rpm. (d) The atomic absorbance of Sb (III) in solutions with the extraction time from 2 to 10 min.

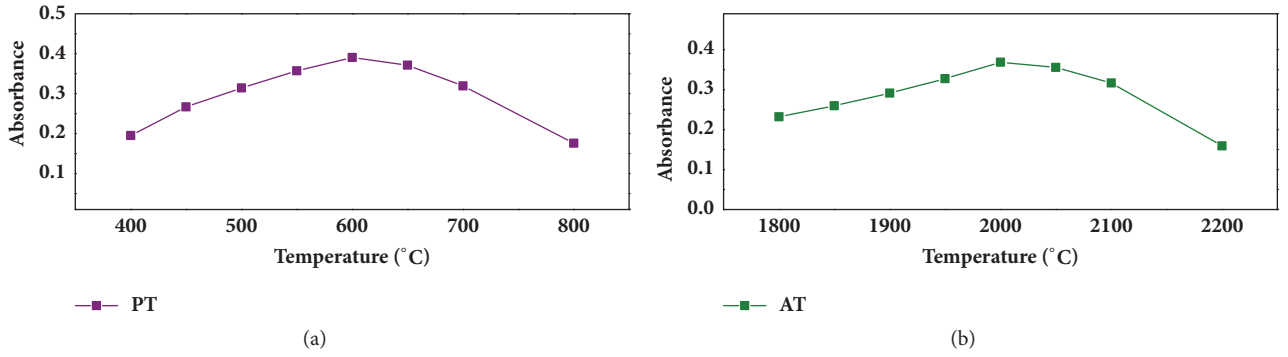

Figure 4: (a) The absorbance of Sb (III) with the pyrolysis temperature (PT) from 400°C to 800°C. (b) The absorbance of Sb (III) with the atomization temperature (AT) from 1800°C to 2200°C.

temperature of 600°C; however the absorbance decreased with increasing of the pyrolysis temperature due to the loss of Sb at higher temperature. In addition, the time of atomization was 5 s. As the results showed in Figure 4, 2000°C was chosen as the atomization temperature and 600°C as the pyrolysis temperature.

3.8. Effect of Interferences. One of the interferences was other metal ions reacting with chelating agents and the other was coextraction. In order to validate the selectivity of Sb (III) in microextraction system, different amounts of ions were added to the 1.0 $\mu g\cdot L^{-1}$ Sb (III) solutions, respectively. After determination, coexisting ions were considered to have

Table 3: Comparison of the proposed method with other methods for determination of antimony (III).

Method	Linear ranges ($ng \cdot mL^{-1}$)	Limits of detection ($ng \cdot mL^{-1}$)	Enrichment factor	Relative standard deviation	References
DLLME-ETAAS[a]	0.05-5	0.05	115	4.5%	[32]
CPE-ETAAS[b]	-	1.82	45	2.6%	[38]
VASEME-ETAAS[c]	0.4-8	0.09	53	5.4%	[20]
HFSLME-TAFFAAS[d]	5-200	0.8	160	7.8%	[17]
SDME-GFAAS	0.02-50	0.01	112	4.2%	This work

[a]Dispersive liquid-liquid microextraction-electrothermal atomic absorption spectrometry.
[b]Cloud point extraction- electrothermal atomic absorption spectrometry.
[c]Vortex-assisted surfactant-enhanced emulsification microextraction-electrothermal atomic absorption spectrometry.
[d]Hollow fiber supported liquid membrane extraction-thermospray flame furnace atomic absorption spectrometry.

Table 4: Determination of Sb (III) in water samples.

Samples	Added ($\mu g \cdot L^{-1}$)	Found ($\mu g \cdot L^{-1}$)	Recovery (%)
Bottle mineral water	0	< Limits of detection	-
	0.1	0.102 ± 0.01	102±1
	0.4	0.401 ± 0.008	100±2
River water	0	< Limits of detection	-
	0.1	0.104 ± 0.015	104±2
	0.4	0.407 ± 0.012	102±3
Tap water	0	< Limits of detection	-
	0.1	0.098 ± 0.011	98±1
	0.4	0.398 ± 0.009	99±2

interferences when the change of Sb (III) absorption value was more than 5%. As shown in the Results, the tolerance limit of coexisting ions including Na^+, K^+, Ca^{2+}, Mg^{2+}, Cl^-, SO_4^{2-}, and PO_4^{3-} was 2000 $mg \cdot L^{-1}$; of coexisting ions including Co^{2+}, Cd^{2+}, Cu^{2+}, Mn^{2+}, Zn^{2+}, and Ag^+ was 200 $mg \cdot L^{-1}$; of coexisting ions including Al^{3+}, Cr^{3+}, Fe^{3+}, Ni^{2+}, and Pb^{2+} was 50 $mg \cdot L^{-1}$.

3.9. Standard Analysis. As shown in the Results, the low limit of detection (LOD, 3σ) was 0.01 $ng \cdot mL^{-1}$, the relative standard deviation of 0.5 $ng \cdot mL^{-1}$ (n=6) was 4.2%, and the linear value ranged from 0.02 to 5 $ng \cdot mL^{-1}$. The regression equation was A=0.6832C+0.0034 (A represented the absorbance values and C represented the concentration of Sb (III) whose unit was $ng \cdot mL^{-1}$). Linear correlation coefficient was 0.999. A comparison of the main features of the proposed method with other reported methods in the literatures was shown in Table 3. This method was more effective for detecting Sb (III) with lower limit detection and had better precision than majority of the other reported methods.

3.10. Samples Analysis. A series of water samples were analyzed by the presented method. The results were shown in Table 4. The recoveries were in the ranges of 98-104% with the different standard of Sb (III) solutions spiked to the water samples. So, it demonstrated a good accuracy of this method.

4. Conclusions

The optimization method, combined with single drop microextraction using BPHA-[C_4mim][PF_6] system for separation of impurities, detected by GFAAS was developed to determinate trace Sb (III) in water samples. After a series of analysis of optimization conditions, an excellent accuracy, precision, and lower limit detection were obtained by this method. The relative standard deviation of the 0.5 $\mu g \cdot L^{-1}$ Sb (III) was 4.2% (n=6). The detection limit (signal-to-noise ratio of 3) and the enrichment coefficient of Sb (III) were 0.01 $\mu g \cdot L^{-1}$ and 112, respectively. What is more, the introduction of BPHA-[C_4mim][PF_6] system was not only ecofriendly comparing with traditional organic solution but also efficient for extraction. After the rapid extraction by SDME with the system of BPHA-[C_4mim][PF_6], the samples could be injected and detected directly. Thus, this method was a simple, effective, and environment-friendly way to determine the trace concentration of Sb (III) in water samples.

Data Availability

The [Graphite Furnace Atomic Absorption Spectrometry] data used to support the findings of this study are included within the article.

Conflicts of Interest

The authors declare that there are no conflicts of interest regarding the publication of this paper.

Acknowledgments

The authors gratefully acknowledge the South China University of Technology for supporting this work and the Science

and Technology Planning Project of Guangdong (Grant no. 2016A020210012) for the research fellowship.

References

[1] W. Shotyk, M. Krachler, and B. Chen, "Antimony: global environmental contaminant," *Journal of Environmental Monitoring*, vol. 7, no. 12, pp. 1135-1136, 2005.

[2] X. Jiang, S. Wen, and G. Xiang, "Cloud point extraction combined with electrothermal atomic absorption spectrometry for the speciation of antimony(III) and antimony(V) in food packaging materials," *Journal of Hazardous Materials*, vol. 175, no. 1-3, pp. 146–150, 2010.

[3] Y. Li, B. Hu, and Z. Jiang, "On-line cloud point extraction combined with electrothermal vaporization inductively coupled plasma atomic emission spectrometry for the speciation of inorganic antimony in environmental and biological samples," *Analytica Chimica Acta*, vol. 576, no. 2, pp. 207–214, 2006.

[4] S. D. Richardson and T. A. Ternes, "Water analysis: emerging contaminants and current issues," *Analytical Chemistry*, vol. 83, no. 12, pp. 4616–4648, 2011.

[5] P. Smichowski, "Antimony in the environment as a global pollutant: a review on analytical methodologies for its determination in atmospheric aerosols," *Talanta*, vol. 75, no. 1, pp. 2–14, 2008.

[6] A. Gonzalvez, M. L. Cervera, S. Armenta, and M. de la Guardia, "A review of non-chromatographic methods for speciation analysis," *Analytica Chimica Acta*, vol. 636, no. 2, pp. 129–157, 2009.

[7] J. O. Vinhal, A. D. Gonçalves, G. F. B. Cruz, and R. J. Cassella, "Speciation of inorganic antimony (III & V) employing polyurethane foam loaded with bromopyrogallol red," *Talanta*, vol. 150, pp. 539–545, 2016.

[8] M. Krachler, H. Emons, and J. Zheng, "Speciation of antimony for the 21st century: Promises and pitfalls," *TrAC - Trends in Analytical Chemistry*, vol. 20, no. 2, pp. 79–90, 2001.

[9] N. Altunay and R. Gürkan, "Separation/preconcentration of ultra-trace levels of inorganic Sb and Se from different sample matrices by charge transfer sensitized ion-pairing using ultrasonic-assisted cloud point extraction prior to their speciation and determination by hydride generation AAS," *Talanta*, vol. 159, pp. 344–355, 2016.

[10] M. J. G. González, O. D. Renedo, and M. J. A. Martínez, "Simultaneous determination of antimony(III) and antimony(V) by UV-vis spectroscopy and partial least squares method (PLS)," *Talanta*, vol. 68, no. 1, pp. 67–71, 2005.

[11] A. Samadi-Maybodi and V. Rezaei, "A cloud point extraction for spectrophotometric determination of ultra- trace antimony without chelating agent in environmental and biological samples," *Microchimica Acta*, vol. 178, no. 3-4, pp. 399–404, 2012.

[12] P. Li, Y.-J. Chen, X. Hu, and H.-Z. Lian, "Magnetic solid phase extraction for the determination of trace antimony species in water by inductively coupled plasma mass spectrometry," *Talanta*, vol. 134, pp. 292–297, 2015.

[13] F. Séby, C. Gleyzes, O. Grosso, B. Plau, and O. F. X. Donard, "Speciation of antimony in injectable drugs used for leishmaniasis treatment (Glucantime®) by HPLC-ICP-MS and DPP," *Analytical and Bioanalytical Chemistry*, vol. 404, no. 10, pp. 2939–2948, 2012.

[14] H. Wu, X. Wang, B. Liu et al., "Simultaneous speciation of inorganic arsenic and antimony in water samples by hydride generation-double channel atomic fluorescence spectrometry with on-line solid-phase extraction using single-walled carbon nanotubes micro-column," *Spectrochimica Acta Part B: Atomic Spectroscopy*, vol. 66, no. 1, pp. 74–80, 2011.

[15] Y. Zhang, M. Mei, T. Ouyang, and X. Huang, "Preparation of a new polymeric ionic liquid-based sorbent for stir cake sorptive extraction of trace antimony in environmental water samples," *Talanta*, vol. 161, pp. 377–383, 2016.

[16] S. Tajik and M. A. Taher, "New method for microextraction of ultra trace quantities of gold in real samples using ultrasound-assisted emulsification of solidified floating organic drops," *Microchimica Acta*, vol. 173, no. 1-2, pp. 249–257, 2011.

[17] C. Zeng, F. Yang, and N. Zhou, "Hollow fiber supported liquid membrane extraction coupled with thermospray flame furnace atomic absorption spectrometry for the speciation of Sb(III) and Sb(V) in environmental and biological samples," *Microchemical Journal*, vol. 98, no. 2, pp. 307–311, 2011.

[18] H. H. Nadiki, M. A. Taher, and H. Ashkenani, "Ionic liquid ultrasound assisted dispersive liquid-liquid/micro-volume back extraction procedure for preconcentration and determination of ultra trace amounts of thallium in water and biological samples," *International Journal of Environmental Analytical Chemistry*, vol. 93, no. 6, pp. 623–636, 2013.

[19] S. Wen and X. Zhu, "Speciation of antimony(III) and antimony(V) by electrothermal atomic absorption spectrometry after ultrasound-assisted emulsification of solidified floating organic drop microextraction," *Talanta*, vol. 115, pp. 814–818, 2013.

[20] M. Eftekhari, M. Chamsaz, M. H. Arbab-Zavar, and A. Eftekhari, "Vortex-assisted surfactant-enhanced emulsification microextraction based on solidification of floating organic drop followed by electrothermal atomic absorption spectrometry for speciation of antimony (III, V)," *Environmental Modeling & Assessment*, vol. 187, no. 1, 2015.

[21] I. López-García, S. Rengevicova, M. J. Muñoz-Sandoval, and M. Hernández-Córdoba, "Speciation of very low amounts of antimony in waters using magnetic core-modified silver nanoparticles and electrothermal atomic absorption spectrometry," *Talanta*, vol. 162, pp. 309–315, 2017.

[22] A. R. Ghiasvand, S. Shadabi, E. Mohagheghzadeh, and P. Hashemi, "Homogeneous liquid-liquid extraction method for the selective separation and preconcentration of ultra trace molybdenum," *Talanta*, vol. 66, no. 4, pp. 912–916, 2005.

[23] S. Igarashi, N. Ide, and Y. Takagai, "High-performance liquid chromatographic-spectrophotometric determination of copper(II) and palladium(II) with 5,10,15,20-tetrakis(4N-pyridyl)porphine following homogeneous liquid-liquid extraction in the water-acetic acid-chloroform ternary solvent system," *Analytica Chimica Acta*, vol. 424, no. 2, pp. 263–269, 2000.

[24] L. Zhang, Y. Morita, A. Sakuragawa, and A. Isozaki, "Inorganic speciation of As(III, V), Se(IV, VI) and Sb(III, V) in natural water with GF-AAS using solid phase extraction technology," *Talanta*, vol. 72, no. 2, pp. 723–729, 2007.

[25] C. Dietz, J. Sanz, and C. Cámara, "Recent developments in solid-phase microextraction coatings and related techniques," *Journal of Chromatography A*, vol. 1103, no. 2, pp. 183–192, 2006.

[26] A. K. Malik, V. Kaur, and N. Verma, "A review on solid phase microextraction - High performance liquid chromatography as a novel tool for the analysis of toxic metal ions," *Talanta*, vol. 68, no. 3, pp. 842–849, 2006.

[27] R. Gürkan and M. Eser, "Application of ultrasonic-assisted cloud point extraction/flame atomic absorption spectrometry (UA-CPE/FAAS) for preconcentration and determination of

low levels of antimony in some beverage samples," *Journal of the Iranian Chemical Society*, vol. 13, no. 9, pp. 1579–1591, 2016.

[28] Z. Fan, "Determination of antimony(III) and total antimony by single-drop microextraction combined with electrothermal atomic absorption spectrometry," *Analytica Chimica Acta*, vol. 585, no. 2, pp. 300–304, 2007.

[29] C. Mitani and A. N. Anthemidis, "On-line liquid phase microextraction based on drop-in-plug sequential injection lab-at-valve platform for metal determination," *Analytica Chimica Acta*, vol. 771, pp. 50–55, 2013.

[30] C. Ye, Q. Zhou, and X. Wang, "Improved single-drop microextraction for high sensitive analysis," *Journal of Chromatography A*, vol. 1139, no. 1, pp. 7–13, 2007.

[31] E. Marguí, M. Sagué, I. Queralt, and M. Hidalgo, "Liquid phase microextraction strategies combined with total reflection X-ray spectrometry for the determination of low amounts of inorganic antimony species in waters," *Analytica Chimica Acta*, vol. 786, pp. 8–15, 2013.

[32] R. E. Rivas, I. López-García, and M. Hernández-Córdoba, "Speciation of very low amounts of arsenic and antimony in waters using dispersive liquid-liquid microextraction and electrothermal atomic absorption spectrometry," *Spectrochimica Acta Part B: Atomic Spectroscopy*, vol. 64, no. 4, pp. 329–333, 2009.

[33] S. R. Yousefi, F. Shemirani, and M. R. Jamali, "Determination of antimony(III) and total antimony in aqueous samples by electrothermal atomic absorption spectrometry after dispersive liquid-liquid microextraction (DLLME)," *Analytical Letters*, vol. 43, no. 16, pp. 2563–2571, 2010.

[34] E. M. Martinis, R. A. Olsina, J. C. Altamirano, and R. G. Wuilloud, "Sensitive determination of cadmium in water samples by room temperature ionic liquid-based preconcentration and electrothermal atomic absorption spectrometry," *Analytica Chimica Acta*, vol. 628, no. 1, pp. 41–48, 2008.

[35] H. Abdolmohammad-Zadeh and G. H. Sadeghi, "A novel microextraction technique based on 1-hexylpyridinium hexafluorophosphate ionic liquid for the preconcentration of zinc in water and milk samples," *Analytica Chimica Acta*, vol. 649, no. 2, pp. 211–217, 2009.

[36] X. Wen, Q. Deng, and J. Guo, "Ionic liquid-based single drop microextraction of ultra-trace copper in food and water samples before spectrophotometric determination," *Spectrochimica Acta Part A: Molecular and Biomolecular Spectroscopy*, vol. 79, no. 5, pp. 1941–1945, 2011.

[37] G.-T. Wei, Z. Yang, and C.-J. Chen, "Room temperature ionic liquid as a novel medium for liquid/liquid extraction of metal ions," *Analytica Chimica Acta*, vol. 488, no. 2, pp. 183–192, 2003.

[38] Z. Fan, "Speciation analysis of antimony (III) and antimony (V) by flame atomic absorption spectrometry after separation/preconcentration with cloud point extraction," *Microchimica Acta*, vol. 152, no. 1-2, pp. 29–33, 2005.

[39] H. Yiping and W. Caiyun, "Ion chromatography for rapid and sensitive determination of fluoride in milk after headspace single-drop microextraction with in situ generation of volatile hydrogen fluoride," *Analytica Chimica Acta*, vol. 661, no. 2, pp. 161–166, 2010.

Hindawi
International Journal of Analytical Chemistry
Volume 2018, Article ID 4015878, 11 pages
https://doi.org/10.1155/2018/4015878

Research Article

Host–Guest Extraction of Heavy Metal Ions with *p-t*-Butylcalix[8]arene from Ammonia or Amine Solutions

Md. Hasan Zahir,[1] **Shakhawat Chowdhury**,[2] **Md. Abdul Aziz**,[3] **and Mohammad Mizanur Rahman**[4]

[1]*Center of Research Excellence in Renewable Energy, Research Institute, King Fahd University of Petroleum and Minerals, Dhahran 31261, Saudi Arabia*
[2]*Department of Civil and Environmental Engineering, Water Research Group, King Fahd University of Petroleum and Minerals, Dhahran 31261, Saudi Arabia*
[3]*Center of Research Excellence in Nanotechnology, King Fahd University of Petroleum and Minerals, Dhahran 31261, Saudi Arabia*
[4]*Center of Research Excellence in Corrosion, King Fahd University of Petroleum and Minerals, Dhahran 31261, Saudi Arabia*

Correspondence should be addressed to Md. Hasan Zahir; hzahir@kfupm.edu.sa

Received 25 March 2018; Revised 4 June 2018; Accepted 21 June 2018; Published 11 July 2018

Academic Editor: Seyyed E. Moradi

The capacities of the *p-t*-butylcalix[8]arene (abbreviated as H_8L) host to extract toxic divalent heavy metal ions and silver from aqueous solution phases containing ammonia or ethylene diamine to an organic phase (nitrobenzene, dichloromethane, or chloroform) were carried out. When the metal ions were extracted from an aqueous ammonia solution, the metal ion selectivity for extraction was found to decrease in the order $Cd^{2+} > Ni^{2+} > Cu^{2+} > Ag^{+} > Co^{2+} > Zn^{2+}$. When the aqueous phase contained ethylene diamine, excellent extraction efficiencies of 97% and 90% were observed for the heavy metal ions Cu^{2+} and Cd^{2+}, respectively. Under the same conditions the extraction of octahedral type metal ions, namely, Co^{2+} and Ni^{2+}, was suppressed. The extraction of transition metal cations by H_8L in ammonia and/or amine was found to be pH dependent. Detailed analysis of extraction behavior was investigated by slope analysis, the continuous variation method, and by loading tests.

1. Introduction

Host–guest chemistry has attracted great attention in the field of separation and/or extraction of alkaline, rare earth, and divalent heavy metal ions with calixarenes and their ester derivatives. Calixarenes have unusual capabilities to identify and distinguish between different ions and molecules, which makes them appropriate to use as specific receptors [1–3]. Calixarenes are macrocyclic phenolic oligomers with phenolic hydroxyl groups, which are able to coordinate the metal ions very tightly. As a result, the aromatic phenolic rings can form a cavity to integrate the guest metal ion. Recently, Yusof et al. reported that the heavy metal ions could be included into the host calix[4]resorcinarenes cavity in water-chloroform extraction systems [4, 5]. Calix[6]arenes can be also modified with a carboxylic acid as host in the *host–guest* extraction of immunoglobulin G (IgG) [6]. In fact, a precise affinity can be created for specific ions and/or molecules by modification the hydroxyl functional group and/or by creating a new cavity size [7]. In calixarenes, the cavity size, position and type of donor groups, and molecular flexibility lead to their high potential for the complexation and extraction of metal ions. Ludwig et al. reported the impact of calixarenes in analytical chemistry and chemical separation technology in a review article [8].

The modification of *p-t*-butylcalix[*n*]arenes (n = 4, 6, 8) has been extensively investigated, facilitating the synthesis of a variety of host compounds with varying shapes and sizes that have been shown to be valuable in ion or molecular recognition studies [9, 10]. In particular, *p-t*-butylcalix[8]arene (abbreviated as H_8L) has shown interesting complexing properties towards C_{60}-fullerene, cesium, or

strontium cations. This means that new synthetic routes with different functionalized derivatives of H_8L could be more versatile [11].

H_8L can form host–guest complexes through hydrophobic and π–π interactions within the cavities of π-donors composed of benzene rings, polycyclic aromatic hydrocarbons, anthraquinones, phenol regioisomers, and fullerene π-systems, due to their considerable electron affinity [12]. From a coordination standpoint, the reaction of H_8L with metal ions is more complex than that of H_6L; however, already few calix[8]crowns have been reported in the open literature [13, 14]. Derivatives of calix[n]arenes could be formed by inserting binding groups such as amines and/or alcohols into the upper and lower rim positions of the calixarene moiety [15]. It has been reported that proton transfer from an OH-group of the parent calixarene to an amine might occur during the reaction period, eventually resulting in a new compound from the association and inclusion of the amine into the cavity of the calixarene [16]. Finally, the abovementioned studies have established that calixarenes can effectively react with most metal ions and the new organometallic compounds can be obtained in good yields [8–10, 17].

H_8L has been utilized in the separation of metallic cations [18, 19], the extraction of methyl esters of some amino-acids [20], uranium (VI) preconcentration [21], lanthanide complexes [22], and molecular recognition of 1,5-diaminoantraquinone [23]. Erdemir et al. investigated the extraction abilities of carboxylic acid and methyl ester derivatives of *p-t*-butylcalix[n]arenes (n = 6, 8) for carcinogenic aromatic amines [24]. Other calixarenes and their derivatives have been utilized in the fields of complexation, separation, electroanalysis, spectroscopy, and chemometrics [25].

A larger ligand, i.e., H_8L, can act as a ditopic receptor for lanthanide and transition metal ions [26] and hence in principle may bind to a single metal ion in various ways. It is important to mention that solvent extraction of transition metal ions, particularly toxic metal ions, using H_8L alone has scarcely been reported in the open literature. Makrlik et al. studied the liquid–liquid extraction of Eu^{3+} trifluoromethanesulfonate into nitrobenzene in the presence of H_6L and H_8L [27]. Sansone et al. reported the separation of An^{3+}/Ln^{3+} from radioactive waste using CMPO (carbamoylmethyl-phosphine oxide) substituted H_6L and H_8L [28]. Gutsche et al. synthesized aminocalixarenes complexes of Ni^{2+}, Cu^{2+}, Pd^{2+}, Co^{2+}, and Fe^{2+} and determined their spectral and chemical characteristics [10]. Their findings indicated that metal-aminocalixarenes are more flexible than had previously been thought. It has also been reported that H_8L can be combined into a polymeric medium to produce a material that shows a high sorption ability towards transition metal ions (Cu^{2+}, Fe^{2+}, Zn^{2+}, Ni^{2+}, Co^{2+}, Cd^{2+}, and Pb^{2+}) in aqueous solution [29]. The authors also performed research on the extraction behavior of transition metal ions with H_4L and H_6L [30, 31].

An effective extractant with high selectivity for metal ions is in high demand for analytical applications, recycling of resources, and waste treatment purposes. Heavy metals such as lead (Pb), copper (Cu), and nickel (Ni) are harmful to humans. Obviously, the harmful impact of some ions, for example, Cd^{2+} and As^{2+}, is of great concern in such research. Cd^{2+} is one of the most toxic elements for humans. At high concentrations, it causes various debilitating conditions such as painful bone disease, bone marrow disorders, kidney problems, and "*Itaiitai*" or *"ouch-ouch"* disease [32]. However, calixarene derivatives may be useful binders for these cations.

In this study, H_8L has been investigated as host extractant for divalent heavy metal ions and silver from ammonia and amine solutions into various types of organic solvents. We also synthesized H_8L ethyl ester derivatives and the extraction behavior of transition metal cations from aqueous solution was also investigated.

2. Experimental Section

2.1. Materials. H_8L was purchased from the Sigma Aldrich Chemical Company, USA. All transition metal nitrate solutions were prepared according to the method in [30, 31]. Other reagents such as chloroform, dichloromethane and nitrobenzene, and ethanol were purchased from Carlo Erba Reagents, France. Ammonia, ethylenediamine and trimethylene diamine, ethyl bromoacetate, NaH, and THF/DMF were bought from Acros Organic, Belgium. The water was deionized. All the remaining reagents were as pure as is commercially available. Stock solutions were standardized by potentiometric and EDTA titrations. Other metal salts were guaranteed to be reagent grade.

2.2. Extraction Procedure. The hosts H_8L and H_8L-ester were prepared by dissolving the appropriate amount in various organic solvents followed by the dilution, typically to 1×10^{-4} M working solution; aqueous solutions of metal solutions were made from analytical purity nitrates of Cd^{2+}, Ni^{2+}, Cu^{2+}, Ag^{2+}, Co^{2+}, and Zn^{2+}. Extraction experiments were typically performed by equilibrating 8 mL of a 5×10^{-5} M solution of the metal ions, 1 ml succinic acid (0.01M), and 1 mL of a buffer solution with 10 mL of a 5×10^{-4} M solution of the H_8L in 1,2-dichloroethane. The mixture was placed in a stoppered 50 mL glass tube at a volume ratio of 10:10 mL (organic phase to aqueous phase). The pH was adjusted by three types of buffer solution: CH_3COOH-CH_3COONa (acidic region), H_3BO_3-NaOH (neutral), and NH_3-NH_4Cl (alkali). In the case of H_8L-ester extractant, picric acid [2.5×10^{-5} M] was used as the counter anion. The extraction equilibrium was attained within 40 min of shaking with nitrobenzene; the extraction into chloroform reached equilibrium within 20 h of shaking. Therefore, the shaking time was fixed at 2 h for nitrobenzene and at 20 h for chloroform. The extractability was not affected by further shaking, indicating that the equilibrium was attained within 12 h. All the experiments were performed in presence of succinic acid to avoid emulsification during the extraction process. The distribution experiments were performed at room temperature.

Before shaking, the samples were left standing in the water bath at 25°C for 15 min to ensure that the extraction solutions were maintained at the same temperature. Then,

a shaker at 200 stroke min^{-1} at 25.0 ± 0.1°C mixed the two phases; a shaking time of 12 h was sufficient to reach the extraction equilibrium. After shaking, the two phases were centrifuged at 2000 rpm. for 10 min, which was sufficient for complete separation. Before the measurement, the pH of the aqueous and organic phases was adjusted to 2.5 using 5 M HNO_3 and 3 M LiOH. The amount of extracted metal ions was calculated from the difference between the metal concentrations in the aqueous phase before and after the equilibration. The concentration of the metal ion in the organic phase was determined by the back-extraction method; 5 cm^3 of the organic phase was transferred into another glass-stoppered tube and shaken with 4 M hydrochloric acid. After phase separation, the equilibrium concentrations of metal cations in the aqueous phase were measured by an inductively coupled plasma atomic emission spectrometer (Seiko model SPS 1200AR). The equilibrium pH in the aqueous solutions was measured by a pH meter (Beckmann model ø45).

The extractability (Ex%) was determined from the decrease in the metal concentration in the aqueous phase:

$$\text{Ex\%} = \left\{ \frac{(\text{Metal})]_{\text{blank}} - [\text{Metal}]_{\text{water}})}{(\text{Metal})]_{\text{blank}}} \right\} \times 100, \quad (1)$$

where $[\text{Metal}]_{\text{blank}}$ and $[\text{Metal}]_{\text{water}}$ denote the metal concentrations in the aqueous phase after extraction with nitrobenzene and with the nitrobenzene solution containing extractants, respectively, and $[\text{Metal}]_{\text{or}}$ denotes the metal concentration extracted into the organic phase.

2.3. Analysis. Morphology of the product particles was examined using scanning electron microscopy (SEM, JEOL JSM6330F). Fourier transform infrared (FT-IR) spectra were collected on a Bruker FT-IR spectrometer by using the KBr pellet technique. ^{1}H-NMR data were recorded on a JEOL JNM-GX 61D FT-NMR spectrometer operating at 400 MHz in $CDCl_3$, using TMS as internal standard.

3. Results and Discussion

3.1. Effect of H_8L Host Concentration. Experiments were performed using H_8L concentrations of 1×10^{-3} - 5×10^{-4} M and a metal ion concentration of 5×10^{-5} M; all other conditions were kept the same. We found that the extraction percentage increased with increasing H_8L concentration. The best extraction was achieved when 5×10^{-4} M H_8L was used. As H_8L was soluble in nitrobenzene up to 4×10^{-2} M and up to 1×10^{-2} M in 1,2-dichloroethane at room temperature, the saturated solution was used as the stock solution.

3.2. Role of Extractant. Three organic solvents (nitrobenzene, dichloromethane, and chloroform) were also tested as inert diluents at a fixed pH for solutions containing an equal amount of metal ions and H_8L. The phase volume ratio was maintained at 1:1 to avoid emulsion formation; this was found to be the most effective ratio. This means that the tendency for association is, in general, greater when the solvent–solute interactions are weaker; however, chloroform is the least effective. The exact cause of this type of behavior is not known. It was observed that the extraction percentage increased with the diluent type in the order of chloroform > dichloromethane > nitrobenzene.

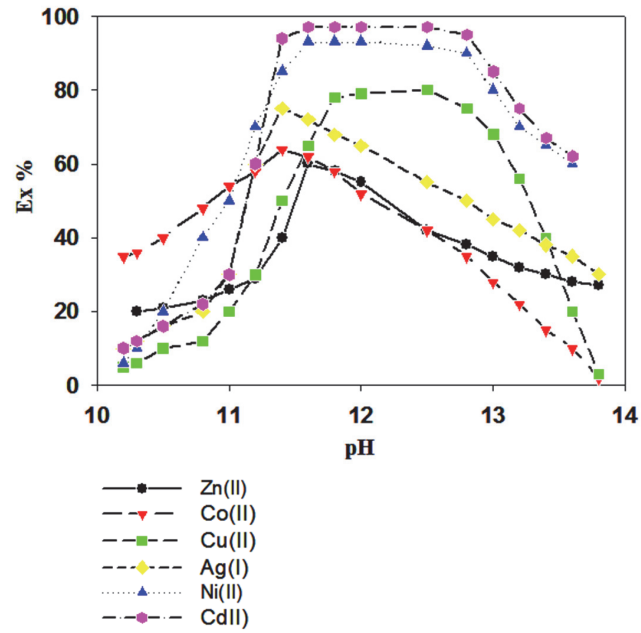

FIGURE 1: Extractability of all tested transition metal ions as a function of pH. Organic phase: $H_8L = 5 \times 10^{-4}$ M; aqueous phase: = (●) 5×10^{-5} M; succinic acid = 0.01 M; and buffer solution: 0.01 M; MES-NaOH (pH 5.0–7.0) and 0.1 M Tris-$HClO_4$ (pH 7.0–9.0). $[Cd^{2+}]$ = (■)1×10^{-4} M, 0.2 M $NaClO_4$. O/A = 1; T = 25°C. O:A represents the ratio between organic (O) and aqueous (A) volumes in the experiments.

3.3. Choice of Stripping Agent. After extraction of Cd^{2+} with H_8L, the metal ions were stripped with 7 mL of various concentrations of mineral acid reagents, specifically 4 M HCl, 0.1–5 M HNO_3, or 2 M H_2SO_4; lower concentrations of nitric acid (< 4.5 M) were not suitable as Cd^{2+} forms a stable complex. Finally, it was observed that 4 M HCl was suitable as a stripping agent.

3.4. Effect of Succinic Acid. Very small amounts of succinic was added to the reaction media to inhibit emulsification particularly in the case of Cd^{2+}, Cu^{2+}, and Cr^{3+} transition metal cations. By keeping all other parameters the same, experiments were performed using different concentrations of succinic acid. The best extraction was achieved when 0.01M succinic was used. It is noteworthy to mention that upon addition of the succinic acid into the highly basic buffer solution, the extraction percentage was stabilized probably due to the pH control.

3.5. Nature of the Extracted Species. At first, we studied the effect of pH on the extraction of several transition metal ions with H_8L in nitrobenzene. Specifically, the solvent extraction percentages of Cd^{2+}, Ni^{2+}, Cu^{2+}, Ag^{+}, Co^{2+}, Zn^{2+}, Cr^{3+}, and Mn^{2+} transition metal cations were examined. Figure 1

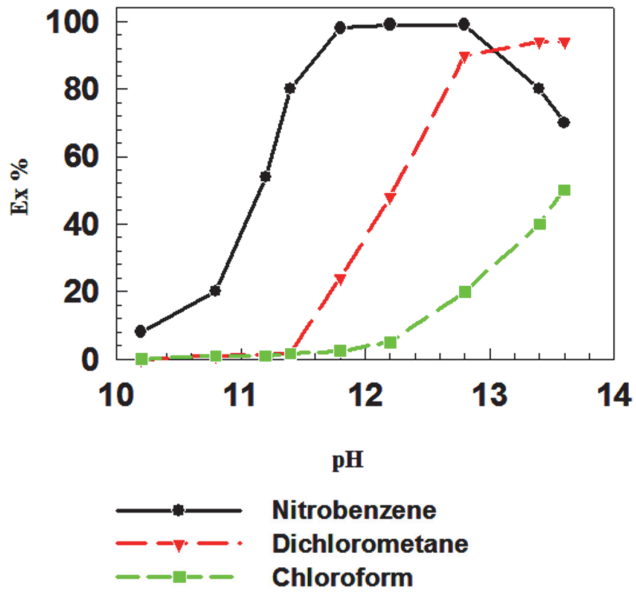

Figure 2: Effect of the organic solvent (nitrobenzene, dichloromethane, or chloroform) on the extraction percentage of Cd^{2+} with H_8L. $H_8L = 5 \times 10^{-4}$ M; aqueous phase [metal ion]: = (●) 5×10^{-5} M. O/A = 1; succinic acid = 0.01 M; and buffer solution, T = 25°C.

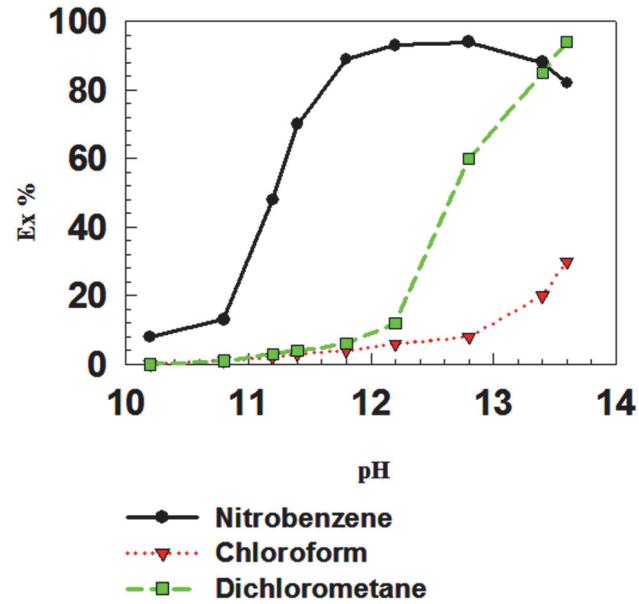

Figure 3: Effect of the organic solvent (nitrobenzene, dichloromethane, or chloroform) on the extraction percentage of Ni^{2+} with H_8L. *p*-calix[8] = 5×10^{-4} M; aqueous phase [metal ion]: = (●) 5×10^{-5} M. succinic acid = 0.01 M and buffer solution, O/A = 1; T = 25°C.

shows that the percentage of metal ions extracted increases as the pH increases from 10.0 to 13.0. In the acidic or neutral pH region, metal ions were not extracted with H_8L, whereas at pH 11.3 more than 60% of metal ions were extracted with H_8L. The maximum extraction percentage was observed in the pH range of the 11.5 to 13.00 for all tested samples. The extractability order is $Cd^{2+} > Ni^{2+} > Cu^{2+} > Ag^{+} > Co^{2+} > Zn^{2+}$. H_8L has phenolic hydroxyl groups which deprotonate at pH > ca.10 and deprotonated H_8L can extract the metal ions. Among the cations tested, almost the same percentages of Cd^{2+} and Ni^{2+} ions were extracted under the experimental conditions. By contrast, no amounts of Cr^{3+} and Mn^{2+} were extracted, possibly due to the formation of a precipitate with ammonia solution. The results indicate that H_8L has a good affinity for complexation with transition metal ions. The study of pH effect indicates that the extraction mechanism depends on a proton exchange mechanism together with hydrogen bonding. Petit et al. also reported a dinuclear cobalt(II) complex of calix[8]arenes compound, prepared by solvothermal reaction of cobalt(II) acetate with *p-t*-butylcalix[8]arene and trimethylamine; the compound was formed by hydrogen bond bridging [33].

The effects of three organic solvents, nitrobenzene, dichloromethane, and chloroform, were examined for both Cd^{2+} (Figure 2) and Ni^{2+} (Figure 3) in the pH range of 10-13.5. Nitrobenzene was very effective as an extractant for both Cd^{2+} and Ni^{2+} metal ions, extracting 96% of these metal ions in the pH range of 11.50-12.70. Dichloromethane was effective in the pH range 11.4-13 for Cd^{2+}, whereas the effective pH range for Ni^{2+} was 12–13. Chloroform was less effective as an extractant at all pH values tested, showing only 50% extraction of Cd^{2+} and Ni^{2+} combined and similar extraction percentages for Cd^{2+} and Ni^{2+} individually. It has been reported that the H_6L complex could be obtained as an adduct with chloroform (1 M); however, chloroform could not be removed from the adduct after calcination at 130°C for 3 days under reduced pressure. This indicates that the chloroform molecule might be encapsulated within the cavity of the calixarene and particularly for p-t-butyl calix[6]arene [H_6L] molecule, which may account for the low extraction percentage obtained in the chloroform solution [25]. Three types of organic solvents were tested and the nitrobenzene is found to be the most efficient. Two other solvents, dichloromethane and chloroform, are least effective. The exact cause of this type of behavior is not known. Masuda et al. observed that the relative descending order of extraction with other solvents is not the same with H_6L and the same order does not necessarily accord the order of their dielectric constants [31]. Actually the extraction percentages of Ce(III) with H_6L were 95%, 27%, and 18% at pH 11.85 in the case of organic solvents nitrobenzene, dichloromethane, and chloroform. The dielectric contestants of nitrobenzene, dichloromethane, and chloroform are 34.82, 7.77, and 4.80, respectively. Therefore, it can be assumed that the dielectric contestant of the medium has some contribution in the extraction process. However, the main factor determining the extraction efficiency in the extraction process must be taken into account and a better term correlating the relative extraction order is solubility parameter. Moreover, Thuéry et al. reported that the reaction at room temperature between H_8L and an excess of trimethylamine in chloroform provided a solid that could be recrystallized in methanol

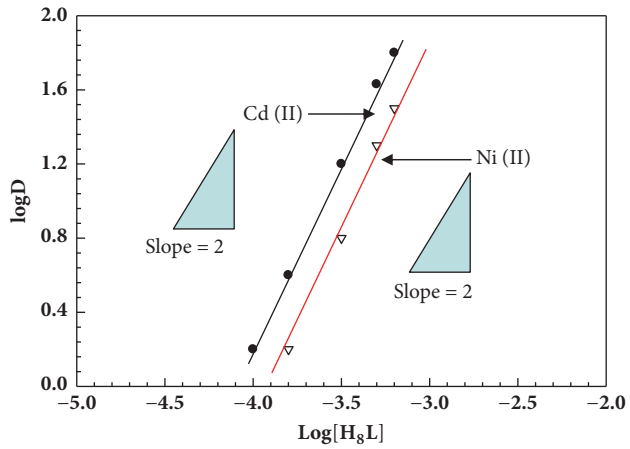

FIGURE 4: Plot of logD vs. log[H_nL] for Cd^{2+} and Ni^{3+} under the same reaction condition of Figure 3.

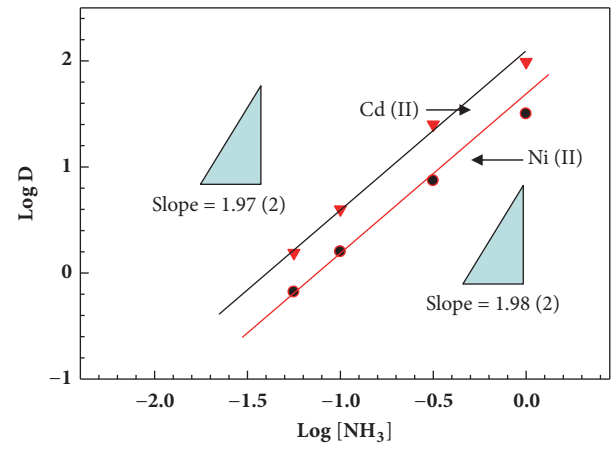

FIGURE 5: Plot of logD vs. log[NH_3] for Cd^{2+} and Ni^{3+} with H_8L under the same reaction condition of Figure 3.

to yield dark red crystals of new compound suitable for X-ray crystallography. Therefore, we can conclude that the chloroform solvents have some affinity and/or suitable for complex formation with H_8L ligand [34].

3.6. Slope Analysis. A traditional and effective means of obtaining both stoichiometric and equilibrium constant information about extraction processes, slope analysis, are based on an examination of the logarithmic variation of the distribution ratio, D, with relevant experimental variables. The log-log plots of the extraction in the form of D vs. a concentration variable indicate the stoichiometry of the formation of the extractable complex and thus lead to the derivation of a suitable equilibrium expression and then to the calculation of equilibrium constants.

Since the extraction reagents exhibited high selectivity for Cd^{2+} and Ni^{2+}, detailed extraction behavior for Cd^{2+} and Ni^{2+} was investigated by slope analysis, the continuous variation method, and by loading tests. The extraction mechanism was studied by evaluating the composition of the extracted Cd^{2+} and Ni^{2+} species. Figure 4 shows the effect of the initial concentration of H_8L in the organic phase on the extraction of Cd^{2+} and Ni^{2+} from an aqueous ammonia solution. With increasing initial concentration of H_8L, straight lines with a slope of 2 were obtained in the logD vs. log[H_8L] plots for Cd^{2+} and Ni^{2+}, indicating that the binding ratio of H_8L with Cd^{2+} and Ni^{2+} is 2:1. Figure 5 shows the effect of the initial concentration of ammonia in the aqueous phase on the extraction of Cd^{2+} and Ni^{2+}. The logD value increases linearly with an increasing initial concentration of ammonia with a slope of 2. These findings suggest that a 2:1 (H_8L: metal) complex was extracted into the organic phase by releasing an equimolar amount of protons from H_8L along with two ammonia molecules.

Distribution experiments were carried out in order to obtain information on the viability of the extraction process, the stoichiometry and distribution equilibrium of the extracted metal ions between phases, and the extent of Cd^{2+} and Ni^{2+} extraction. During this experiment, the

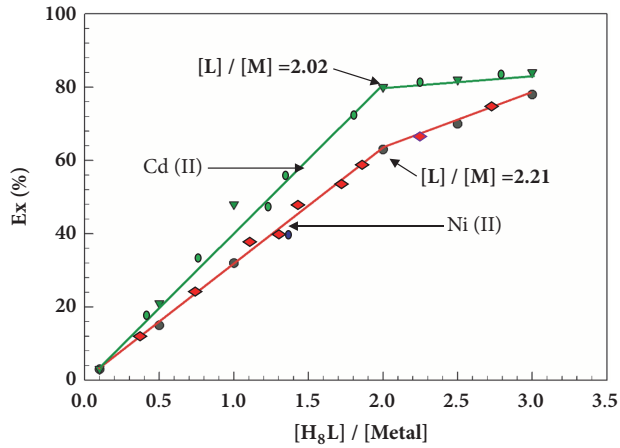

FIGURE 6: Plots of percentage extraction vs. molar ratio [L]/[M] for the extraction of Cd^{2+} and Ni^{3+} with H_8L under the same reaction condition of Figure 3. O:A = 1:1. Symbol (empty green inverted triangle), (filled green circle) (repeated) (filled red diamond) (filled red circle) (repeated)-H_8L; O/A = 1; T = 25°C.

concentrations of Cd^{2+} and Ni^{2+} were kept constant at 1×10^{-3} M, while the concentration of the extractant was varied from 1×10^{-4} to 2×10^{-3} M. This means that the relative concentration of the extractant H_8L (defined as the molar ratio of the initial extractant concentration and the concentration of the extracted metal) changed from 0.1 to 3.4 (Figure 6). A plot of the residual concentration of Cd^{2+} and Ni^{2+} in the aqueous phase, against the relative concentration of extractant, is presented in Figure 6. Initially, experiments were completed three times to examine their reproducibility. These results are also presented in Figure 6. As can be seen, the extraction method showed good reproducibility. An extraction percentage higher than 75% was obtained using H_8L at low concentrations of Cd^{2+} and Ni^{2+}. For Cd^{2+} and Ni^{2+} extracted by the same reaction condition, the higher Ex % of Cd^{2+} must have a high extraction equilibrium constant. That is why the slope of straight line after the inflection point

in Figure 6 becomes more horizontal in green line (Cd^{2+}) than red line (Ni^{2+}).

As mentioned above the molar ratio of H_8L: metal was 2:1. These extraction studies suggest that the 2:1 (H_8L: metal) complex was extracted into the organic phase releasing 1 M protons from 1 M H_8L, accompanying two ammonia molecules [Figures 4 and 5]. The extraction equilibrium and the extraction equilibrium constant K_{ex} can be expressed as

$$M(NH_3)_i^{2+} + 2H_8L_{(o)} + 2NH_3 = M(NH_3)_{i+2}H_6L_{(o)} + 2H^+ \quad (2)$$

$$K_{ex} = \frac{[M(NH_3)_{i+2}H_6L]_o [H^+]^{2+}}{[M(NH_3)_i^{2+}][H_8L]_o^2 [NH_3]^2} \quad (3)$$

where (o) indicates the species in the organic phase. Equation (3) can be simplified as follows using the distribution ratio of the metal ($D = [M(NH_3)_{i+2}H_8L]_o / [M(NH_3)_i^{2+}]$):

$$K'_{ex} = \frac{D[H]^2}{[H_6L]_o^2 [NH_3]^2} \quad (4)$$

$$\log D = \log K'_{ex} + 2\log[H_8L]_o + 2pH + 2\log[NH_3] \quad (5)$$

From the above observations, it is suggested that the ammonia molecules and amine complex participate in the extraction of transition metal ions with H_8L.

The extraction of transition metal ions with H_8L from the aqueous phase, containing 0.1 M ethylenediamine $[C_2H_4(NH_2)_2]$ and 0.1 M trimethylenediamine $[(CH_2)_3(NH_2)_2]$ instead of ammonia, into the dichloromethane solution was also examined. It is worth noting that extraction of Co^{2+} and Ni^{2+} from the aqueous phase containing ethylene diamine was suppressed (Ex% = 0). On the other hand, Cu^{2+} and Cd^{2+} were extracted remarkably well (Cu^{2+} = 100% and Cd^{2+} = 90%) from the aqueous phase containing ethylene diamine. The interaction of calixarenes and amines in the dichloromethane solution likely involves the following two-step process: (i) proton transfers from the calixarene to the amine to form the amine cation and then (ii) the calixarene anion forms an endo-calix complex by association with the amine cation [35]. However, we think these reactions simultaneously take place and reach equilibrium at certain conditions.

To understand complexation in the aqueous phase, the distribution ratio of the $M(en)_2$ and $M(en)_3$ [$(en)_2$= ethylene diamine and $(en)_3$ = trimethylene diamine] species in the aqueous phase about each metal ion before extraction, using the formation constant with ethylene di and triamine, was calculated. Table 1 shows the distribution ratios of the $M(en)_2$ and $M(en)_3$ species in the aqueous phase before extraction and the extraction percentage for extraction with H_8L into dichloromethane. The distribution ratios for the complexations with H_8L are comparable and indicative of high efficiency (Table 1). The values of the distribution ratios of $M(en)_2$ and $M(en)_3$ species in the aqueous phase before extraction are integers. As mentioned above, the extraction

Table 1: Extraction percentage (Ex%) of the transition metal ions with H_8L from ethylene diamine into dichloromethane at 25°C and distribution ratio of $M(en)_2$ and $M(en)_3$ in the aqueous phase before extraction. Uncertainties are given in parentheses as standard errors of the mean (N = 3).

	%E	$M(en)_2$* (%)	$M(en)_3$** (%)
Co(II)	0	0	100
Ni(II)	0	0	100
Cu(II)	97.0 (2)	100	40
Zn(II)	46.0 (3)	3	97
Ag(I)	52.7 (5)	99	35
Cd(II)	90.1 (1)	15	85

∗**$(en)_2$** = ethylene diamine, ∗∗**$(en)_3$** = ethylene triamine.

of Co^{2+} and Ni^{2+} metal ions was suppressed. Thus, most of the existing species in the aqueous phase are $M(en)_3$, while few $M(en)_2$ species were present, whereas in the case of Cu^{2+} most of the extracted species present in the aqueous phase were $M(en)_2$ species. These data suggest that the existence of $M(en)_2$ species diverts and/or controls the extraction with H_8L from the aqueous phase containing ethylene diamine to some extent. This can be explained by steric factors influencing the binding of the ligands to the metal ions. It means that probably the small molecule are encapsulated by larger molecular and steric barriers keep the guest from escaping the host. From the above results, masking effects of metal ions with amines were also observed, particularly metal ions showing high affinity with amines.

We additionally studied the composition of the Cu^{2+} and Cd^{2+} extracted species according to the molar ratio method. A plot of logD vs. log[H_8L] was constructed and a straight line was found with a slope of 1, indicating a molar ratio of H_8L:metal = 1:1, which is different from the composition of species in the case of the ammonia aqueous phase. The effect of pH on the extraction of Cu^{2+} was also verified. As logD increases linearly with an increase in pH, where a slope of 2 was obtained.

Thus, the extraction equilibrium can be expressed as (en= $H_2N(CH_2)_2NH_2$)

$$M_{(en)2}^{2+} + H_8L_{(O)} = M_{(en)2}H_6L_{(O)} + 2H^+ \quad (6)$$

Table 2 shows the elemental analysis data of the Cu^{2+}-H_8L and Cd^{2+}-H_8L complexes. These data indicate that the extracted species from the aqueous phase containing ethylene diamine was $M(en)_2$ not $M(en)_3$, in agreement with our initial assumption based on Table 1.

It has been reported that, in the extraction of metal ions using calix[n]arenes, the metal ion selectivity is related to the ring size of the calix[n]arene and to the radii of the metal ions [9, 10]. The present extraction study using H_8L accompanied by amines indicated that size is key to the selectivity, as the diameter of the H_8L ring (4-4.4 Å) is sufficient to fit the $M(en)_2$ complex (where the distance between the both ends of amino proton is ca. 4.0 Å). A possible structure of Cu^{2+}-H_8L is given in Scheme 1. An X-ray results is essential to

Table 2: Elemental analysis of Cu^{2+}-H_8L and Cd^{2+}-H_8L complexes and estimated chemical formula.

	Cu^{2+}: estimate chemical formula $Cu(en)_2H_6L.5H_2O$				Cd^{2+}: estimate chemical formula $Cd(en)_2\ H_6L.3H_2O$		
	H(%)	C(%)	N(%)		H(%)	C(%)	N(%)
Obs.	8.37	70.89	3.56	Obs.	8.18	69.90	3.49
Calc.	8.73	70.40	3.57	Calc.	8.41	69.83	3.54

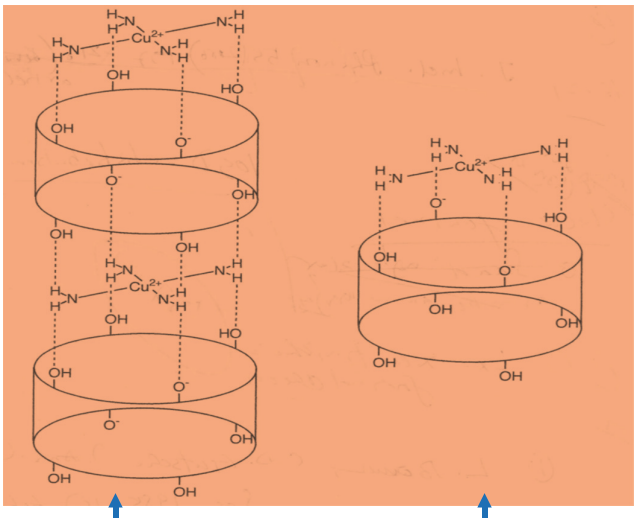

(a) [$Cu(en_2$]n-(H_8L)n (b) $Cu(en)_2$-H_8L

Scheme 1: Structure of $Cu(en)_2$-H_8L complex.

determine a compound structure. At present, our research is now progressing in this direction.

As mentioned above Cd^{2+} is very toxic and inhaling cadmium dust leads to kidney problems which can be fatal. Therefore, complexation studies of Cd^{2+}-H_8L complexes were also performed using FESEM, FTIR, and ^1H NMR spectroscopy for more information of Cd^{2+} extraction with H_8L. FESEM images of H_8L and Cd^{2+}-H8L showed very unique surface morphology. The H_8L had rod-like particles with almost 10 μm long and less than 1 μm wide [Figure 7(a)]. However, the Cd^{2+}-H_8L morphology was totally changed in compare with H_8L alone. The Cd^{2+}-H_8L sample had two types of particle sizes as shown in Figures 7(a) and 7(b), respectively. The nanosize spherical particles were Cd^{2+} ions and the square or bigger size particles were H_8L as evidence by EDX analysis. The EDX and elemental analysis showed almost the same results. It is interesting that the Cd^{2+} ions were homogeneously dispersed and/or distributed over the H_8L ligand. Figure 8(a) shows the EDX spectrum of big particles marked by red arrow in Figure 7(b). The atomic percentage of C was 69.26 for the big size particles. Very little amount of Cd^{2+} was also obtained during EDX analysis of big size particles. On the other hand, the spherical particles had mostly Cd^{2+} ion and atomic percentage of Cd was 33.78 [Figure 8(b), the EDX spectrum of spherical particle was based on Figure 7(c), marked by red arrow]. Almost the same results were obtained for different location based on particles size. The EDX results shown in Figures 8(a) and 8(b) indicate the presence of Cd, C, Au, Cu, and O. The Au and Cu were found due to gold coating over the sample and Cu substrate was used.

The FTIR spectrum of H_8L and Cd^{2+}-H_8L is shown in Figures 9(a) and 9(b), respectively. In the FTIR spectra of the complexes, the intensities or wave numbers of the stretching vibration of the OH groups change drastically with complexation by breakage of the especially strong intramolecular hydrogen bonding existing in the free ligands [30]. The IR absorption bands at 3187 cm^{-1} due to υN-H: free ethylene diamine [36] shifted to 3361 cm^{-1} upon extraction of Cd^{2+} with H_8L. This indicates that hydrogen bonding was likely present in the $M(en)_2$-H_8L complex. The associated natures of $C(CH_3)_3$, $-CH_2-$, and hydroxyl group have been reported previously [30]. The band $C(CH_3)_3$ gives a sharp absorption band at ca. 2944 cm^{-1}, and this peak intensity was weakened after making a complex with Cd^{2+} cation. The ν(C=C) vibration bands shift by about 30 cm^{-1} (i.e., from 1605 to 1638 cm^{-1}) toward higher frequencies. It has been also recorded that the $-CH_2-$ vibrations almost disappeared and the very strong peak at 1489 cm^{-1} was disappeared. The differences in the infrared spectra may be caused by hydrogen bonding. As a whole, all the peaks of Cd^{2+}-H_8L composites were shifted to higher energy direction, indicating the strong interaction between Cd^{2+} and H_8L.

The solution behavior of the complexes was determined by ^1H-NMR spectroscopy in $CDCl_3$ at room temperature. In the spectra of H_8L [Figure 10(a)], and Cd^{2+}-H_8L [Figure 10(b)], each spectrum shows one singlet resonance for protons of -$C(CH_3)_3$ at $\delta = 1.25$. For H_8L, singlet resonances of Ar-H are observed at $\delta = 7.12$ and 7.14 ppm, respectively; for Ar-OH these resonances are at $\delta = 9.63$, respectively. A new signal appeared at chemical shift of $\delta = 2.62$ which was not observed in the H_8L. In our previous study, we also observed one singlet at around δ 3.00 for Ce^{3+}-H_8L and Ce^{3+}-H_6L probably for the bridging methane groups due to the different environments of the hydrogen atoms on the methylene group [30]. In the ^1H NMR spectra, peaks at 3.5 and 4.4 ppm were observed (due to the nonequivalent methylene protons (Ar-CH_AH_B-Ar) in the free H_8L which converge to 3.8 ppm in the $Cd(en)_2$-H_8L complex after extraction. This indicates that the cone conformation of H_8L converts into the 1,3,5,7-alternate conformation.

In this study, the H_8L-ester compounds were also synthesized according to published procedures [37]. The extraction percentage of any metal ion was poor throughout the entire

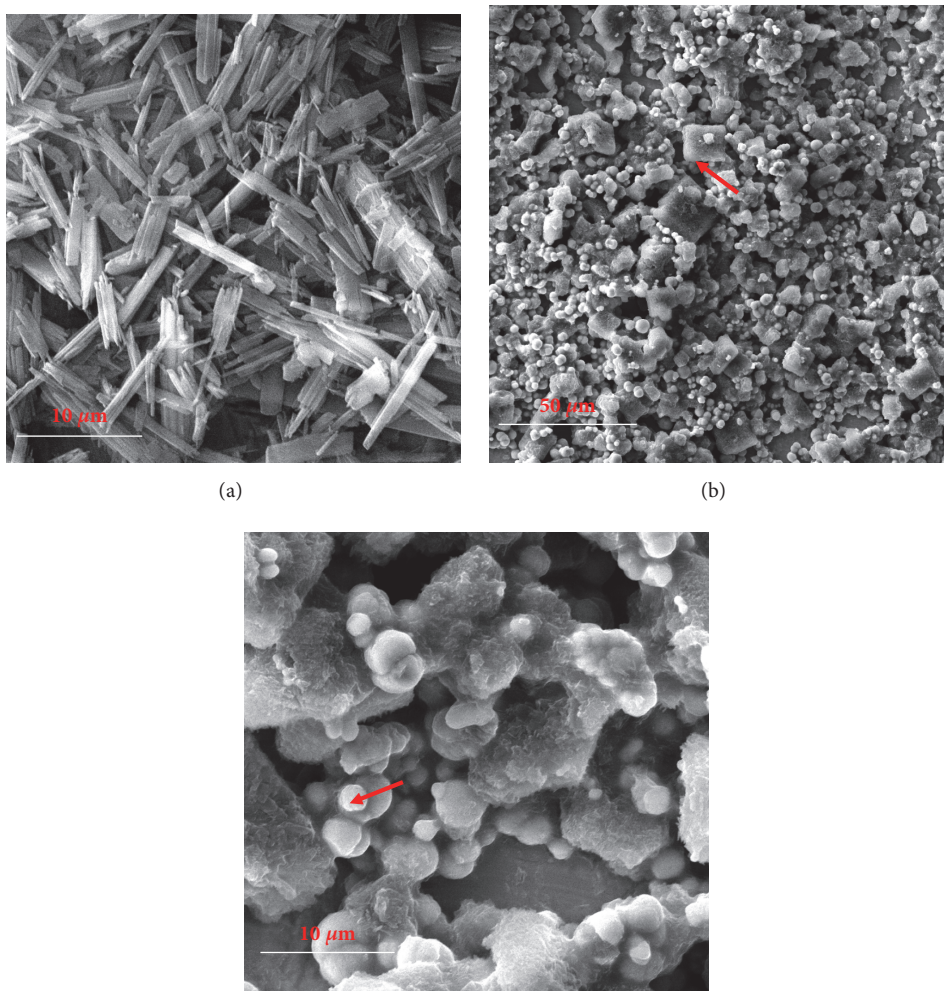

(a) (b)

(c)

Figure 7: FESEM images of the samples: (a) H_8L, (b) Cd^{2+}-H_8L, and (c) sample (b) at high magnification.

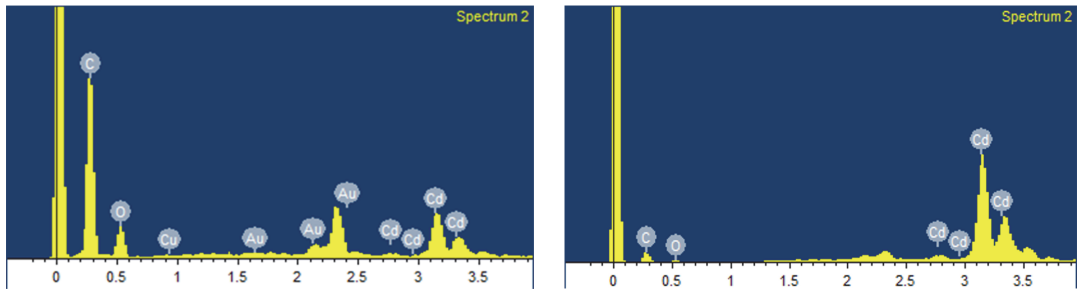

(a) (b)

Figure 8: EDX spectra of (a) H_8L and (b) Cd^{2+}-H_8L. EDX spectra for the region marked by an arrow in (b), and (c) of Cd^{2+}-H_8L in Figure 7.

range of pH used. In fact, the liquid–liquid extraction ability of transition metal ions with the H_8L-ester/$CH_2COOC_2H_5$ derivative was low in comparison with H_8L alone. It is thought that the H_8L becomes an anion due to deprotonation. The H_8L-ester, which is modified from calix[8]arene, is more flexible than both the calix[4]arene and calix[6]arene derivatives; however, it did not show a good extraction capability for Co^{2+}, Ni^{2+}, Zn^{2+}, and Ag^{+}, as shown in Figure 11.

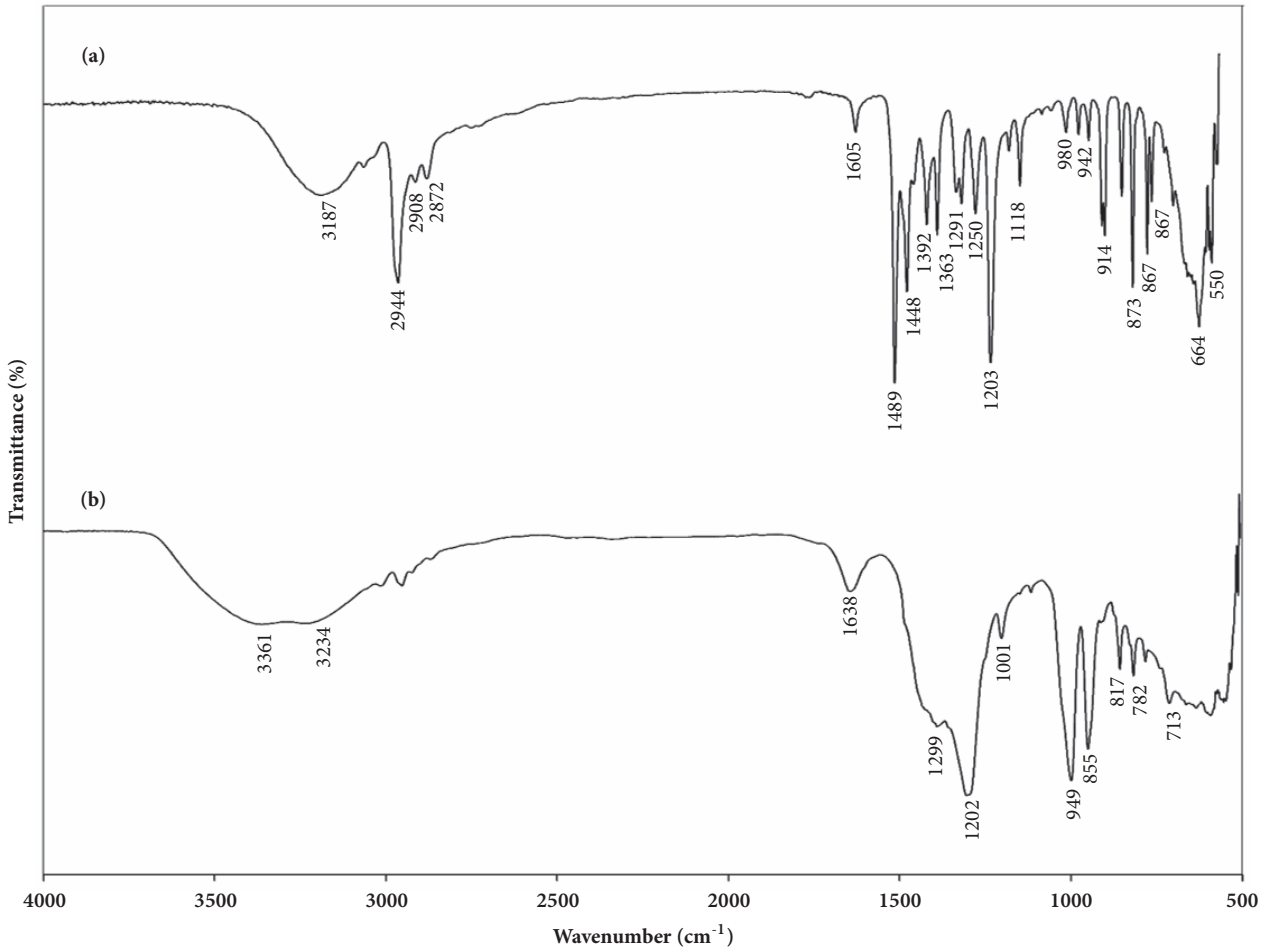

Figure 9: FTIR spectra of (a) H_8L and (b) Cd^{2+}-H_8L.

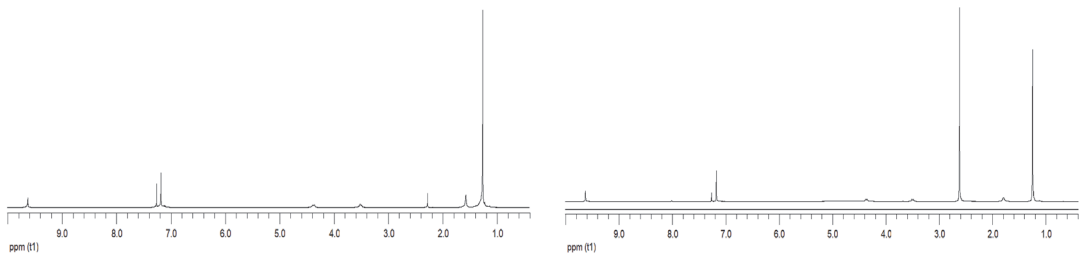

(a) (b)

Figure 10: ^1H NMR spectra of (a) H_8L at 25°C in $CDCl_3$ and (b) Cd-H8L at 25°C in $CDCl_3$ at 400 MHz.

4. Conclusions

The host–guest extraction and/or complexation of divalent heavy metal cations and silver by H_8L and its ethyl ester host was investigated by changing various experimental parameters. The effect of the organic solvent on the extraction procedure was examined. In the solvents, the affinity of H_8L to bind transition metal cations was found to be much higher in the case of Cd^{2+} and Ni^{2+} when ammonia was used as the aqueous phase. The results from the extraction study suggested that, in the case of ammonia, the ratio of the extracted species is 2:1 (H_8L:metal), whereas in the presence of ethylene diamine instead of ammonia, the composition of the extracted species is 1:1, indicating selectivity towards tetrahedral type metal ions. The ester-H_8L compounds were found to be not effective for the extraction of transition metal cations under the present reaction conditions. The extraction behavior of the metal ions was closely related to the pH at equilibrium and the matrix and/or medium (i.e., ammonia or amine) of the aqueous solution and organic phase.

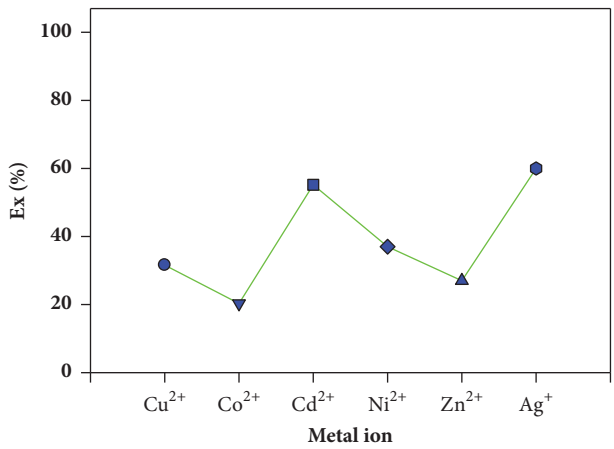

Figure 11: Metal ions percentage extraction (E%) at pH 11.5 by H_8L-ester. O/A = 1; T = 25°C.

Data Availability

The data used to support the findings of this study are available from the corresponding author upon request.

Conflicts of Interest

The authors declare no conflicts of interest.

References

[1] V. Böhmer and J. Vicens, "Special Calixarenes, Synthesis and Properties," in *Calixarenes: A Versatile Class of Macrocyclic Compounds*, vol. 3 of *Topics in Inclusion Science*, pp. 39–62, Springer Netherlands, Dordrecht, 1990.

[2] C. D. Gutsche, "Calixarenes," *The Royal Society of Chemistry, Cambridge*, p. 181, 1989.

[3] K. Ohto, M. Yano, K. Inoue et al., "Effect of coexisting alkaline metal ions on the extraction selectivity of lanthanide ions with calixarene carboxylate derivatives," *Polyhedron*, vol. 16, no. 10, pp. 1655–1661, 1997.

[4] N. N. M. Yusof, Y. Kikuchi, and T. Kobayashi, "Predominant hosting lead(II) in ternary mixtures of heavy metal ions by a novel of diethylaminomethyl-calix[4]resorcinarene," *International Journal of Environmental Science and Technology*, vol. 11, no. 4, pp. 1063–1072, 2014.

[5] N. N. M. Yusof, Y. Kikuchi, and T. Kobayashi, "Ionic imprinted calix[4]resorcinarene host for Pb(II) adsorbent using diallylaminomethyl-calix[4]resorcinarene copolymer," *Chemistry Letters*, vol. 42, no. 10, pp. 1119–1121, 2013.

[6] M. Martínez-Aragón, E. Goetheer, and A. de Haan, "Host–guest extraction of immunoglobulin G using calix[6]arenas," *Separation and Purification Technology*, vol. 65, no. 1, pp. 73–78, 2009.

[7] T. Oshima, M. Goto, and S. Furusaki, "Complex formation of cytochrome c with a calixarene carboxylic acid derivative: A novel solubilization method for biomolecules in organic media," *Biomacromolecules*, vol. 3, no. 3, pp. 438–444, 2002.

[8] R. Ludwig, "Calixarenes in analytical and separation chemistry," *Fresenius' Journal of Analytical Chemistry*, vol. 367, no. 2, pp. 103–128, 2000.

[9] C. D. Gutsche, B. Dhawan, K. H. No, and R. Muthukrishnan, "Calixarenes. 4. The Synthesis, Characterization, and Properties of the Calixarenes from p-tert-Butylphenol," *Journal of the American Chemical Society*, vol. 103, no. 13, pp. 3782–3792, 1981.

[10] C. D. Gutsche and K. C. Nam, "Calixarenes. 22. Synthesis, Properties, and Metal Complexation of Aminocalixarenes," *Journal of the American Chemical Society*, vol. 110, no. 18, pp. 6153–6162, 1988.

[11] X. Chen, R. A. Boulos, A. D. Slattery, J. L. Atwood, and C. L. Raston, "Unravelling the structure of the C60 and p-But-calix[8]arene complex," *Chemical Communications*, vol. 51, no. 57, pp. 11413–11416, 2015.

[12] J. L. Atwood, L. J. Barbour, M. W. Heaven, and C. L. Raston, "Controlling van der Waals Contacts in Complexes of Fullerene C60," *Angewandte Chemie International Edition*, vol. 42, no. 28, pp. 3254–3257, 2003.

[13] C. Geraci, G. Chessari, M. Piattelli, and P. Neri, "Cation encapsulation within a ten-oxygen spheroidal cavity of conformationally preorganized 1,5-3,7-calix[8]bis-crown-3 derivatives," *Chemical Communications*, no. 10, pp. 921-922, 1997.

[14] C. Redshaw, "Coordination chemistry of the larger calixarenes," *Coordination Chemistry Reviews*, vol. 244, no. 1-2, pp. 45–70, 2003.

[15] T. Kajiwara, N. Iki, and M. Yamashita, "Transition metal and lanthanide cluster complexes constructed with thia-calix[n]arene and its derivatives," *Coordination Chemistry Reviews*, vol. 251, no. 13-14, pp. 1734–1746, 2007.

[16] R. Ludwig and N. T. K. Dzung, "Calixarene-based molecules for cation recognition," *Sensors*, vol. 2, no. 10, pp. 397–416, 2002.

[17] C. J. Liu, J. T. Lin, S. H. Wang, J. C. Jiang, and L. G. Lin, "Chromogenic calixarene sensors for amine detection," *Sensors and Actuators B: Chemical*, vol. 108, no. 1-2, pp. 521–527, 2005.

[18] R. M. Izatt, J. D. Lamb, R. T. Hawkins, P. R. Brown, S. R. Izatt, and J. J. Christensen, "Selective M+-H+ Coupled Transport of Cations through a Liquid Membrane by Macrocyclic Calixarene Ligands," *Journal of the American Chemical Society*, vol. 105, no. 7, pp. 1782–1785, 1983.

[19] S. R. Izatt, R. T. Hawkins, J. J. Christensen, and R. M. Izatt, "Cation Transport from Multiple Alkali Cation Mixtures Using a Liquid Membrane System Containing a Series of Calixarene Carriers," *Journal of the American Chemical Society*, vol. 107, no. 1, pp. 63–66, 1985.

[20] L. Mutihac and R. Mutihac, "Liquid-liquid extraction and transport through membrane of amino acid methylesters by calix[n]arene derivatives," *Journal of Inclusion Phenomena and Macrocyclic Chemistry*, vol. 59, no. 1-2, pp. 177–181, 2007.

[21] S. Ayata and M. Merdivan, "P-tert-Butylcalix[8]arene loaded silica gel for preconcentration of uranium(VI) via solid phase extraction," *Journal of Radioanalytical and Nuclear Chemistry*, vol. 283, no. 3, pp. 603–607, 2010.

[22] L. N. Puntus, A.-S. Chauvin, S. Varbanov, and J.-C. G. Bünzli, "Lanthanide complexes with a calix[8]arene bearing phosphinoyl pendant arms," *European Journal of Inorganic Chemistry*, no. 16, pp. 2315–2326, 2007.

[23] G. Suganthi, C. Meenakshi, and V. Ramakrishnan, "Molecular recognition of 1,5 diamino anthraquinone by p-tert-butyl-calix(8) arene," *Journal of Fluorescence*, vol. 20, no. 5, pp. 1017–1022, 2010.

[24] S. Erdemir, M. Bahadir, and M. Yilmaz, "Extraction of carcinogenic aromatic amines from aqueous solution using calix[n]arene derivatives as carrier," *Journal of Hazardous Materials*, vol. 168, no. 2-3, pp. 1170–1176, 2009.

[25] I. Yoshida, S. Fujii, K. Ueno, S. Shinkai, and T. Matsuda, " Solvent Extraction of Copper(II) Ion with ," *Chemistry Letters*, vol. 18, no. 9, pp. 1535–1538, 1989.

[26] E. Tashev, M. Atanassova, S. Varbanov et al., "Synthesis of octa(1,1,3,3-tetramethylbutyl)octakis(dimethylphosphinoylmethyleneoxy) ca lix[8]arene and its application in the synergistic solvent extraction and separation of lanthanoids," *Separation and Purification Technology*, vol. 64, no. 2, pp. 170–175, 2008.

[27] E. Makrlík, P. Vaňura, and P. Selucký, "Solvent extraction of europium trifluoromethanesulfonate into nitrobenzene in the presence of p-tert-butylcalix[6]arene and p-tert-butylcalix[8]arene," *Journal of Radioanalytical and Nuclear Chemistry*, vol. 287, no. 1, pp. 277–280, 2011.

[28] F. Sansone, M. Fontanella, A. Casnati et al., "CMPO-substituted calix[6]- and calix[8]arene extractants for the separation of An3+/Ln3+ from radioactive waste," *Tetrahedron*, vol. 62, no. 29, pp. 6749–6753, 2006.

[29] R. Pathak and G. N. Rao, "Synthesis and metal sorption studies of p-tert-butylcalix[8]arene chemically bound to polymeric support," *Analytica Chimica Acta*, vol. 335, no. 3, pp. 283–290, 1996.

[30] Md. Hasan Zahir, "Synthesis and Characterization of Trivalent Cerium Complexes of p-tert-Butylcalix[4,6,8]Arenes: Effect of Organic Solvents," *Journal of Chemistry*, vol. 2013, pp. 1–9, 2013.

[31] Y. Masuda and Md. H. Zahir, "The host-guest extraction chemistry of lighter lanthaniod (III) metal ions with p-t-butylcalix[6]arene from the ammonia alkaline solution in presence of succinic acid," *Analytical Sciences*, vol. 17, pp. a483–a486, 2001.

[32] A. K. De, "Environmental Chemistry, New age international Ltd," *Inorganic Chemistry and Analysis through Problems and Exercises*, pp. 80-81, 2005.

[33] S. Petit, G. Pilet, D. Luneau, L. F. Chibotaru, and L. Ungur, "A dinuclear cobalt(ii) complex of calix[8]arenes exibiting strong magnetic anisotropy," *Journal of the Chemical Society, Dalton Transactions*, no. 40, pp. 4582–4588, 2007.

[34] P. Thuéry and M. Nierlich, "The first metal complex of an acyclic hexaphenol: structure of the binuclear complex of uranyl ions with an analogue of p-tert-butylcalix[6]arene," *Journal of the Chemical Society, Dalton Transactions*, no. 9, pp. 1481-1482.

[35] E. Akceylan, M. Bahadir, and M. Yilmaz, "Removal efficiency of a calix[4]arene-based polymer for water-soluble carcinogenic direct azo dyes and aromatic amines," *Journal of Hazardous Materials*, vol. 162, no. 2-3, pp. 960–966, 2009.

[36] C. J. Pouchert, *The Aldrich library of IR spectra*, Aldrich Chemical Company, Inc., 3rd edition.

[37] G. M. L. Consoli, F. Cunsolo, M. Piattelli, and P. Neri, "Study on the esterification of p-tert-butylcalix[8]arene," *The Journal of Organic Chemistry*, vol. 61, no. 6, pp. 2195–2198, 1996.

Hindawi
International Journal of Analytical Chemistry
Volume 2018, Article ID 1710438, 11 pages
https://doi.org/10.1155/2018/1710438

Research Article

TEMPO-Functionalized Nanoporous Au Nanocomposite for the Electrochemical Detection of H_2O_2

Dongxiao Wen,[1] Qianrui Liu,[2] Ying Cui,[1] Huaixia Yang ,[1] and Jinming Kong [2]

[1] *Pharmacy College, Henan University of Chinese Medicine, Zhengzhou 450008, China*
[2] *School of Environmental and Biological Engineering, Nanjing University of Science and Technology, Nanjing 210094, China*

Correspondence should be addressed to Huaixia Yang; yanghuaixia886@163.com and Jinming Kong; j.kong@njust.edu.cn

Received 8 March 2018; Accepted 26 April 2018; Published 10 June 2018

Academic Editor: Seyyed E. Moradi

A novel nanocomposite of nanoporous gold nanoparticles (np-AuNPs) functionalized with 2,2,6,6-tetramethyl-1-piperidinyloxy radical (TEMPO) was prepared; assembled carboxyl groups on gold nanoporous nanoparticles surface were combined with TEMPO by the "bridge" of carboxylate-zirconium-carboxylate chemistry. SEM images and UV-Vis spectroscopies of np-AuNPs indicated that a safe, sustainable, and simplified one-step dealloying synthesis approach is successful. The TEMPO-np-AuNPs exhibited a good performance for the electrochemical detection of H_2O_2 due to its higher number of electrochemical activity sites and surface area of 7.49 m^2g^{-1} for load bigger amount of TEMPO radicals. The TEMPO-functionalized np-AuNPs have a broad pH range and shorter response time for H_2O_2 catalysis verified by the response of amperometric signal under different pH and time interval. A wide linear range with a detection limit of 7.8×10^{-7} M and a higher sensitivity of 110.403 μA $mM^{-1}cm^{-2}$ were obtained for detecting H_2O_2 at optimal conditions.

1. Introduction

Hydrogen peroxide (H_2O_2) is the smallest and simplest peroxide, which could be generated in many biological processes and cause severe oxidative damage [1–3]. It has been applied in many biosynthetic reactions and also plays an important role in various fields, especially in immune cell activation, vascular remodelling, apoptosis, stomatal closure, root growth, and so on [1, 4]. Because of this, many practical explorations have been done in the detection and monitoring of H_2O_2 in pharmaceutical [1–6], biological [5, 6], clinical [1, 3, 7], chemical, textile [1, 2, 8–10], and food industries [1–6, 10]. The dynamic equilibrium of the production and consumption of H_2O_2 is closely interlinked with the quality of our life; therefore, the development of new materials and techniques for quantitative detection of H_2O_2 at a trace level has presented a significant role in the fundamental studies of diagnostic and monitoring applications. However, most existing techniques suffer from many drawbacks, such as inherent instability, time consuming, poor selectivity, low activity, complicated, and costly immobilization procedures [1–3, 9–11]. Thus, it is necessary to develop new electrochemical sensors overcoming those drawbacks for accurate and sensitive detection of H_2O_2.

A number of new materials such as metals nanomaterials, carbon nanotubes, quantum dots, nanocomposites, and redox substances have been employed for the detection of H_2O_2 [1–9]. In recent studies, nanoscale hollow materials have attracted scientists' attention for their unique porous structural and versatile properties. There have been some reports already about its applications in fuel cell and remarkable catalytic oxidation activities to CO, methanol, hydrazine, and so on [12–15]. Particularly, nanoporous gold nanoparticles (np-AuNPs), one of the most important nanoscale hollow materials, combining their high surface areas with tunable surface plasmon resonance (SPR) features, can serve larger immobilized surface and excellent catalytic sites in chemical reactions and also provide a substrate material to manufacture functionalized nanocomposite [12, 15]. Meanwhile, TEMPO plays a key role in chemistry and biology as an organic redox catalyst for alcohol, aldehydes, and ketones [16–21] and has shown its catalytic oxidation potential to

H_2O_2 due to the electrochemical oxidation of stable nitroxyl radical [22, 23]. Recently, the nitroxyl radical of TEMPO has been reported to attach to solid surfaces by chemical routes to form supramolecular assemblies with high coverage of catalytic radicals [24, 25]. Based on considerations above, in order to take full advantage of their inherent catalytic oxidation activity of the np-AuNPs and the TEMPO, we explore the synergistic effect of TEMPO-functionalized np-AuNPs for the peroxidase-like activity response and use this feature for H_2O_2 detection.

Most nanoporous materials are prepared by using traditional dealloying, template, electrochemical methods, and directed self-assembly [9, 10, 26], and the dealloying approach is mostly adopted to synthesize various nanoporous hollow structures [12–15], using AgCl templates to get the nanoporous gold [12, 26, 27]. However, this traditional dealloying approach is limited by its harsh cumbersome and high-heat conditions [12, 28]. In this work, we prepared the zero-dimensional hollow np-AuNPs via an improved one-step dealloying synthesis in moderate conditions instead of traditional two-step dealloying methods. To improve the peroxidase-like activity of the np-AuNPs and TEMPO, we assembled mercaptoacetic acid (MA) on the surfaces of np-AuNPs/GCE, and then the 4-carboxy-TEMPO was connected to the mercaptoacetic acid through Zr^{4+} as the bridge bond. The np-AuNPs were characterized by scanning electron microscopy (SEM) and UV-Vis spectroscopy, and the TEMPO-contained nanocomposites characterized its electrochemical active area by cyclic voltammetry in different electrolytic buffer. Finally, its amperometric response of TEMPO-np- AuNPs/ GCE to detect H_2O_2 was exploited.

2. Experimental

2.1. Chemical Reagents. Silver nitrate (99%), $HAuCl_4{\cdot}3H_2O$ (>99.9%), hydroquinone (>99%), H_2O_2 (30wt% aqueous), and mercaptoacetic acid (MA) were obtained by Sinopharm Chemical Reagent Co., Ltd. (Beijing). The polyvinylpyrrolidone (PVP, MW 1,300,000) was purchased from J&K Scientific Ltd. Zirconium dichloride oxide octahydrate ($ZrOCl_2{\cdot}8H_2O$) and 4-carboxy-2,2,6,6-tetramethylpiperidine-1-oxyl free radical (4-carboxy-TEMPO) came from Sigma-Aldrich (St. Louis, MO) and TCI (Shanghai) Development Co., Ltd., respectively. 0.1 M PBS supporting electrolyte was prepared by orthophosphoric acid and its salts (0.1 M Na_2HPO_4, 0.1 M NaH_2PO_4), pH=4.0-9.0. All reagents were of analytical grade.

2.2. Apparatus. A scanning electron microscopy (SEM, Hitachi S-4800, Japan) was employed to study the morphology of nanoporous gold nanoparticles and TEMPO-MA-np-AuNPs on the electrode. The UV-Vis absorption peak was carried on a UV-3600 spectrophotometer (SHIMADZU). All data of electrochemical studies were obtained with an electrochemical workstation (CHI 760D, Chenhua, Shanghai) at the room temperature. A platinum wire auxiliary electrode, a saturated calomel reference electrode, and a modified glassy carbon electrode (GCE, Φ=3 mm, as the working electrode) are included in a standard three-electrode cell. All ultrapure water (≥18.25 MΩ) for experiments was obtained from a Millipore Milli-Q water purification system.

2.3. Preparation of Nanoporous Gold Nanoparticles. The nanoporous gold nanoparticles (np-AuNPs) were prepared according to the literature with some modification [12]. Briefly, 160 μL solution of hydroquinone (28 mM) and 10 mM $AgNO_3$ aqueous solution (60 μL) were mixed firstly into 4.5 mL PVP solution (90 mM) in sequence. Then the mixed system came to an equilibrium stirring for 5s, 650 r.m.p. Next, 40 mM $HAuCl_4$ (100 μL) was added dropwise into the system at room temperature under gentle stirring. After 3 min standing, the color of the reaction liquid turned to stable (reddish brown), and then the residual AgCl, which is formed during the reaction, was removed by the additional concentrated NH_4OH (1 mL). Finally, the resulting solution was centrifuged and washed repeatedly with ultrapure water, 7,000 r.p.m. 5 min, to collect the np-AuNPs. Finally, 1.0 mg of np-AuNPs sample was fully suspended in a mixed solution (1.0 mL ethanol, 1.0 mL of 90 mM PVP) by ultrasonication.

2.4. Electrode Fabrication of Tempo-Np-Au NPs/GCE. The bare glassy carbon electrode (GCE) was polished with 0.30μM Al_2O_3 slurries on the chamois leather until a mirror-like surface is obtained. Next, it was ultrasonically cleaned with absolute ethanol and ultrapure water, dried with N_2. Then, the electrode was subjected to cyclic voltammetry (CV) in 0.1 M KCl with the potential of -0.4V and 1.6 V, at a scan rate of 100 mVs^{-1}, until the reproducible cyclic voltammograms were obtained.

A quantity of 1μL of the prepared np-AuNPs suspension was dropped on the surface of freshly pretreated bare GCE above. After the GCE was air dried at room temperature, 20 μL of 0.2 mM MA solution was added onto the np-AuNPs/GCE surface and incubated for 1.0 h at room temperature; by so doing, a MA self-assembled monolayer formed on the surface of np-AuNPs (MA-np-AuNPs/GCE) via chemisorption and the chemistry of formation of MA-SAM on the np-AuNPs surface; a procedure probably involves the oxidative addition to form the S-Au bond by losing the hydrogen as H_2 or H_2O [29, 30]. Subsequently, the TEMPO-np-AuNPs/GCE was prepared by carboxylate- zirconium-carboxylate chemistry [31–33]. After washing the MA-np-AuNPs/GCE with ultrapure water to remove the remaining MA, the electrode was immersed in $ZrOCl_2{\cdot}8H_2O$ 60% ethanol solution (5.0 mM) for 30 min. The modified electrode was taken out and then washed with absolute ethanol, dried with N_2. Next, the electrode was incubated in 20 μL of 0.2 mM 4-carboxy-TEMPO solution for 30 min, followed by rinsing with ultrapure water to remove remaining reactants. TEMPO-functionalized nanoporous Au nanocomposite electrode was prepared. The establishment of this sensor for H_2O_2 detection is depicted in Figure 1.

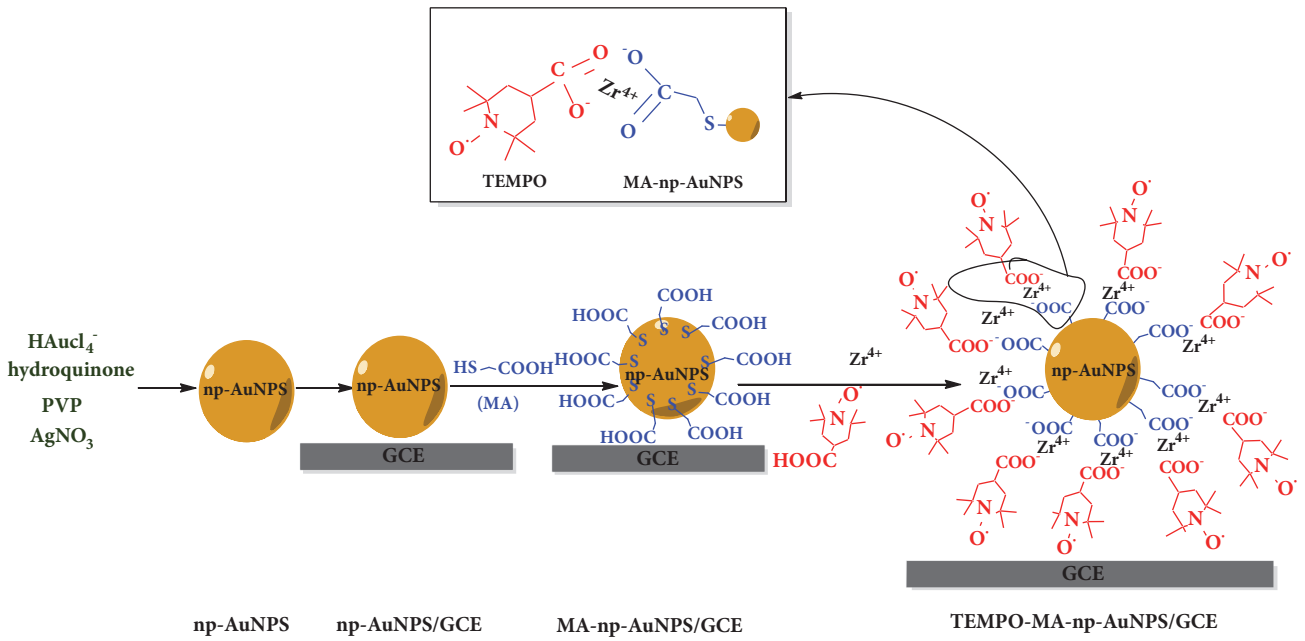

FIGURE 1: Preparation of TEMPO-MA-np-AuNPs/GCE for the electrochemical determination of H_2O_2.

3. Results and Discussion

3.1. Characterization of Modified Electrode by SEM and UV-Vis. By following procedures above, we successfully synthesized the free-standing np-AuNPs under moderate conditions by using a one-step aqueous solution-based approach, which circumvents the limits of stringent and harsh multistep protocols of traditional dealloying approaches. As shown in Figures 2(a) and 2(b), SEM images indicate that the as-synthesized np-AuNPs have a shape of spherical and exhibit an extremely roughened surface, which is consistent with the result of Srikanth's report [12].

As it has been known to all, AgNPs and AuNPs including np-AuNPs are attractive due to their surface plasmon resonance (SPR) properties. Ag^+ AuNPs and np-AuNPs often exhibit different spectral absorptions in the UV-Vis wavelength region [26, 34]. Therefore, we can use absorption spectroscopy to monitor the process of reaction; the UV-Vis spectral absorptions of the as-prepared np-AuNPs are shown In Figure 2(c). A peak appeared at 324 nm, which is the typical UV-Vis absorbance peak of Ag^+ [34]. After 100μL $HAuCl_4$ solution was added in the system, a significant increase of signal appeared at 530 nm, which is caused by the grown of AuNPs on the surface of AgCl templates in the kinetic-controlled process [35]. Subsequently, with NH_4OH added to stop the reaction, the surface plasmon resonance (SPR) peak of 530 nm underwent a red shift to 596 nm-700 nm with longer and broader profile, which belongs to the characteristic peak of porous gold nanoparticles. The typical SPR peak of AuNPs always exhibited around 530 nm; the Ag° broad peak maximum usually occurs at 410 nm, in solution [34]. It was found that, after the centrifuge step to remove residual AgCl, the absorbance peak at 324 nm disappeared, indicating the formation of the np-AuNPs.

3.2. Characterization of Modified Electrode by Cyclic Voltammetry. To characterize the modified electrode TEMPO-np-AuNPs, the typical cyclic voltammetry was performed. The cyclic voltammogram (CV) curves of different modified electrodes in the absence of oxygen in 0.1 M PBS supporting electrolyte (pH = 7.0), at 50 mVs^{-1}, are shown in Figure 3(a). For the bare GCE, there are no redox peaks (A). With the np-AuNPs added on the GCE surface, a broad peak arose at 1.2-1.5V (B) due to the increased effective electroactive area of np-AuNPs. What is more, when MA self-assembled on the np-AuNPs, an obvious peak increase was observed due to the S-Au bond formation (C). By comparing the CVs of C and D, a new pair of well-behaved redox peaks of 0.38 V (cathodic peak) and 0.82 V (anodic oxidation peak) was obtained after 4-carboxy-TEMPO was finally attached to the former-electrode surface. In addition, the decreases of a pair of peaks at -0.1 V/1.2-1.5 V due to the steric hindrance also indicted that 4-carboxy-TEMPO was successfully connected with MA-np-AuNPs via carboxylate-zirconium-carboxylate chemistry.

Further, we characterized the formed np-AuNPs with electroactive activity through CV at different scan rates from 10 mVs^{-1} to 200 mVs^{-1}. As shown in Figure 3(b), the intensities of the electric current increased linearly along with the increase of scan rates (k_1 = 3.934 (± 0.122)), which confirmed that the electroactive np-AuNPs attached on the GCE electrode surface by adsorption according to the theory of homogeneous redox catalysis [22], rather than other interactions. As mentioned above, the CV of TEMPO-np-AuNPs has a new pair of redox peak (0.38 V/0.82 V), while the CV of np-AuNPs did not. As displayed in Figure 2(c), with the scan rates increasing, the current intensity of this redox couple enhanced with a slight redshift; both the I_{pa} (black spots) and I_{pc} (red spots) peak currents were linearly proportional to

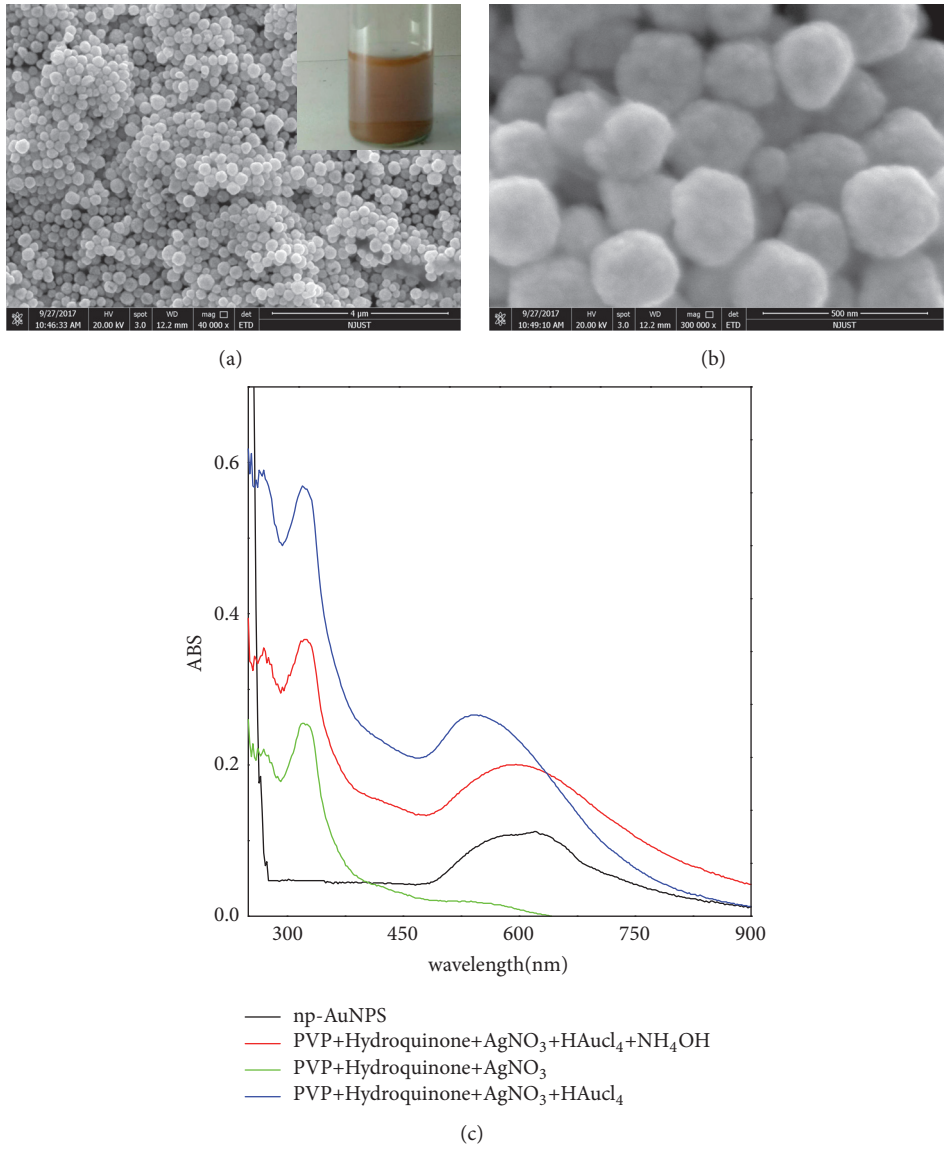

Figure 2: SEM images (a and b) of nanoporous gold nanoparticles (np-AuNPs) and typical UV-Vis absorption spectra (c) of the reactions during the prepared process of np-AuNPs.

the scan rate. Their slopes, respectively, were k_{pa} = 0.290 (± 0.005) and k_{pc} = -0.456 (± 0.011). Those behaviors illustrate that the modified np-AuNPs (TEMPO-np-AuNPs) had the adsorption with the GCE electrode surface, which are in accordance with the np-AuNPs and literatures [42, 43].

3.3. Electrochemical Measurement of Np-AuNPs Active Surface Areas. The effective areas of different surface modification were estimated by CV method. As shown in Figure 3(d), the anodic oxidation current of the three curves all rose at about 1.2 V and had a typical reduction peak around 0.75 V, which is caused by the reversible redox reaction in 0.5 M H_2SO_4. However, the MA-np-AuNPs (B) exhibit a higher peak at 0.75 V and sustain a large redshift as compared with np-AuNPs (A), indicating that it is hard to be oxidized with H_2SO_4 due to the increased impedance of charge transfer after MA is immobilized on the surface of np-AuNPs. When the TEMPO is chemically modified on MA-np-AuNPs (C), the cathodic peak (around 0.75 V) had an obvious enhancement, which may be caused by the diffusion layer of TEMPO· and is a three-dimensional steady-state. Besides, the rough porous surface of np-AuNPs contributed to generate the multimodal of the curve (e.g., 0.20 V-0.45 V of curve C).

For each experiment, the amount of np-AuNPs used was the same; CV of np-AuNPs in 0.5 M H_2SO_4 (A) were measured to calculate their electroactive surface areas via integrating the area of the gold oxide reduction curve. An electroactive surface area of 7.49 m^2g^{-1} for np-AuNPs is obtained by Randles-Sevcik equation and assuming a specific charge of 450 μC cm^{-2} for the gold oxide reduction [12, 44]. Notably, the active surface areas of np-AuNPs are higher than that of the commercial Au electrodes, Au nanoparticle, Au

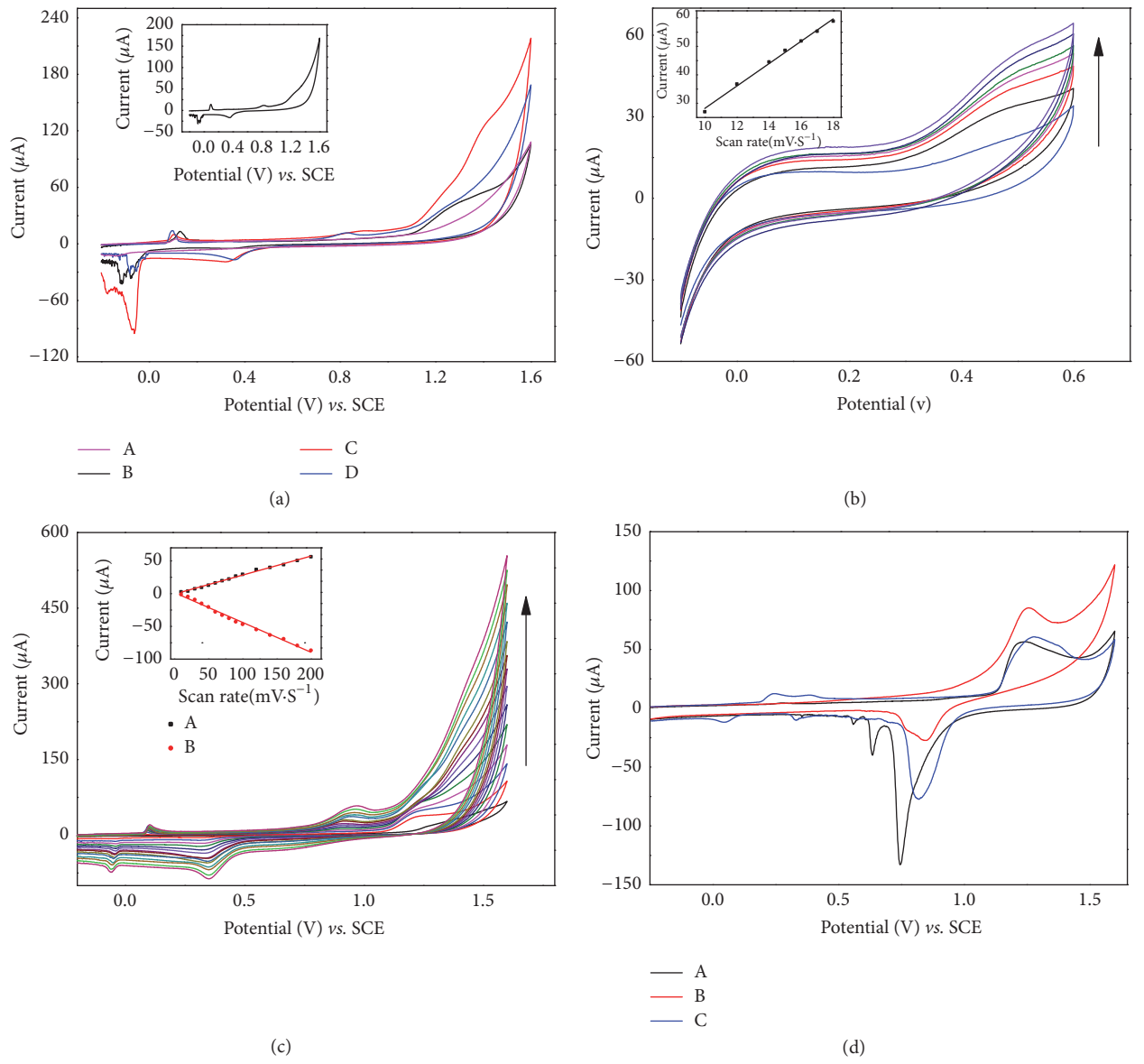

FIGURE 3: **(a)** Different modified GCE in 0.1 M PBS (pH = 7.0) under N_2. Scan rate: 50mVs^{-1}. (A) Bare GCE, (B) np-AuNPs/GCE, (C) MA-np-AuNPs/GCE, and (D and inset) TEMPO-np-AuNPs/GCE. CVs of np-AuNPs **(b)** and TEMPO-np-AuNPs (**c**) on the GC electrode surface under N_2, 0.1 M PBS (pH = 7.0) at different scan rates from 10mVs^{-1} to 200mVs^{-1}. Inset: (**b**) the linear relationship between the scan rate and the currents at a potential of 0.55V. (**c**) The linear relationship between anodic (black spots, at 0.95 V) and cathodic (red spots, at 0.38 V) peak currents and scan rate. **(d)** CVs of different electrodes in 0.5 M H_2SO_4 under N_2, 0.1 M PBS (pH = 7.0) at a scan rate of 100 mVs^{-1}.(A) np-AuNPs, (B) MA-np-AuNPs, and (C) TEMPO-np-AuNPs.

nanocoral, and other kinds of Au electrodes [45], near 49 times high according to report. The large surface-to-volume ratio of metal nanoparticles is closely related to its high electrical conductivity, catalytic ability, and surface reaction activity such as for the detection of H_2O_2 [2, 45].

3.4. Electrochemical Detection of H_2O_2. As we have known already, the electrochemical behavior of np-AuNPs modified GCE electrode for H_2O_2 was studied by CV. As shown in Figure 4(a), when 3 mM H_2O_2 was added to 0.1 M phosphate buffer saline (pH=7.0) under N_2, compared to the bare GCE, distinct increases of the AuNPs/GCE and np-AuNPs/GCE response currents were observed. Interestingly, the np-AuNPs/GCE had a significant advantage in the difference of the current intensity (ΔI) under the same condition in the presence of H_2O_2. As one of the most famous catalytic materials, Au nanomaterials with different shapes and structures have been suggested good responses for electrocatalytic H_2O_2 [1–3].The current responses toward H_2O_2 concentration over the range of 0.5 μM-100 μM on the np-AuNPs/GCE (Figure 4(b)) were studied. The current intensity had a steady rise with the increasing of H_2O_2 concentration. The HO· radical resulted from H_2O_2 would

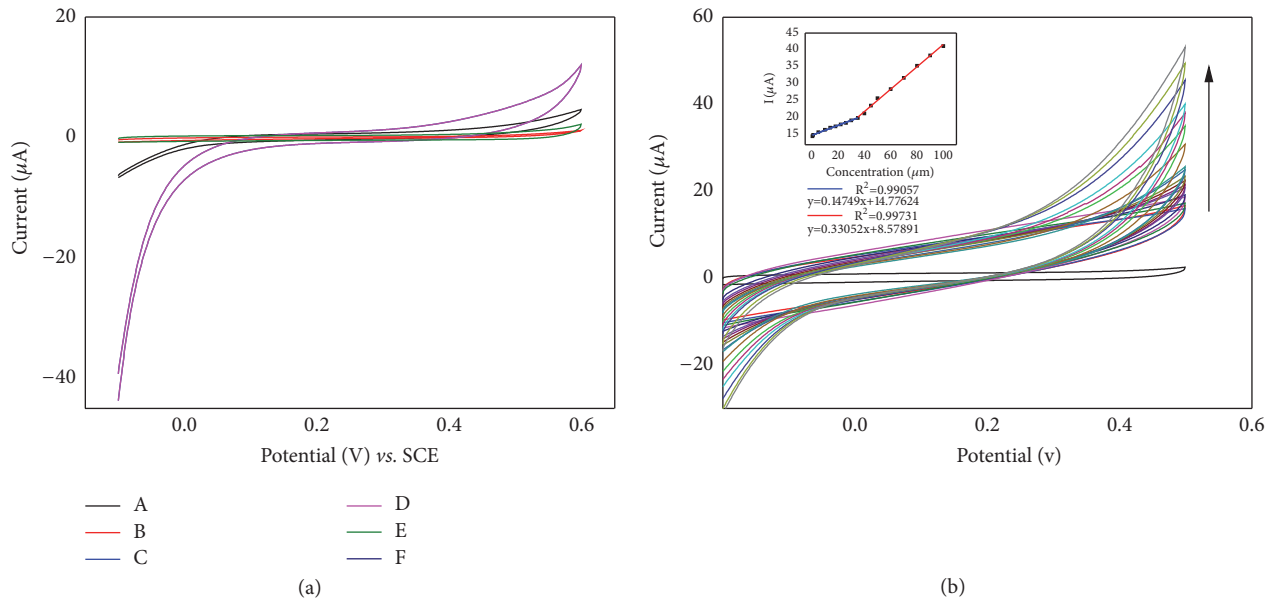

FIGURE 4: **(a)** CVs of electrodes in the absence (A-C) and presence (D-F) of H_2O_2 (3mM) in N_2-saturated 0.1 M PBS (pH = 7.0). Scan rate: 20mVs^{-1}. (A and E) Bare GCE (curves B and F) AuNPs/GCE (curves C and D) np-AuNPs/GCE. **(b)** CVs of np-AuNPs/GCE in 0.1 M PBS (pH = 7.0) with N_2 toward different concentrations of H_2O_2 over the range of 0.5 μM to 100 μM. Applied potential: 0.55 V. Inset: plot of electrocatalytic current of H_2O_2 versus its concentrations.

be stabilized by the np-AuNPs [3, 46]. The surface property of np-AuNPs may influence the catalytic ability of H_2O_2 and the charge-transfer processes. When the H_2O_2 concentration is below 26 μM, it exhibited a linear correlation of I (μA) = 0.14749 C (μM) +14.77624 (R^2 = 0.99057, RSD = 4.2%) between 0.5 μM and 26 μM. With the increase of stable surface charge transfer for the continuous regeneration of charge-transfer complex [47], it may fill the concave surface of np-AuNPs, and the slope (K_b) of the oxidation catalytic linear response grew to 0.3305 (R^2 = 0.9973) in the range of 26 μM-100 μM. Results of np-AuNPs /GCE show a good catalytic detection activity to H_2O_2.

CV voltammograms of different product on GC electrode in the absence and presence of hydrogen peroxide were shown in Figure 5(a). When H_2O_2 was put into 0.1 M PBS electrolyte buffer, an obvious increase of the peak current at 0.95 V in the CV of TEMPO-np-AuNPs is observed unlike that of smooth curves in other CVs. To ascertain the synergistic peroxidase-like activity between the TEMPO and np-AuNPs, we compared the net current strengths (ΔI) of TEMPO-np-AuNPs and np-AuNPs, where the ΔI refers to the difference strength value within H_2O_2 in and without it. The nitroxide mediator can improve the free diffuse state, which is adjacent to the electrode surface [22, 23]. The ΔI of np-AuNPs sharply rose to 403 μA after it was modified with the TEMPO. All of these manifest that TEMPO-np-AuNPs have a higher potential peroxidase-like activity to H_2O_2. Usually, the H_2O_2 biosensor is constructed via the transfers of the two consecutive single electron transfers (Scheme 1) [22]. First of all, the TEMPO-np-AuNPs undergo a stable reversible one-electron oxidation to produce the intermediate at the TEMPO-functionalized electrode. Finally, the intermediate provides an electrocatalytic electron transfer way to detect H_2O_2.

3.5. Factors Influencing Detection. We all know that time and pH can directly affect the stability of the reaction proceeding and catalytic of enzymes. The analytical performance of the sensor is usually closely linked with the stability of the materials on electrode, which was partially influenced by the time and pH of electrolyte solution. So the pH and time were tested for their electrical catalytic activity to an optimal condition in this work. Firstly, the effect of pH on the potential of electrocatalytic activity on the TEMPO-np-AuNPs was tested at the range of 2.0 to 9.0 under the presence of 5 mM H_2O_2.

As can be seen in Figures 5(b) and 5(c), there is a slight negative shift in the potential catalytic site due to the reversible anodic oxidation of nitroxide derivatives and the inherent peroxidase-like activity response to H_2O_2 of np-AuNPs. Besides, the current intensity at 0.95V has an obvious enhancement under acidic environment and a distinct reduction followed when it was substituted with alkaline buffer (pH > 7.0). Briefly, TEMPO-np-AuNPs can reach the highest catalytic activity to H_2O_2, which is consistent with the result of the one-electron behavior of TEMPO/TEMPO$^+$ [22], under similar physiological conditions (0.1 M PBS, pH 7.0). Results show that pH can inappreciably influence the catalytic activity of TEMPO-np-AuNPs at the range of 5.0 to 8.5. Compared with the pH decided enzyme-modified electrode detection methods, this sensor can advance the application of TEMPO-np-AuNPs to detect H_2O_2 *in vivo* measurements [1].

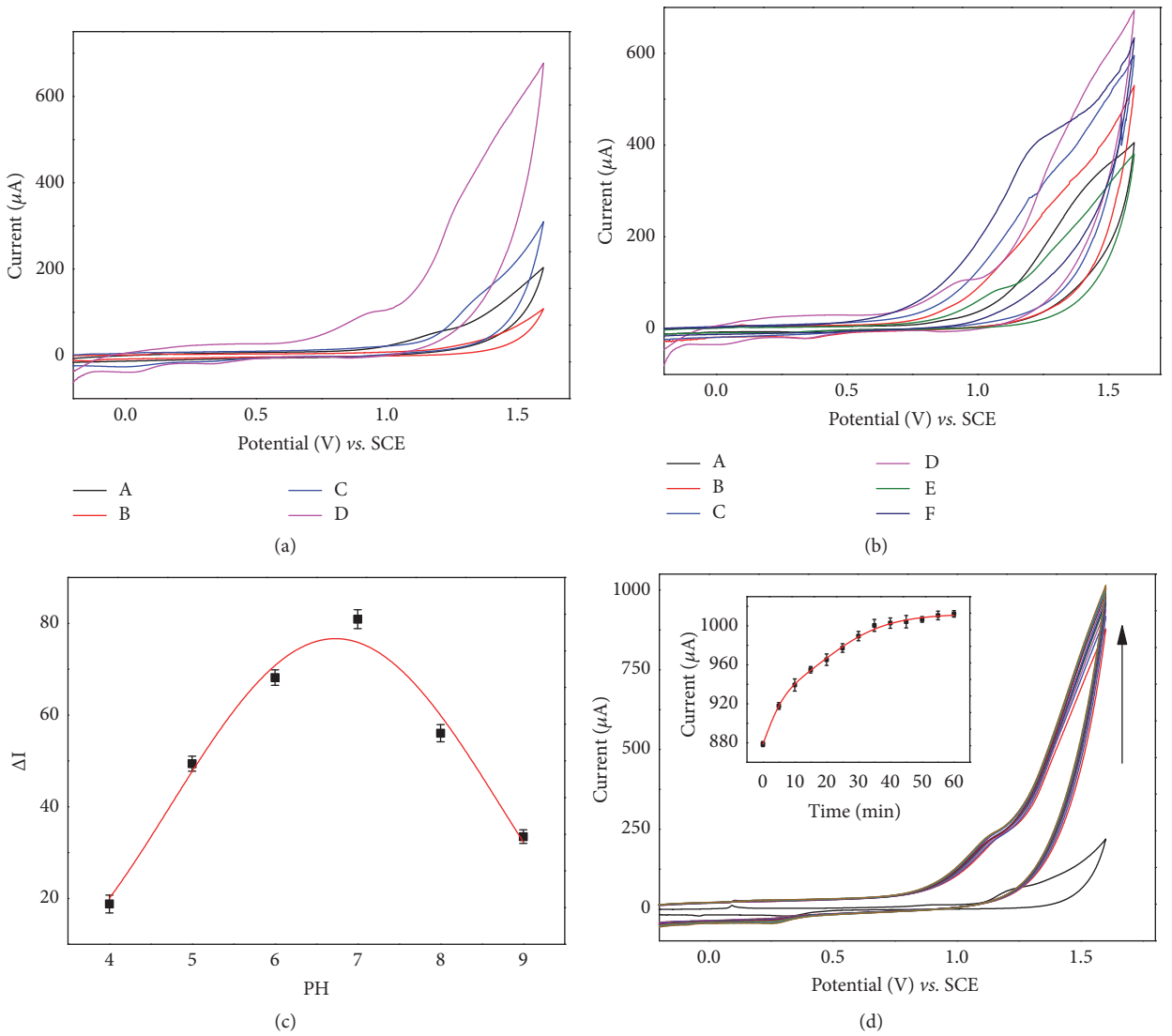

FIGURE 5: **(a)** CVs of different GCE under the absence (A and B) and presence (C and D) of 5mM H_2O_2 in N_2-saturated 0.1 M PBS (pH = 7.0) at a scan rate of 50mVs^{-1}. (A) Bare GCE (B and C) np-AuNPs/GCE, and (D) 4-carboxy-TEMPO-np-AuNPs/GCE. Optimization of experimental conditions: **(b)** CVs of the TEMPO -np-AuNPs/GCE in different pH values at the range of 2.0~9.0 and **(c)** the relationship between the net current at 0.95V with different pH. **(d)** CVs of TEMPO-np-AuNPs/GCE in 0.1 M PBS (pH = 7.0), in the presence 5 mM H_2O_2, in different times from 0 min to 60 min, N_2-saturated, 50mVs^{-1}. Inset: the changes of the electric current (1.6 V) with the time increasing.

Further, we investigated the time factor in the presence of 5 mM H_2O_2. Figure 5(d) shows TEMPO-np-AuNPs can catalyze H_2O_2 to produce O_2, immediately, which then comes to an equilibrium state with a maximum current strength in 40 min. By comparing the current strength at 1.6 V, we found that the floating electric potential of 40 min only takes 13.64% in the whole catalytic oxidation process. It is possible that this remaining increase is closely related to the irregular gaps and surface of the np-AuNPs, which may lead to the time retardation to the reversible one-electron behavior of the redox couple TEMPO/$TEMPO^+$ [46]. So we selected 40 min stirring constantly after H_2O_2 was added to the 0.1 M PBS with the buffer system of pH=7.0 to ensure the sufficient current response in the following measurements.

3.6. Steady-State Amperometric Response of H_2O_2. To evaluate the applied potential of TEMPO-MA-np-AuNPs/GCE as peroxidase-like. We investigated the response of the amperometric signal under the optimal condition with the 0.95 V as the applied potential (E_{app}). As shown in Figure 6, the TEMPO-np-AuNPs/GCE not only can achieve a quick steady-state current within 10 s, but also has a stronger response (C) compared to the np-AuNPs/GCE (B).

Moreover, with the addition of same amount H_2O_2 in every interval of 100 s, the TEMPO- np-AuNPs nanocomposite on the GCE exhibited a good linear chronoamperometric response to H_2O_2 from 2.0 μM to 500 μM, which is shown in Figure 6. As what we have seen, when the concentration of H_2O_2 is below 10.0 μM, the slope of the

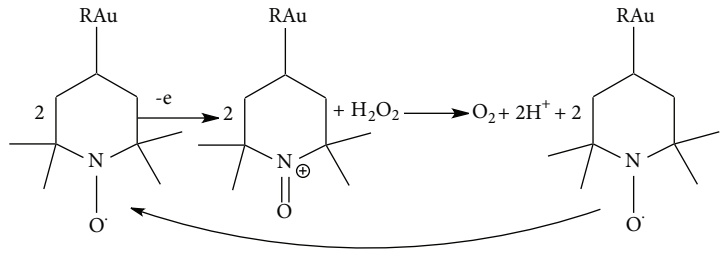

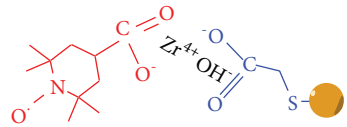

Mechanism process:

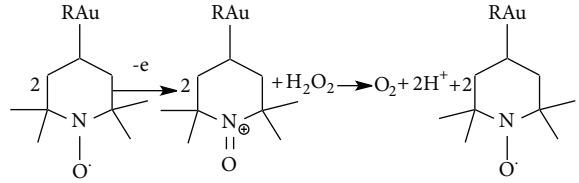

Scheme 1: Equilibrium of single electron between TEMPO-np-AuNPs and H_2O_2.

linear (K_b= 0.66608, R^2=0.98185) is lower than that in a higher concentration range. In other words, the sensitivity of electrocatalytic oxidation activity to H_2O_2 is improved with the concentration of H_2O_2 increased in the solution and there are no substrate inhibition effects occurring at high concentration of H_2O_2. With successive addition of H_2O_2 (n = 5) as shown in Figures 6(b) and 6(c), we can obtain two linear regression equations: (1) below 10.0 μM, y = 0.66608x+4.51516 (R^2 = 0.98185); (2) 10.0 μM to 500 μM, y = 0.1078x+0.6047(R^2 = 0.9998). Error bars represent the standard deviations of five independent measurements. The repeatability of the system is assured by a relative standard deviation (RSD) of 2.8%. We use conventional three times the standard deviation of [LOD = 3(RSD/slope)] to estimate the limit of detection (LOD) of H_2O_2, which is 0.78 μM in our work and lower than some Au nanomaterials and nitroxide derivatives for H_2O_2 detection as listed in Table 1. The results of the stability measurements indicated that np-AuNPs still keep its stable original roughened surface and porous structure after 30 days of storage at 4°C. Moreover, compared with previous results, the TEMPO-np-AuNPs/GCE can retain 98.6% of its initial current response results in the same measurement conditions. Therefore, the TEMPO-np-AuNPs nanocomposite has a remarkable superiority for the electrochemical detection of H_2O_2 over the conventional electrochemical sensing materials and most of the reported Au nanomaterials and nitroxide derivatives probes (Table 1).

3.7. Interference Study. Some coexisting potential electroactive species may affect the sensor response, such as sucrose (SC), glucose (GC), dopamine (DA), and ascorbic acid (AA) [3, 48]. Good selectivity is crucial to ensure and facilitate the accurate assessment for biosensor in a particular application. For better detection *in vivo*, the interference study of TEMPO-np-AuNPs/GCE for the electrochemical detection of H_2O_2 was carried out to evaluate its practical feasibility. Results were shown in Figure 6(d); a discernible slight fluctuation is hard to see after the abundant successive addition of each interfering species (SC/GC/DA/AA), while no obvious interference signal was observed. Notably, the TEMPO-np-AuNPs/GCE had an 18μA response (E_{app} = + 0.95 V) as soon as another 0.1mM H_2O_2 was injected into the complex system of interference. The initial small responses caused by SC, GC, DA, and AA belong to normal current fluctuations, which is a deductible interference compared with that caused by H_2O_2. TEMPO-np-AuNPs/GCE exhibited an acceptable selectivity towards the practical *in vivo* electrochemical detection of H_2O_2.

Table 1: Comparison of recent Au nanomaterials and nitroxide derivatives for H_2O_2 detection.

Electrode design	L. R. (M)	D.L. (μM)	Stability	Reference
HRP/Cys/AuNP/ITO	8.0×10^{-6}~3.0×10^{-3}	2.00	83% (12 weeks)	[6]
HRP/$CaCO_3$-AuNPs/ATP/Au	5.0×10^{-7}~5.2×10^{-3}	0.10	96.4% (30 days)	[36]
HRP-nano-Au	1.2×10^{-5}~1.1×10^{-3}	6.10	75% (5 weeks)	[37]
HRP/AuNPs/poly(St-co-AA)	8.0×10^{-6}~7.0×10^{-3}	4.00	97.8 % (60 days)	[38]
Au/CeO_2 nanocomposite	0~3.0×10^{-4}	5.00	---	[9]
AuNPs-N-GQDs/GC	2.5×10^{-5}~1.3×10^{-2}	0.12	89%, 3 weeks	[10]
Poly(BCB)/Au-NPs/GCE	6.0×10^{-5}~1.0×10^{-2}	0.23	95 %(2 week)	[39]
GC/MTMOS-$Au^{73}Ag^{27}$	1.0×10^{-5}~7.0×10^{-5}	1.00	---	[40]
Hb/Au nanoflowers/CNTs/GCE	1.0×10^{-6}~6.0×10^{-4}	7.30	---	[41]
TEMPO/GCE	1.0×10^{-7}~1.0×10^{-8}	0.05	100%,3 months	[22]
ChOx/TEMPO/GCE	2×10^{-5}~ 2.5×10^{-3}	20.0	---	[23]
TEMPO-MA-np-AuNPs/GCE	2.5×10^{-6}~5.0×10^{-4}	0.78	98.6%(30 days)	**This work**

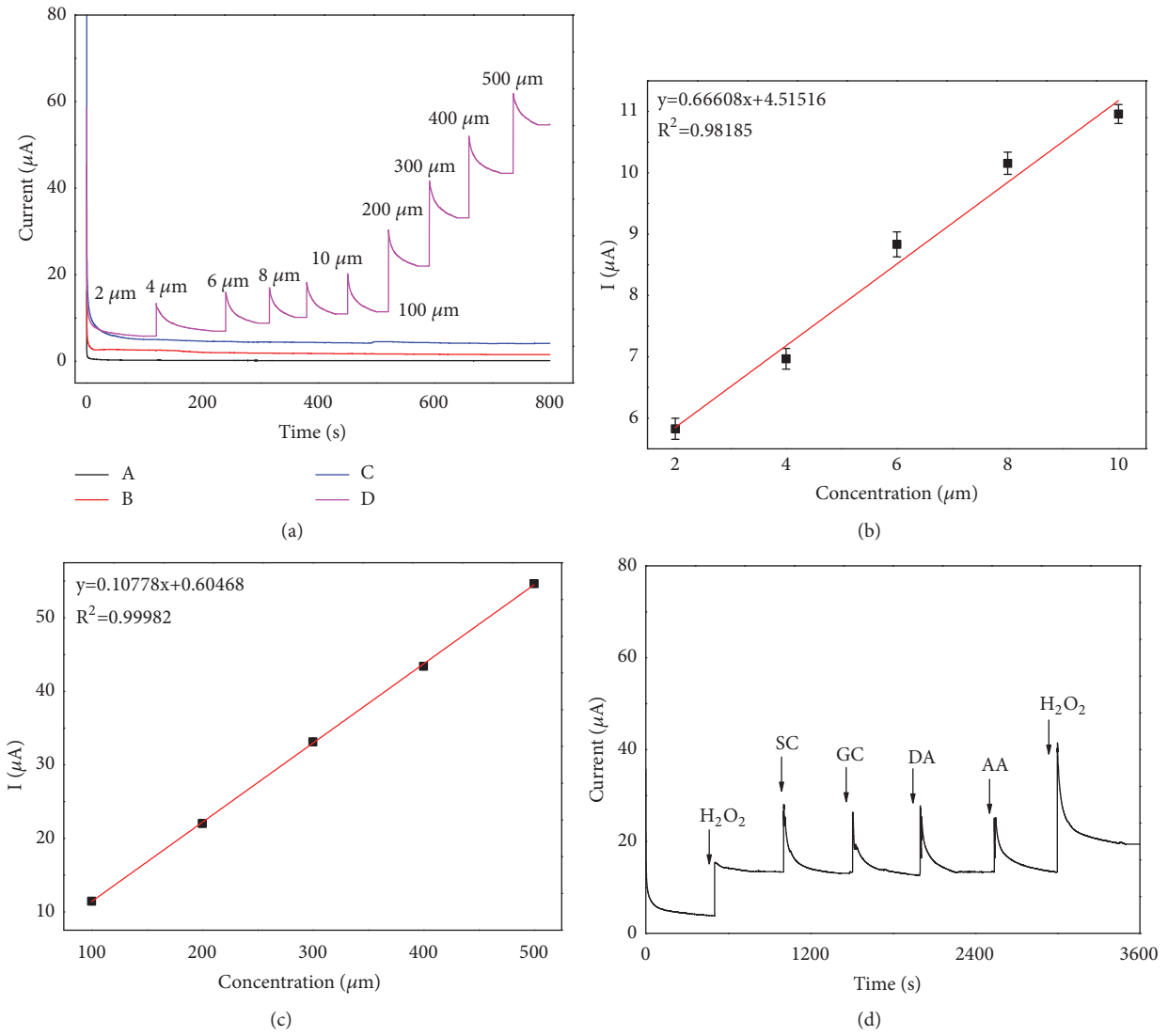

Figure 6: **(a)** Chronoamperometric responses observed at (A) bare GCE, (B) np-AuNPs/GCE, (C) TEMPO-np-AuNPs/GCE, and (D) TEMPO-np-AuNPs/GCE after successively injecting H_2O_2, in 0.1 M PBS (pH=7.0). Applied potential: 1.10 V and the calibration plot between the oxidation current and the H_2O_2 concentration **(b and c).** **(d)** Amperometric response of H_2O_2 and interferants at TEMPO-np-AuNPs/GCE at 1.10V in PBS (0.1 M, pH = 7.0). Injection sequence: 0.1mM H_2O_2, 100 mM SC, 100 mM GC, 100 mM DA, 100 mM AA, and 0.2 mM H_2O_2.

4. Conclusions

In this work, we demonstrated a strategy for producing large specific surface area nanoporous gold nanoparticles and manufactured the TEMPO-functionalized np-AuNPs nanocomposite; the electrooxidation to H_2O_2 with a high density of radicals on the TEMPO-np-AuNPs surface was also investigated. It is worth noting that this new nonenzymatic H_2O_2 probe is prepared under a gentle, secure, low-cost, and simple procedure. When the np-AuNPs are combined with 4-carboxy-TEMPO, the advantages of their unique properties for the electrochemical detection of H_2O_2 come to a double effective enhancement. Compared the peroxidase-like activity based on the direct electron transfer of the TEMPO-np-AuNPs/GCE to the electrochemical hydrogen peroxide biosensors of TEMPO-based ligand, we obtained a wide linear range for H_2O_2 detection. The enzyme-like activity with low detection limit, high sensitivity, low-cost, anti-interference, good reproducibility, and stability of this nanocomposite with TEMPO-based ligand make a contribution to improve the detection current signal of H_2O_2. Furthermore, this TEMPO-functionalized np-AuNPs nanocomposite study plays a significant role in facilitating the research of biosensors, gold nanomedicine, catalysis, or cancer therapy.

Data Availability

All the data used to support the findings of this study are included within the article or are available from the corresponding author upon request. These data are available for unrestricted use, distribution, and reproduction in any medium, provided the original work is properly cited.

Conflicts of Interest

The authors declare that they have no conflicts of interest.

Acknowledgments

This work was supported by the National Natural Science Foundation of China (Grant no. 21575066).

References

[1] W. Chen, S. Cai, Q.-Q. Ren, W. Wen, and Y.-D. Zhao, "Recent advances in electrochemical sensing for hydrogen peroxide: A review," *Analyst*, vol. 137, no. 1, pp. 49–58, 2012.

[2] S. Chen, R. Yuan, Y. Chai, and F. Hu, "Electrochemical sensing of hydrogen peroxide using metal nanoparticles: A review," *Microchimica Acta*, vol. 180, no. 1-2, pp. 15–32, 2013.

[3] Z. Miao, D. Zhang, and Q. Chen, "Non-enzymatic hydrogen peroxide sensors based on multi-wall carbon nanotube/Pt nanoparticle nanohybrids," *Materials* , vol. 7, no. 4, pp. 2945–2955, 2014.

[4] M. Giorgio, M. Trinei, E. Migliaccio, and P. G. Pelicci, "Hydrogen peroxide: a metabolic by-product or a common mediator of ageing signals?" *Nature Reviews Molecular Cell Biology*, vol. 8, no. 9, pp. 722–728, 2007.

[5] K.-J. Huang, D.-J. Niu, X. Liu et al., "Direct electrochemistry of catalase at amine-functionalized graphene/gold nanoparticles composite film for hydrogen peroxide sensor," *Electrochimica Acta*, vol. 56, no. 7, pp. 2947–2953, 2011.

[6] J. Wang, L. Wang, J. Di, and Y. Tu, "Electrodeposition of gold nanoparticles on indium/tin oxide electrode for fabrication of a disposable hydrogen peroxide biosensor," *Talanta*, vol. 77, no. 4, pp. 1454–1459, 2009.

[7] Y.-D. Lee, C.-K. Lim, A. Singh et al., "Dye/peroxalate aggregated nanoparticles with enhanced and tunable chemiluminescence for biomedical imaging of hydrogen peroxide," *ACS Nano*, vol. 6, no. 8, pp. 6759–6766, 2012.

[8] L. Gu, N. Luo, and G. H. Miley, "Cathode electrocatalyst selection and deposition for a direct borohydride/hydrogen peroxide fuel cell," *Journal of Power Sources*, vol. 173, no. 1, pp. 77–85, 2007.

[9] C. Ampelli, S. G. Leonardi, A. Bonavita et al., "Electrochemical H2O2 sensors based on Au/CeO2 nanoparticles for industrial applications," *Chemical Engineering Transactions*, vol. 43, pp. 733–738, 2015.

[10] J. Jian and C. Wei, "In situ growth of surfactant-free gold nanoparticles on nitrogen-doped graphene quantum dots for electrochemical detection of hydrogen peroxide in biological environments," *Analytical Chemistry*, vol. 87, no. 3, pp. 1903–1910, 2015.

[11] A. A. Ensafi, N. Ahmadi, B. Rezaei, and M. M. Abarghoui, "A new electrochemical sensor for the simultaneous determination of acetaminophen and codeine based on porous silicon/palladium nanostructure," *Talanta*, vol. 134, pp. 745–753, 2015.

[12] S. Pedireddy, H. K. Lee, W. W. Tjiu et al., "One-step synthesis of zero-dimensional hollow nanoporous gold nanoparticles with enhanced methanol electrooxidation performance," *Nature Communications*, vol. 5, article no. 4947, 2014.

[13] C. Boyer, M. R. Whittaker, C. Nouvel, and T. P. Davis, "Synthesis of hollow polymer nanocapsules exploiting gold nanoparticles as sacrificial templates," *Macromolecules* , vol. 43, no. 4, pp. 1792–1799, 2010.

[14] C. Zhang, A. Zhu, R. Huang, Q. Zhang, and Q. Liu, "Hollow nanoporous Au/Pt core-shell catalysts with nanochannels and enhanced activities towards electro-oxidation of methanol and ethanol," *International Journal of Hydrogen Energy*, vol. 39, no. 16, pp. 8246–8256, 2014.

[15] Z. Liu, A. Nemec-Bakk, N. Khaper, and A. Chen, "Sensitive Electrochemical Detection of Nitric Oxide Release from Cardiac and Cancer Cells via a Hierarchical Nanoporous Gold Microelectrode," *Analytical Chemistry*, vol. 89, no. 15, pp. 8036–8043, 2017.

[16] R. A. Green, J. T. Hill-Cousins, R. C. D. Brown, D. Pletcher, and S. G. Leach, "A voltammetric study of the 2,2,6,6-tetramethylpiperidin-1-oxyl (TEMPO) mediated oxidation of benzyl alcohol in tert-butanol/water," *Electrochimica Acta*, vol. 113, pp. 550–556, 2013.

[17] M. Rafiee, K. C. Miles, and S. S. Stahl, "Electrocatalytic Alcohol Oxidation with TEMPO and Bicyclic Nitroxyl Derivatives: Driving Force Trumps Steric Effects," *Journal of the American Chemical Society*, vol. 137, no. 46, pp. 14751–14757, 2015.

[18] B. Karimi, M. Rafiee, S. Alizadeh, and H. Vali, "Eco-friendly electrocatalytic oxidation of alcohols on a novel electro generated TEMPO-functionalized MCM-41 modified electrode," *Green Chemistry*, vol. 17, no. 2, pp. 991–1000, 2015.

[19] P.-Y. Blanchard, O. Alévêque, T. Breton, and E. Levillain, "TEMPO mixed SAMs: Electrocatalytic efficiency versus surface coverage," *Langmuir*, vol. 28, no. 38, pp. 13741–13745, 2012.

[20] R. Ciriminna, G. Palmisano, and M. Pagliaro, "Electrodes functionalized with the 2,2,6,6-tetramethylpiperidinyloxy radical for the waste-free oxidation of alcohols," *ChemCatChem*, vol. 7, no. 4, pp. 552–558, 2015.

[21] S. Eken Korkut, D. Akyüz, K. Özdoğan, Y. Yerli, A. Koca, and M. K. Şener, "TEMPO-functionalized zinc phthalocyanine: Synthesis, magnetic properties, and its utility for electrochemical sensing of ascorbic acid," *Dalton Transactions*, vol. 45, no. 7, pp. 3086–3092, 2016.

[22] B. Limoges and C. Degrand, "Electrocatalytic oxidation of hydrogen peroxide by nitroxyl radicals," *Journal of Electroanalytical Chemistry*, vol. 422, no. 1-2, pp. 7–12, 1997.

[23] S. Abdellaoui, K. L. Knoche, K. Lim, D. P. Hickey, and S. D. Minteer, "TEMPO as a Promising Electrocatalyst for the Electrochemical Oxidation of Hydrogen Peroxide in Bioelectronic Applications," *Journal of The Electrochemical Society*, vol. 163, no. 4, pp. H3001–H3005, 2016.

[24] V. Lloveras, E. Badetti, V. Chechik, and J. Vidal-Gancedo, "Magnetic interactions in Spin-labeled Au nanoparticles," *The Journal of Physical Chemistry C*, vol. 118, no. 37, pp. 21622–21629, 2014.

[25] L. Zhang, Y. B. Vogel, B. B. Noble et al., "TEMPO Monolayers on Si(100) Electrodes: Electrostatic Effects by the Electrolyte and Semiconductor Space-Charge on the Electroactivity of a Persistent Radical," *Journal of the American Chemical Society*, vol. 138, no. 30, pp. 9611–9619, 2016.

[26] Y. Sun and Y. Xia, "Increased sensitivity of surface plasmon resonance of gold nanoshells compared to that of gold solid colloids in response to environmental changes," *Analytical Chemistry*, vol. 74, no. 20, pp. 5297–5305, 2002.

[27] W. S. Chew, S. Pedireddy, Y. H. Lee et al., "Nanoporous Gold Nanoframes with Minimalistic Architectures: Lower Porosity Generates Stronger Surface-Enhanced Raman Scattering Capabilities," *Chemistry of Materials*, vol. 27, no. 22, pp. 7827–7834, 2015.

[28] A. Wittstock, J. Biener, and M. Bäumer, "Nanoporous gold: A new material for catalytic and sensor applications," *Physical Chemistry Chemical Physics*, vol. 12, no. 40, pp. 12919–12930, 2010.

[29] P. E. Laibinis, M. A. Fox, J. P. Folkers, and G. M. Whitesides, "Comparisons of Self-Assembled Monolayers on Silver and Gold: Mixed Monolayers Derived from HS(CH2)21X and HS(CH2)10Y (X, Y = CH3, CH2OH) Have Similar Properties," *Langmuir*, vol. 7, no. 12, pp. 3167–3173, 1991.

[30] A. Badia, S. Singh, L. Demers, L. Cuccia, G. R. Brown, and R. B. Lennox, "Self-assembled monolayers on gold nanoparticles," *Chemistry - A European Journal*, vol. 2, no. 3, pp. 359–363, 1996.

[31] J. Kong, A. R. Ferhan, X. Chen, L. Zhang, and N. Balasubramanian, "Polysaccharide templated silver nanowire for ultrasensitive electrical detection of nucleic acids," *Analytical Chemistry*, vol. 80, no. 19, pp. 7213–7217, 2008.

[32] M. Mazur, P. Krysiński, and G. J. Blanchard, "Use of zirconium-phosphate-carbonate chemistry to immobilize polycyclic aromatic hydrocarbons on boron-doped diamond," *Langmuir*, vol. 21, no. 19, pp. 8802–8808, 2005.

[33] Q. Hu, W. Hu, J. Kong, and X. Zhang, "PNA-based DNA assay with attomolar detection limit based on polygalacturonic acid mediated in-situ deposition of metallic silver on a gold electrode," *Microchimica Acta*, vol. 182, no. 1-2, pp. 427–434, 2015.

[34] D. Wan, H.-L. Chen, Y.-S. Lin, S.-Y. Chuang, J. Shieh, and S.-H. Chen, "Using spectroscopic ellipsometry to characterize and apply the optical constants of hollow gold nanoparticles," *ACS Nano*, vol. 3, no. 4, pp. 960–970, 2009.

[35] P. Silvert, R. Herrera-Urbina, and K. Tekaia-Elhsissen, "Preparation of colloidal silver dispersions by the polyol process," *Journal of Materials Chemistry*, vol. 7, no. 2, pp. 293–299.

[36] F. Li, Y. Feng, Z. Wang, L. Yang, L. Zhuo, and B. Tang, "Direct electrochemistry of horseradish peroxidase immobilized on the layered calcium carbonate-gold nanoparticles inorganic hybrid composite," *Biosensors and Bioelectronics*, vol. 25, no. 10, pp. 2244–2248, 2010.

[37] C. X. Leia, S. Q. Huc, N. Gao, G. L. Shen, and R. Q. Yu, "An amperometric hydrogen peroxide biosensor based on immobilizing horseradish peroxidase to a nano-Au monolayer supported by sol-gel derived carbon ceramic electrode," *Bioelectrochemistry*, vol. 65, no. 1, pp. 33–39, 2004.

[38] S. Xu, G. Tu, B. Peng, and X. Han, "Self-assembling gold nanoparticles on thiol-functionalized poly(styrene-co-acrylic acid) nanospheres for fabrication of a mediatorless biosensor," *Analytica Chimica Acta*, vol. 570, no. 2, pp. 151–157, 2006.

[39] S. A. Kumar, S.-F. Wang, and Y.-T. Chang, "Poly(BCB)/Au-nanoparticles hybrid film modified electrode: Preparation, characterization and its application as a non-enzymatic sensor," *Thin Solid Films*, vol. 518, no. 20, pp. 5832–5838, 2010.

[40] S. Manivannan and R. Ramaraj, "Core-shell Au/Ag nanoparticles embedded in silicate sol-gel network for sensor application towards hydrogen peroxide," *Journal of Chemical Sciences*, vol. 121, no. 5, pp. 735–743, 2009.

[41] Y.-C. Gao, K. Xi, W.-N. Wang, X.-D. Jia, and J.-J. Zhu, "A novel biosensor based on a gold nanoflowers/hemoglobin/carbon nanotubes modified electrode," *Analytical Methods*, vol. 3, no. 10, pp. 2387–2391, 2011.

[42] J.-J. Feng, G. Zhao, J.-J. Xu, and H.-Y. Chen, "Direct electrochemistry and electrocatalysis of heme proteins immobilized on gold nanoparticles stabilized by chitosan," *Analytical Biochemistry*, vol. 342, no. 2, pp. 280–286, 2005.

[43] F. Meng, X. Yan, J. Liu, J. Gu, and Z. Zou, "Nanoporous gold as non-enzymatic sensor for hydrogen peroxide," *Electrochimica Acta*, vol. 56, no. 12, pp. 4657–4662, 2011.

[44] F. Jia, C. Yu, K. Deng, and L. Zhang, "Nanoporous metal (Cu, Ag, Au) films with high surface area: general fabrication and preliminary electrochemical performance," *The Journal of Physical Chemistry C*, vol. 111, no. 24, pp. 8424–8431, 2007.

[45] T.-M. Cheng, T.-K. Huang, H.-K. Lin et al., "(110)-Exposed gold nanocoral electrode as low onset potential selective glucose sensor," *ACS Applied Materials & Interfaces*, vol. 2, no. 10, pp. 2773–2780, 2010.

[46] J. Yun, B. Li, and R. Cao, "Positively-charged gold nanoparticles as peroxidiase mimic and their application in hydrogen peroxide and glucose detection," *Chemical Communications*, vol. 46, no. 42, pp. 8017–8019, 2010.

[47] H. Cui, Z.-F. Zhang, M.-J. Shi, Y. Xu, and Y.-L. Wu, "Light emission of gold nanoparticles induced by the reaction of bis(2,4,6-trichlorophenyl) oxalate and hydrogen peroxide," *Analytical Chemistry*, vol. 77, no. 19, pp. 6402–6406, 2005.

[48] G. Yin, L. Xing, X.-J. Ma, and J. Wan, "Non-enzymatic hydrogen peroxide sensor based on a nanoporous gold electrode modified with platinum nanoparticles," *Chemical Papers*, vol. 68, no. 4, pp. 435–441, 2014.